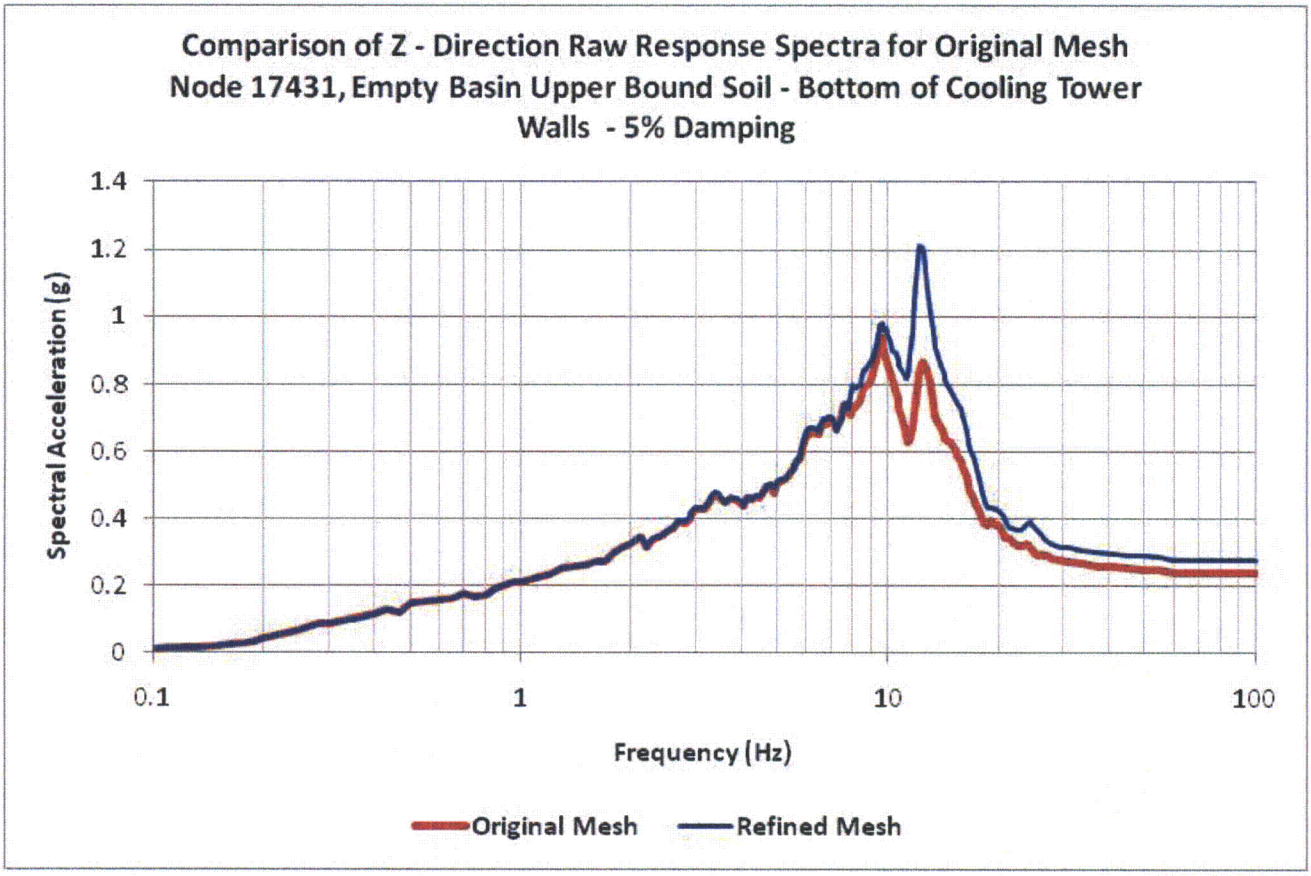

Figure 03.07.02-24.123: Comparison of Z - Direction Raw Response Spectra for Original Mesh Node 17431, Empty Basin Upper Bound Soil - Bottom of Cooling Tower Walls - 5% Damping

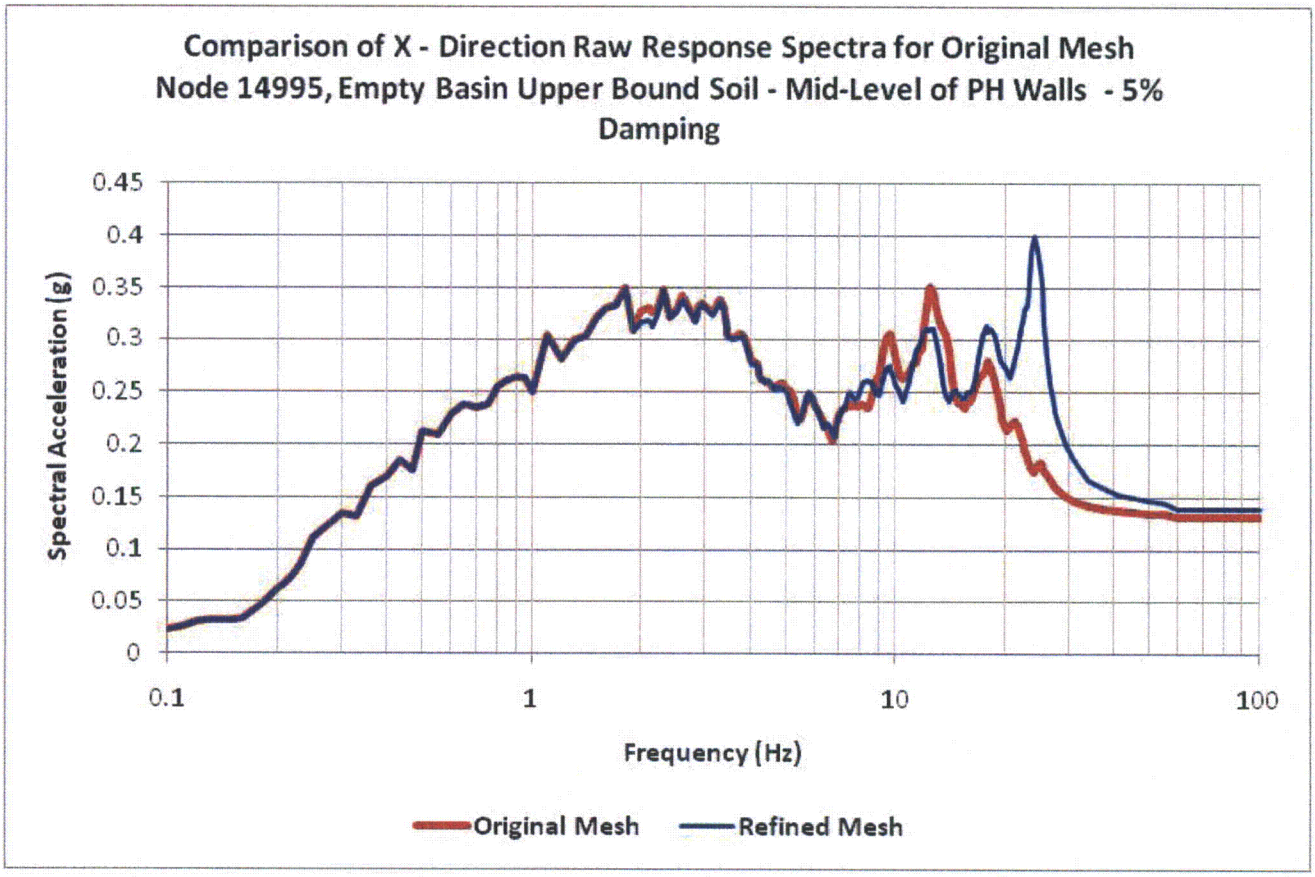

Figure 03.07.02-24.124: Comparison of X - Direction Raw Response Spectra for Original Mesh Node 14995, Empty Basin Upper Bound Soil - Mid-Level of PH Walls - 5% Damping

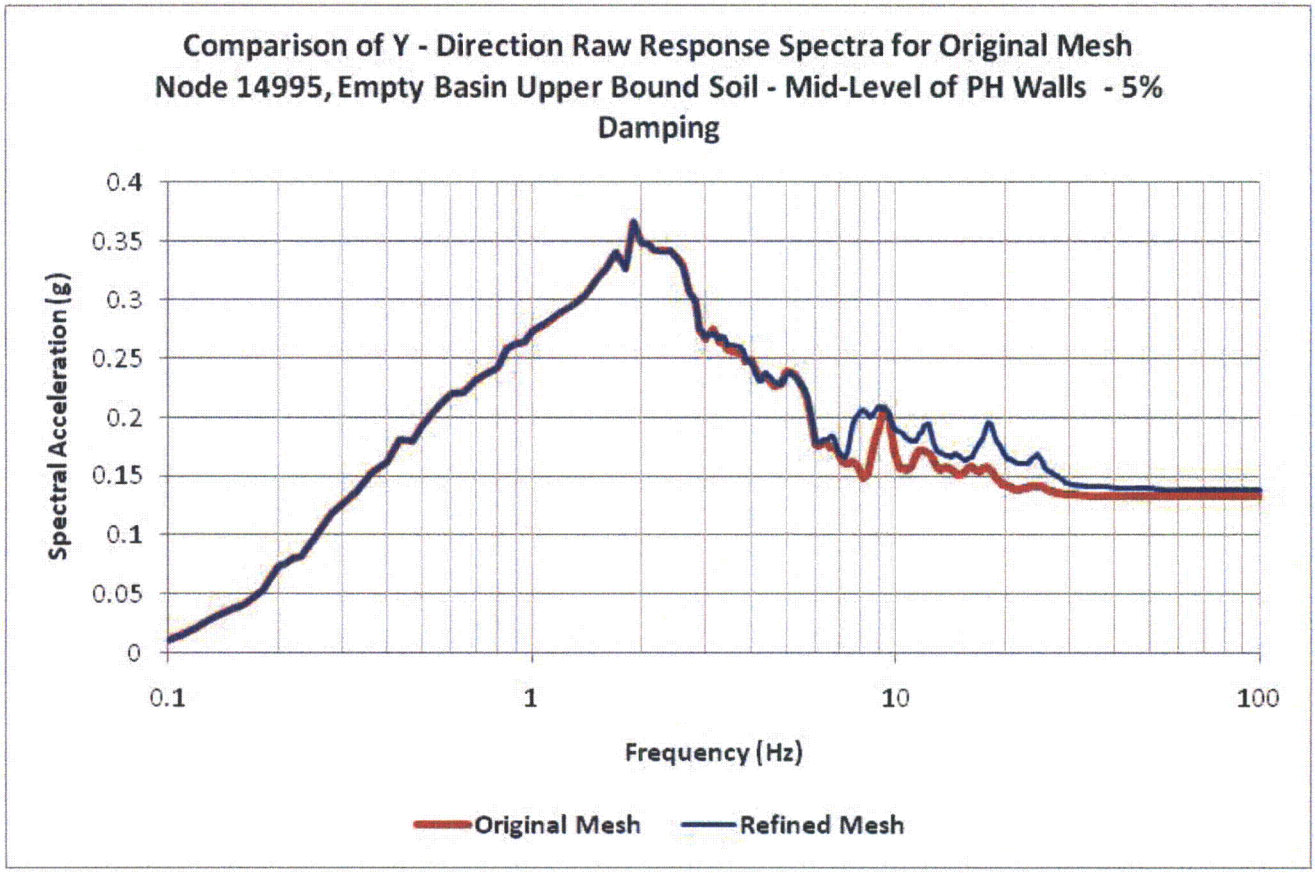

Figure 03.07.02-24.125: Comparison of Y - Direction Raw Response Spectra for Original Mesh Node 14995, Empty Basin Upper Bound Soil - Mid-Level of PH Walls - 5% Damping

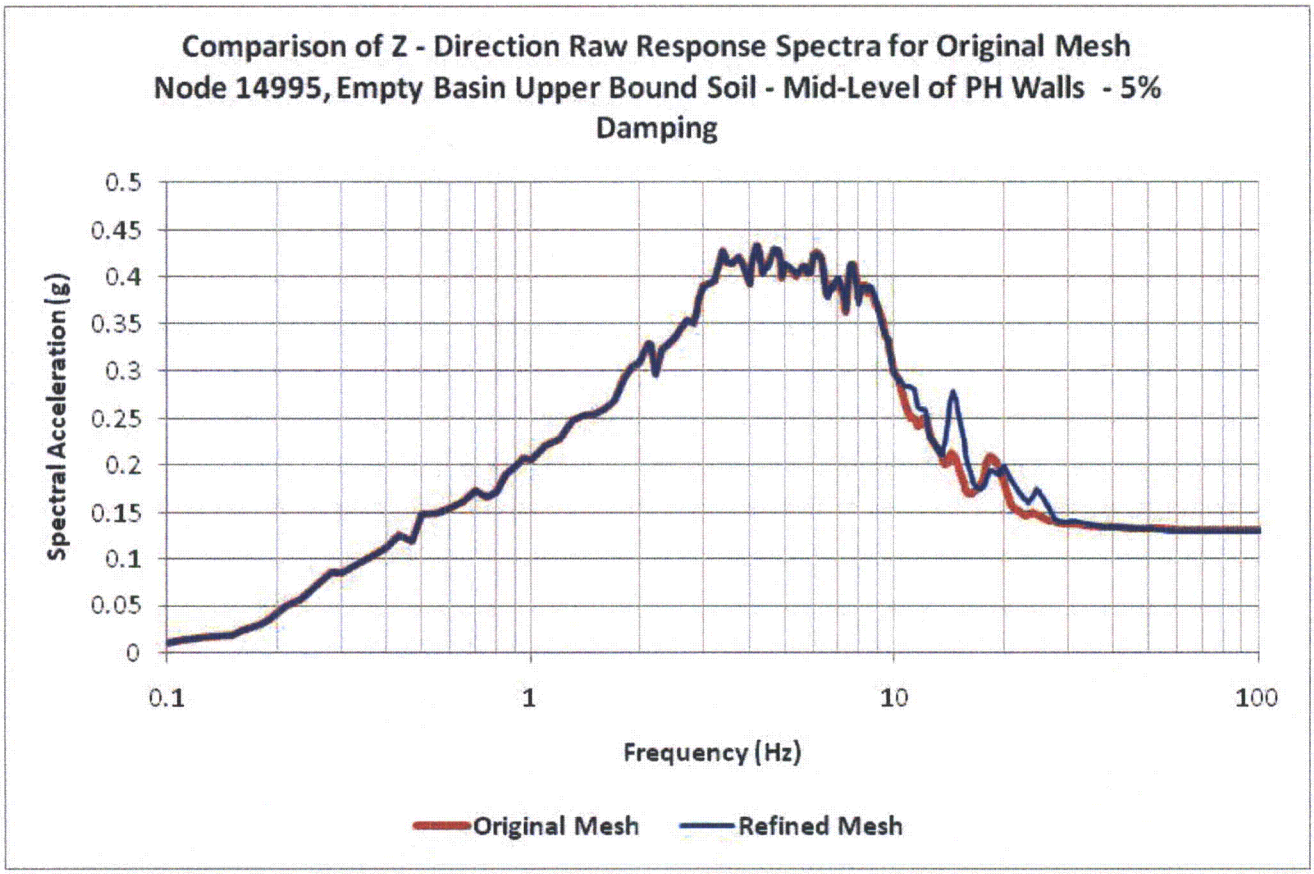

Figure 03.07.02-24.126: Comparison of Z - Direction Raw Response Spectra for Original Mesh Node 14995, Empty Basin Upper Bound Soil - Mid-Level of PH Walls - 5% Damping

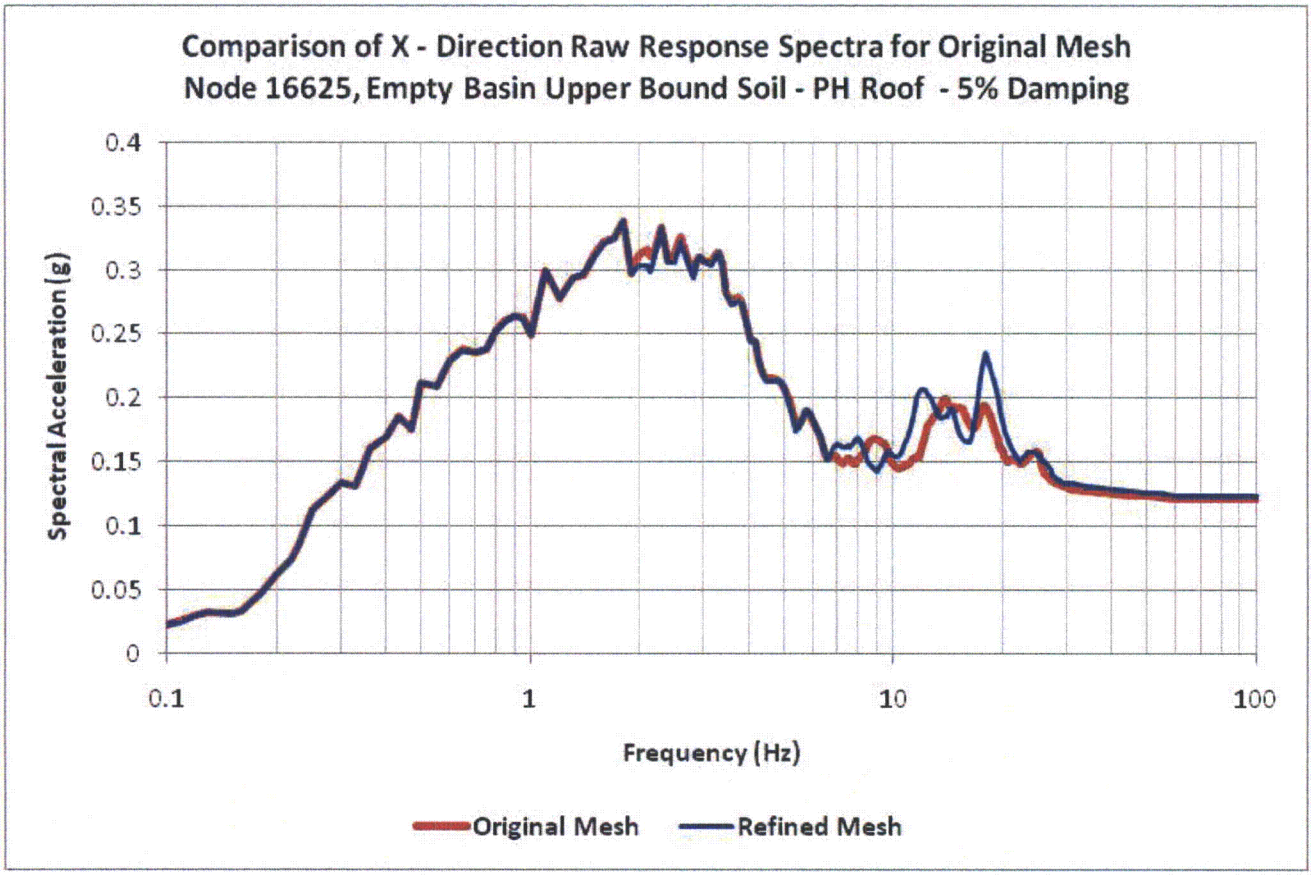

Figure 03.07.02-24.127: Comparison of X - Direction Raw Response Spectra for Original Mesh Node 16625, Empty Basin Upper Bound Soil - PH Roof - 5% Damping

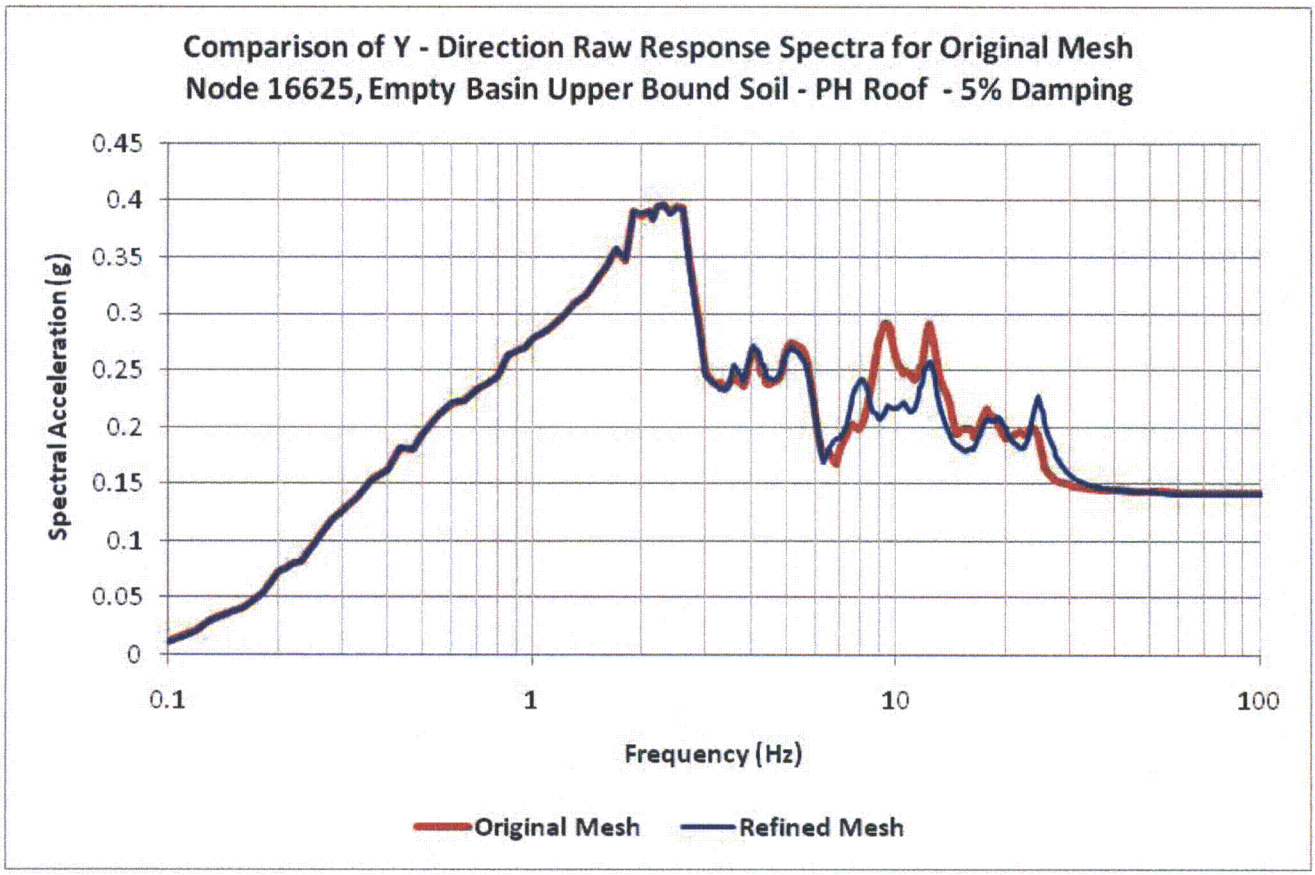

Figure 03.07.02-24.128: Comparison of Y - Direction Raw Response Spectra for Original Mesh Node 16625, Empty Basin Upper Bound Soil - PH Roof - 5% Damping

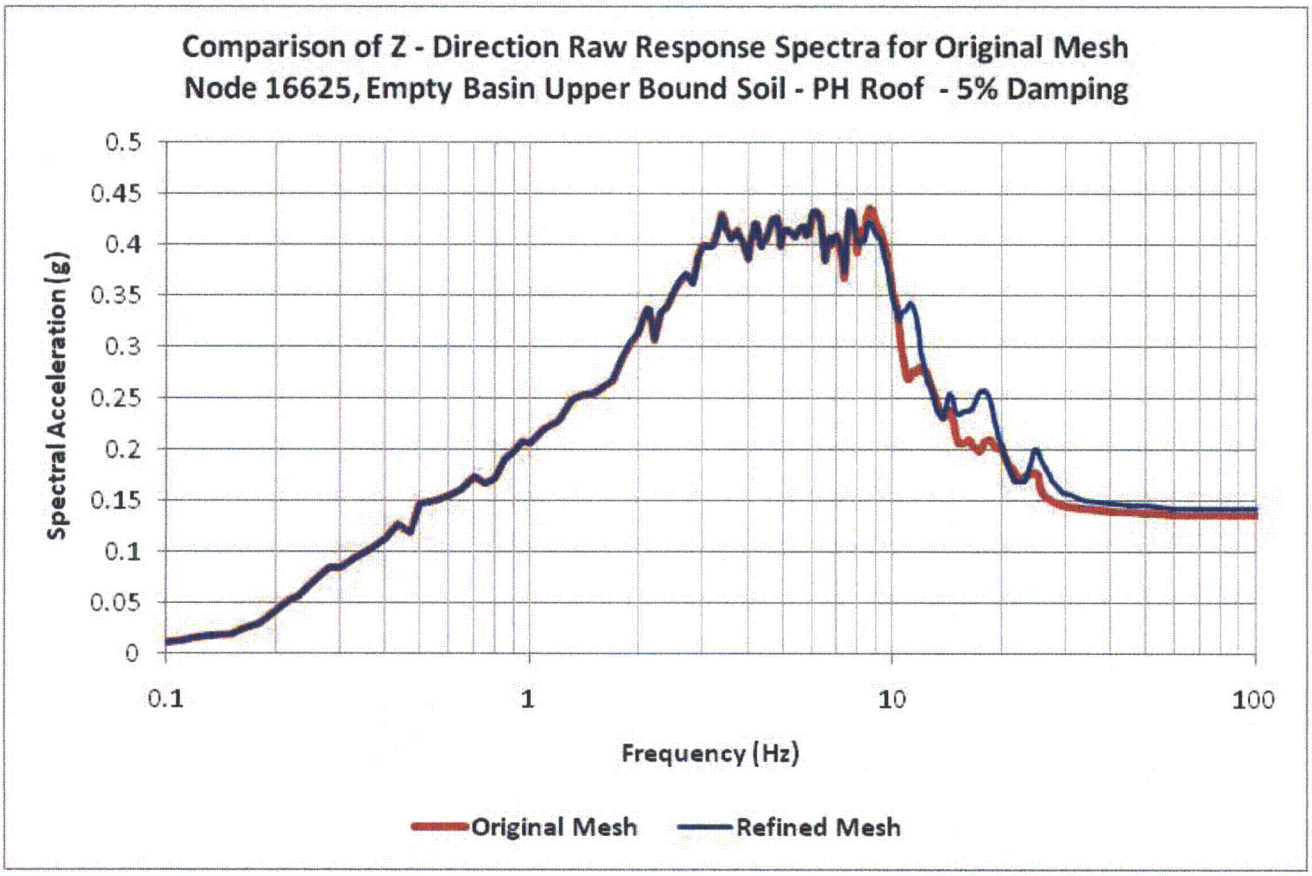

Figure 03.07.02-24.129: Comparison of Z - Direction Raw Response Spectra for Original Mesh Node 16625, Empty Basin Upper Bound Soil - PH Roof - 5% Damping

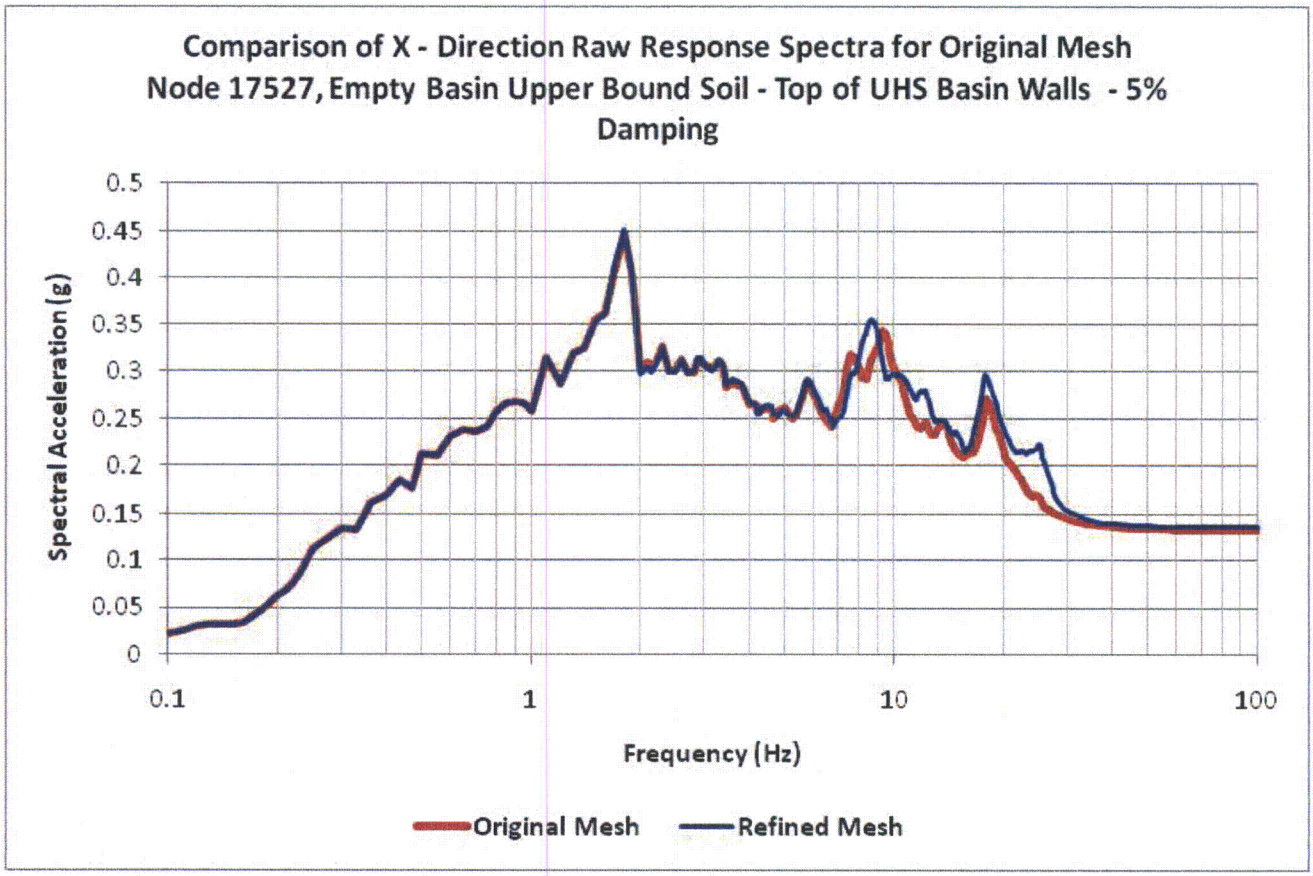

Figure 03.07.02-24.130: Comparison of X - Direction Raw Response Spectra for Original Mesh Node 17527, Empty Basin Upper Bound Soil - Top of UHS Basin Walls - 5% Damping

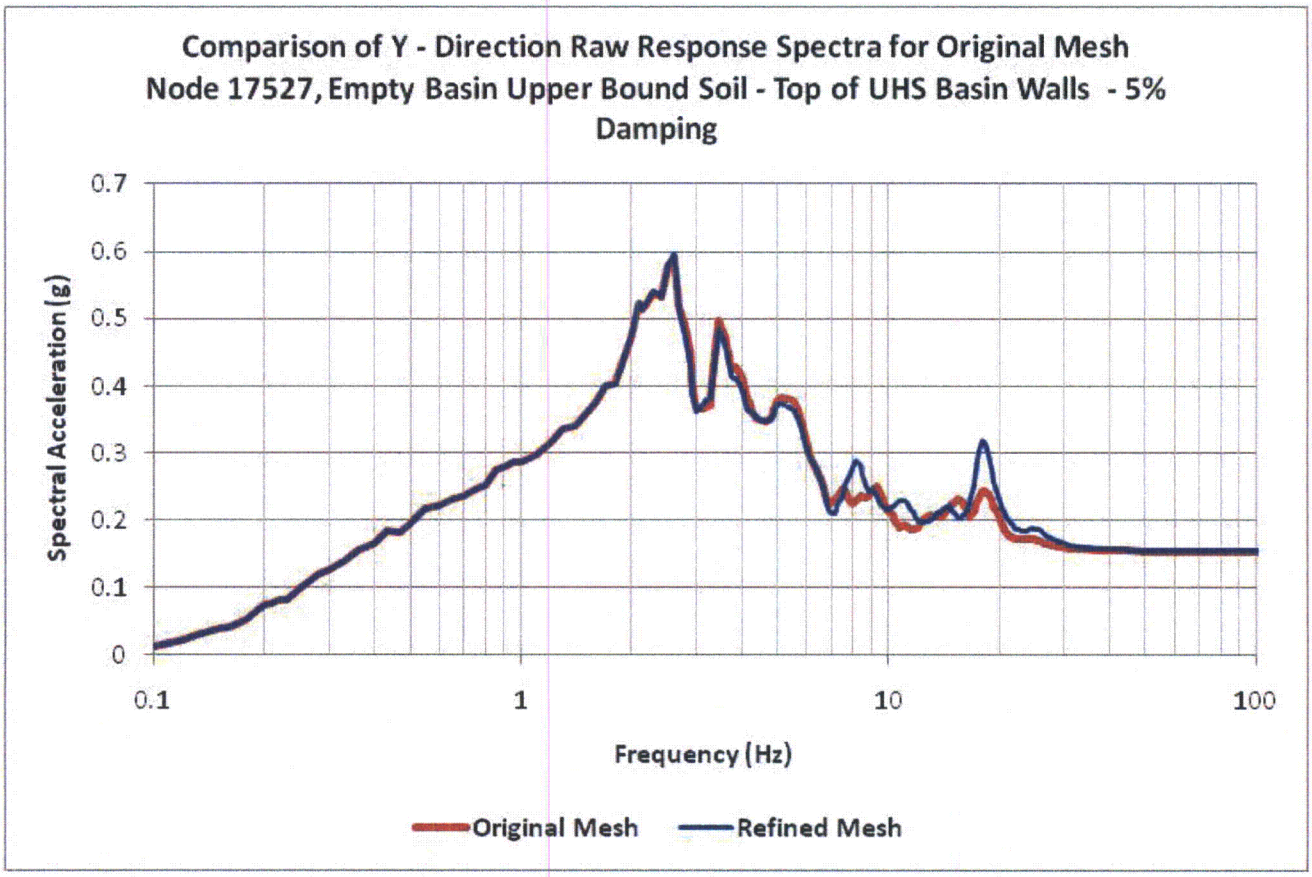

Figure 03.07.02-24.131: Comparison of Y - Direction Raw Response Spectra for Original Mesh Node 17527, Empty Basin Upper Bound Soil - Top of UHS Basin Walls - 5% Damping

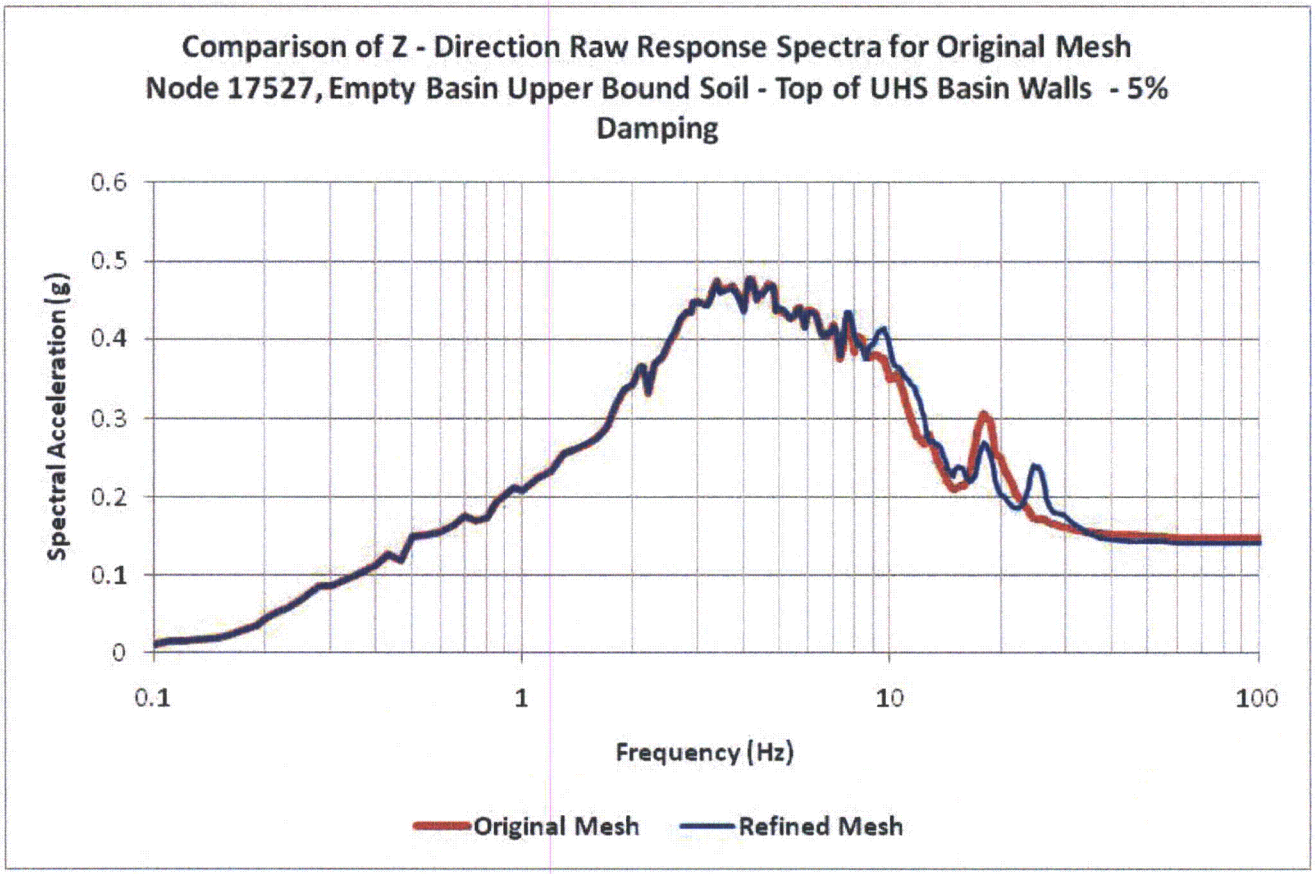

Figure 03.07.02-24.132: Comparison of Z - Direction Raw Response Spectra for Original Mesh Node 17527, Empty Basin Upper Bound Soil - Top of UHS Basin Walls - 5% Damping

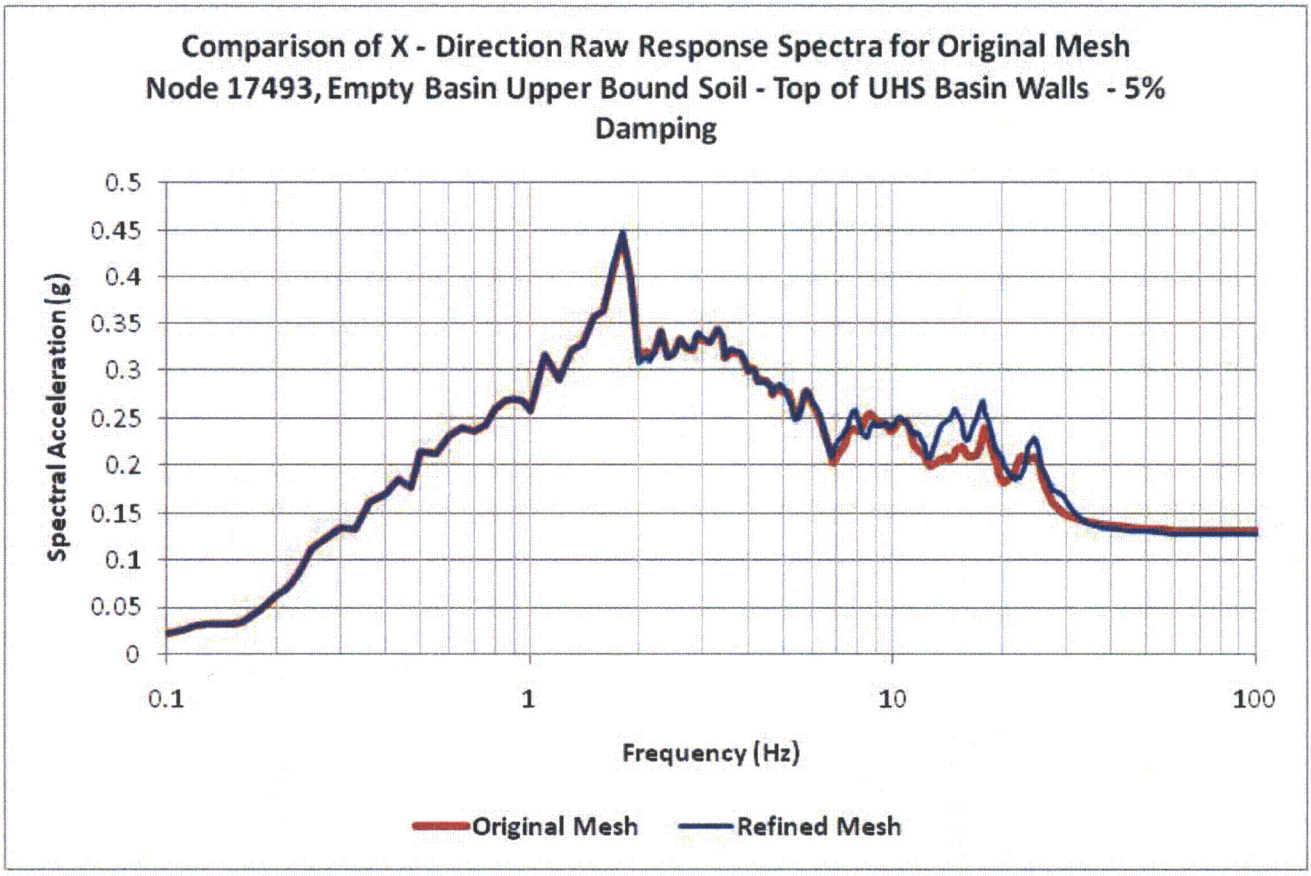

Figure 03.07.02-24.133: Comparison of X - Direction Raw Response Spectra for Original Mesh Node 17493, Empty Basin Upper Bound Soil - Top of UHS Basin Walls - 5% Damping

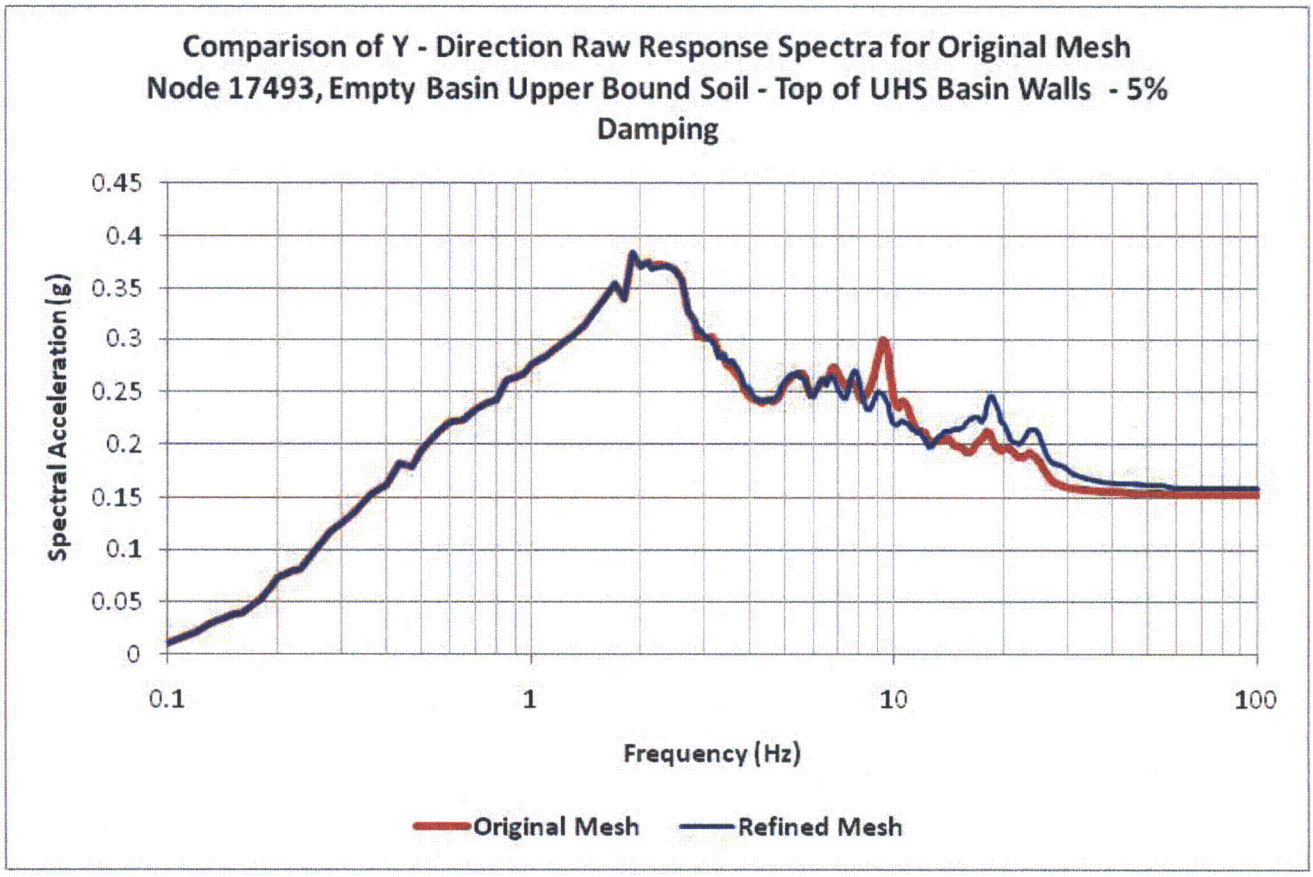

Figure 03.07.02-24.134: Comparison of Y - Direction Raw Response Spectra for Original Mesh Node 17493, Empty Basin Upper Bound Soil - Top of UHS Basin Walls - 5% Damping

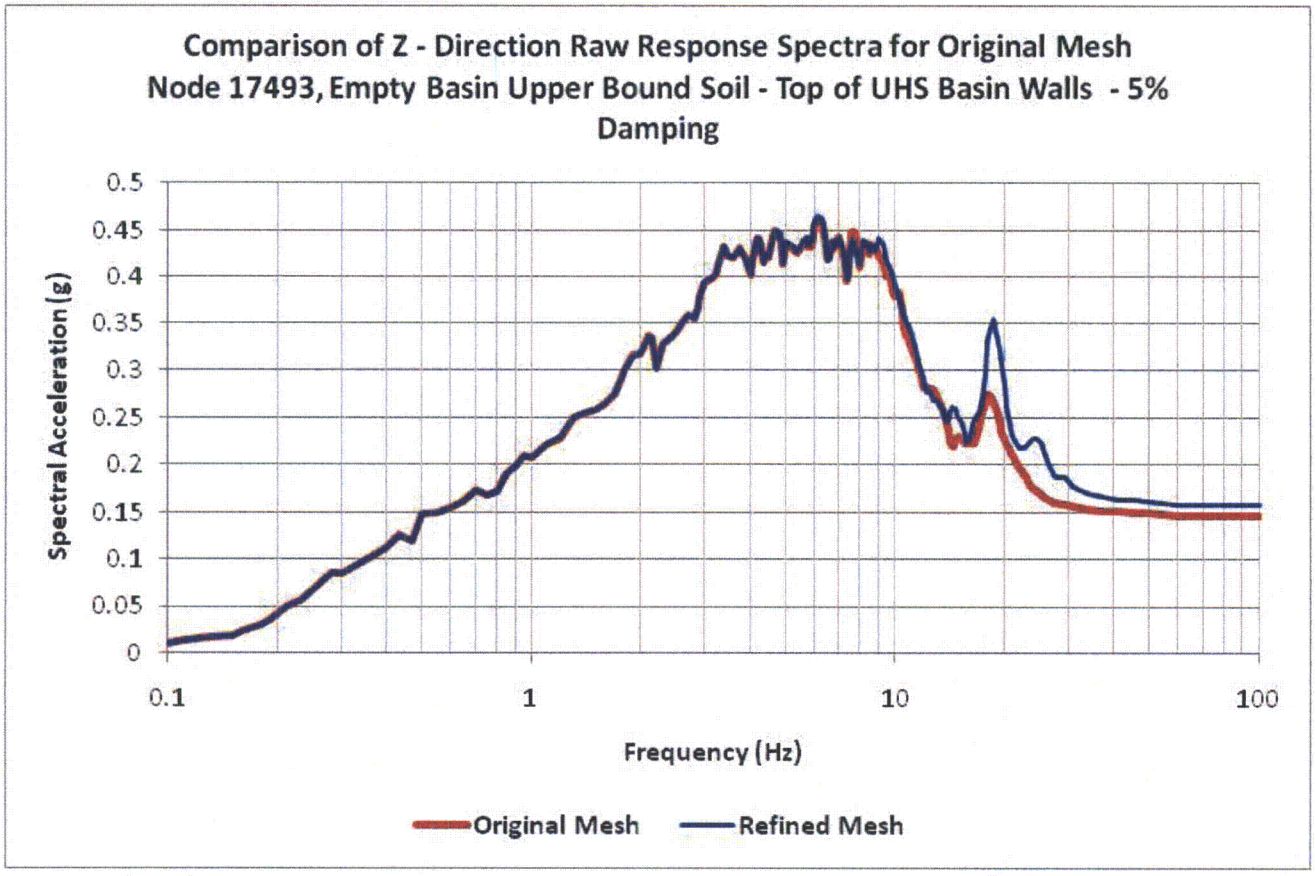

Figure 03.07.02-24.135: Comparison of Z - Direction Raw Response Spectra for Original Mesh Node 17493, Empty Basin Upper Bound Soil - Top of UHS Basin Walls - 5% Damping

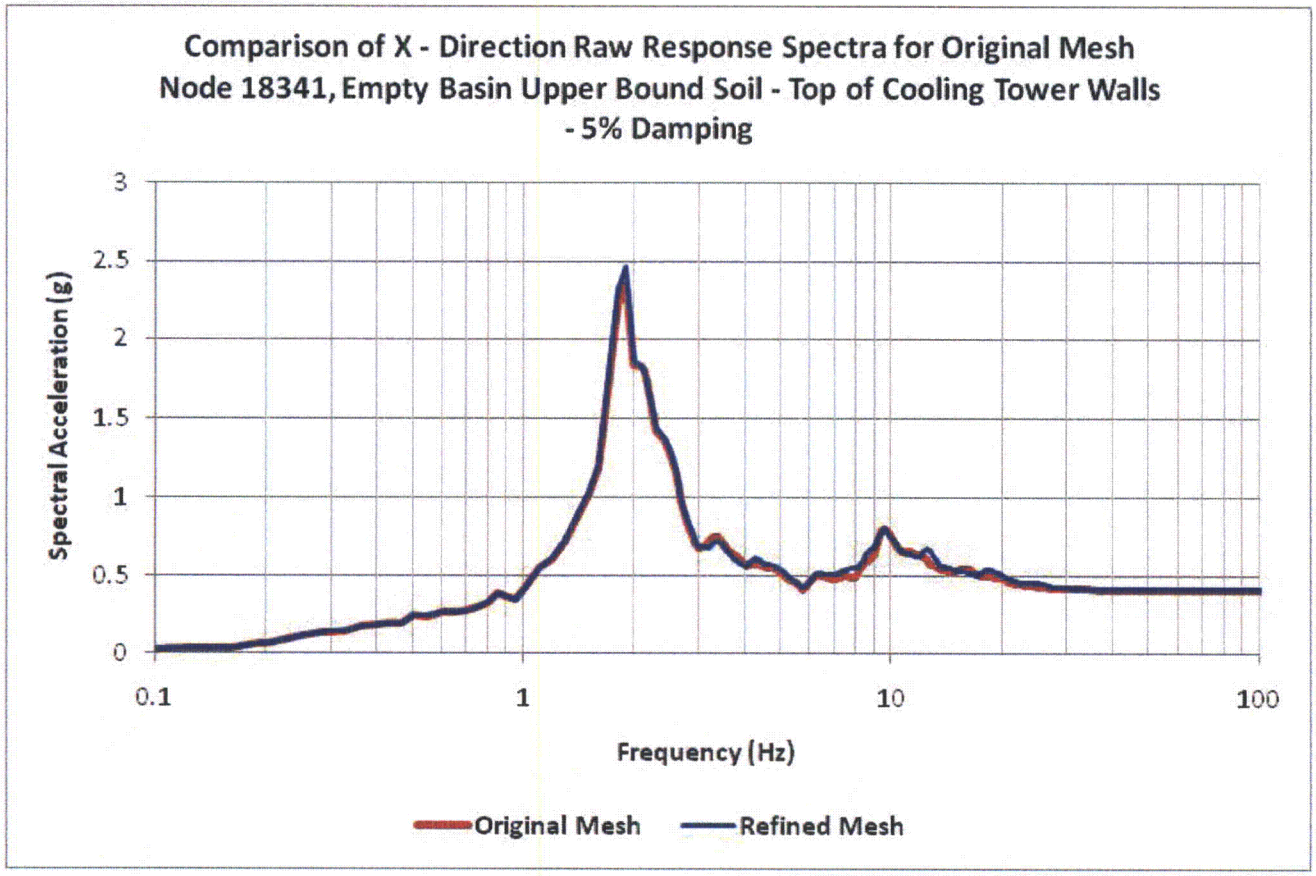

Figure 03.07.02-24.136: Comparison of X - Direction Raw Response Spectra for Original Mesh Node 18341, Empty Basin Upper Bound Soil - Top of Cooling Tower Walls - 5% Damping

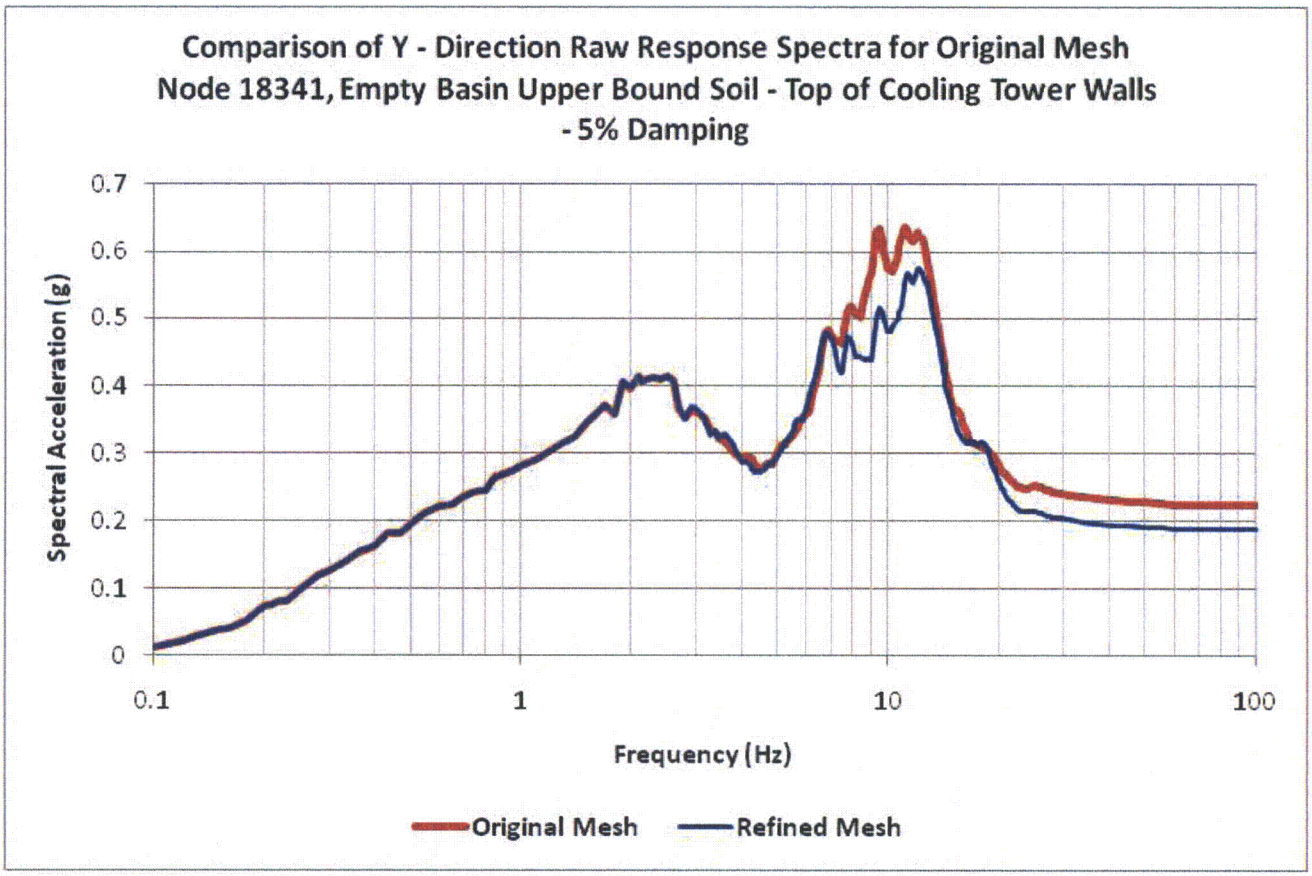

Figure 03.07.02-24.137: Comparison of Y - Direction Raw Response Spectra for Original Mesh Node 18341, Empty Basin Upper Bound Soil - Top of Cooling Tower Walls - 5% Damping

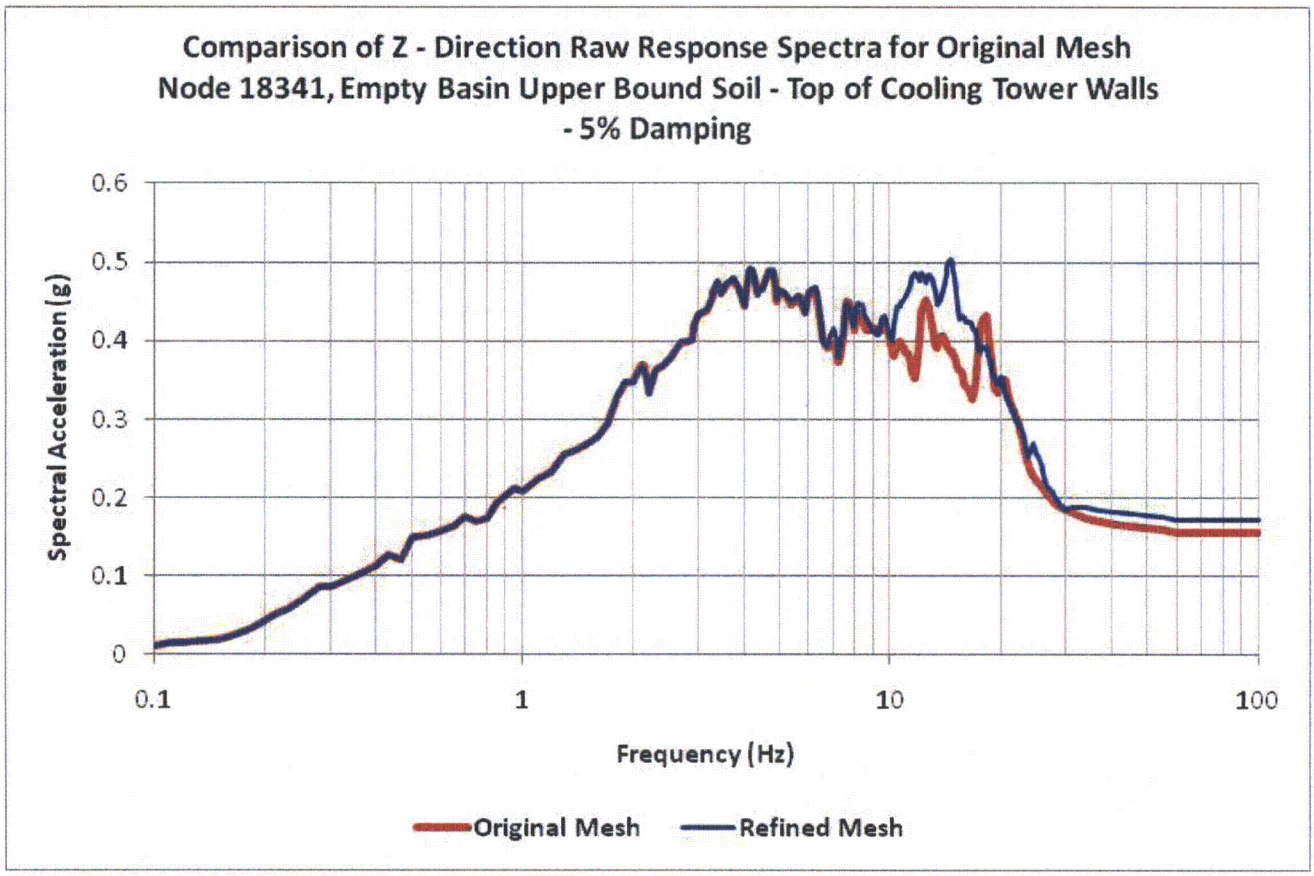

Figure 03.07.02-24.138: Comparison of Z - Direction Raw Response Spectra for Original Mesh Node 18341, Empty Basin Upper Bound Soil - Top of Cooling Tower Walls - 5% Damping

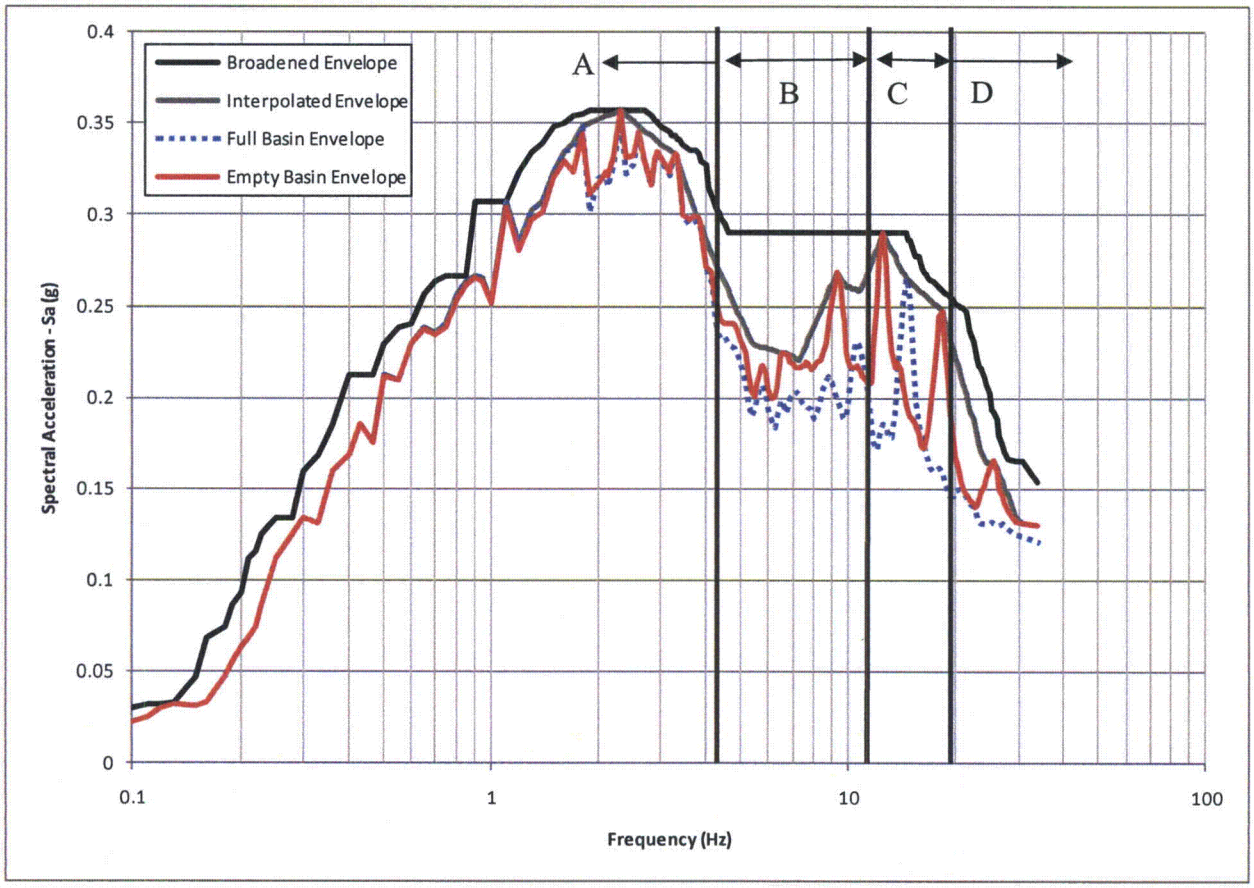

Figure 03.07.02-24.139a: Scaled X Direction Response Spectra at Node 10015 - PH Operating Floor Demonstrating the Behavior of the Compensation for Intermediate Data Sets Feature.

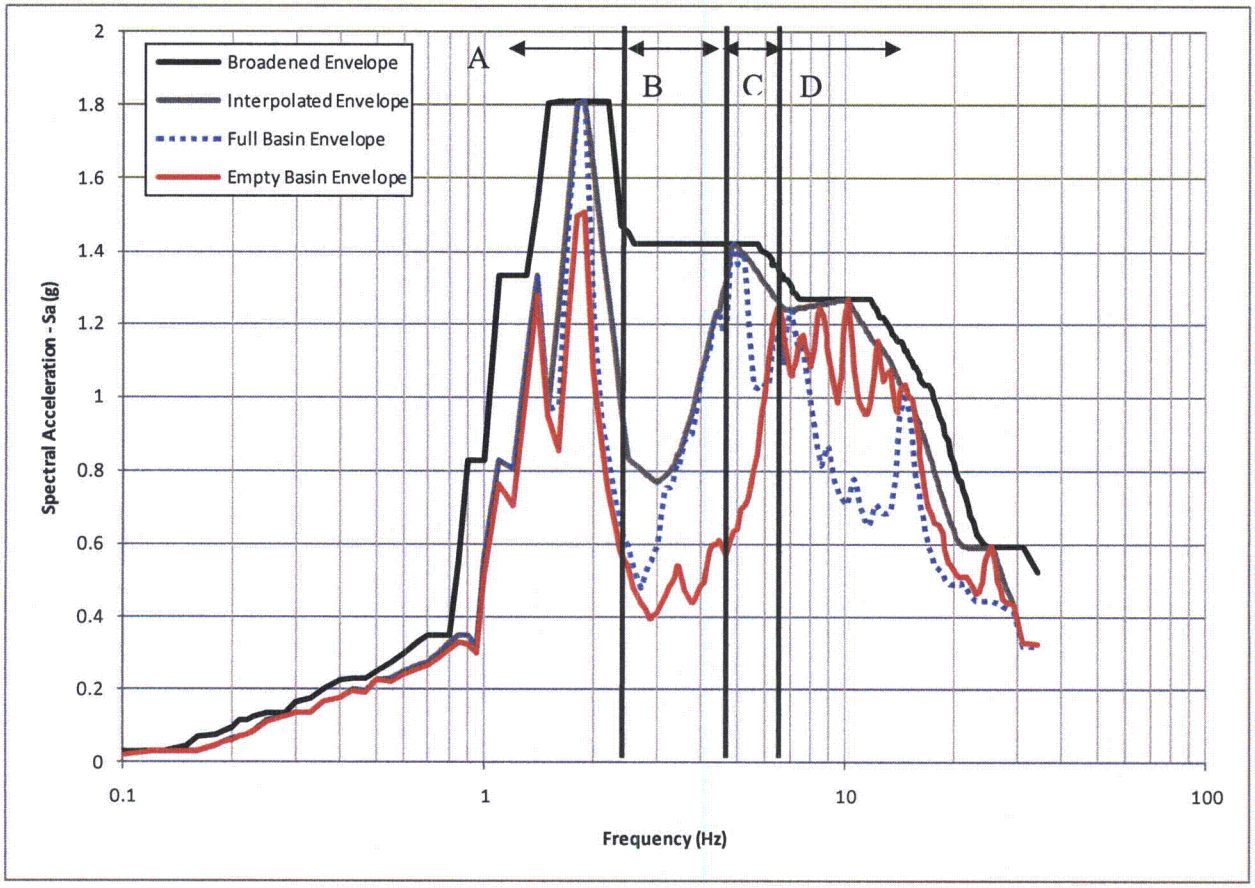

Figure 03.07.02-24.139b: Scaled X Direction Response Spectra at Node group6 - Mid-level of UHS Basin Walls

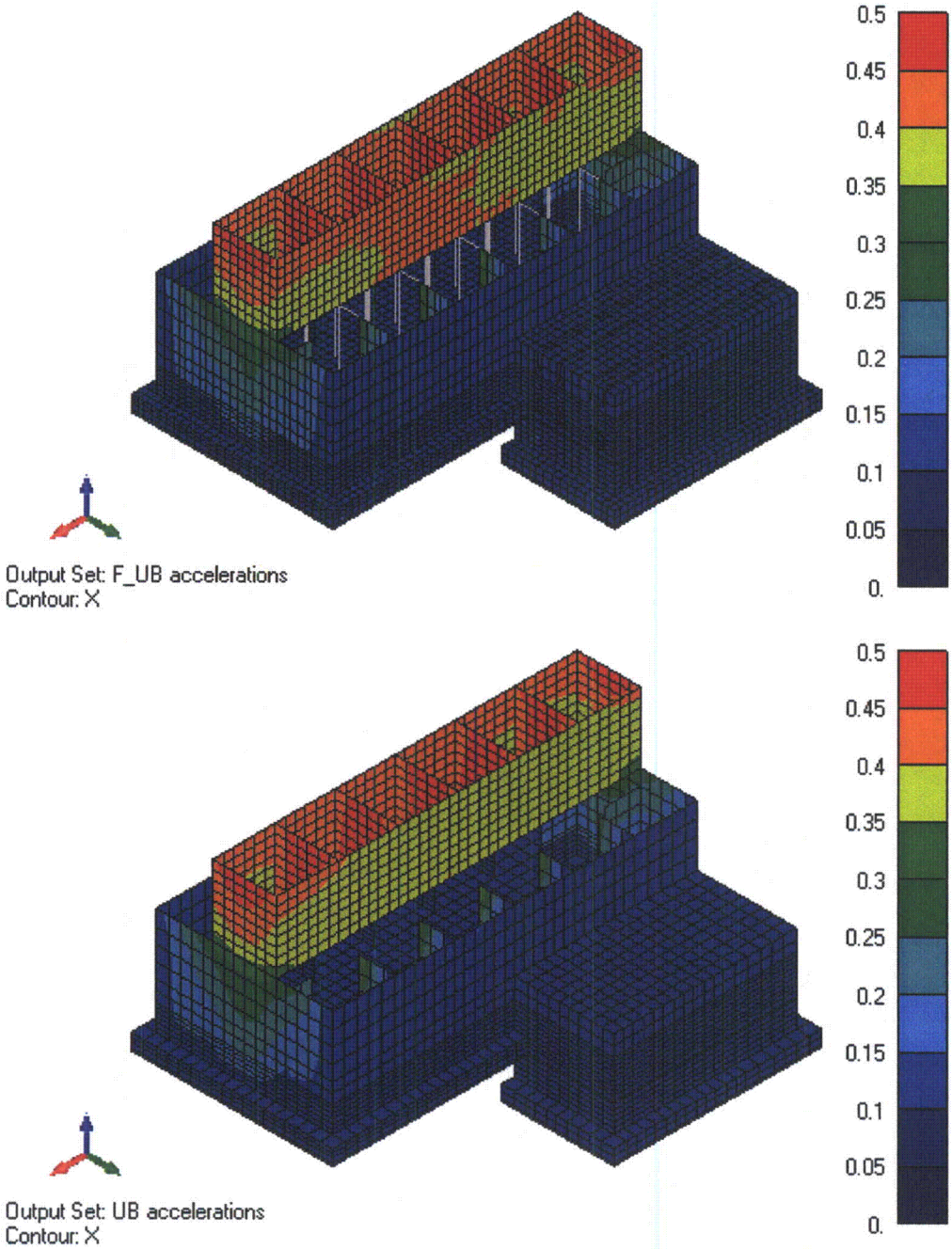

Figure 03.07.02-24.140: Acceleration contour plots of Refined Mesh Model (top) and Original Mesh Model (bottom) for X-Direction accelerations from Full Basin Upper Bound Soil Case.

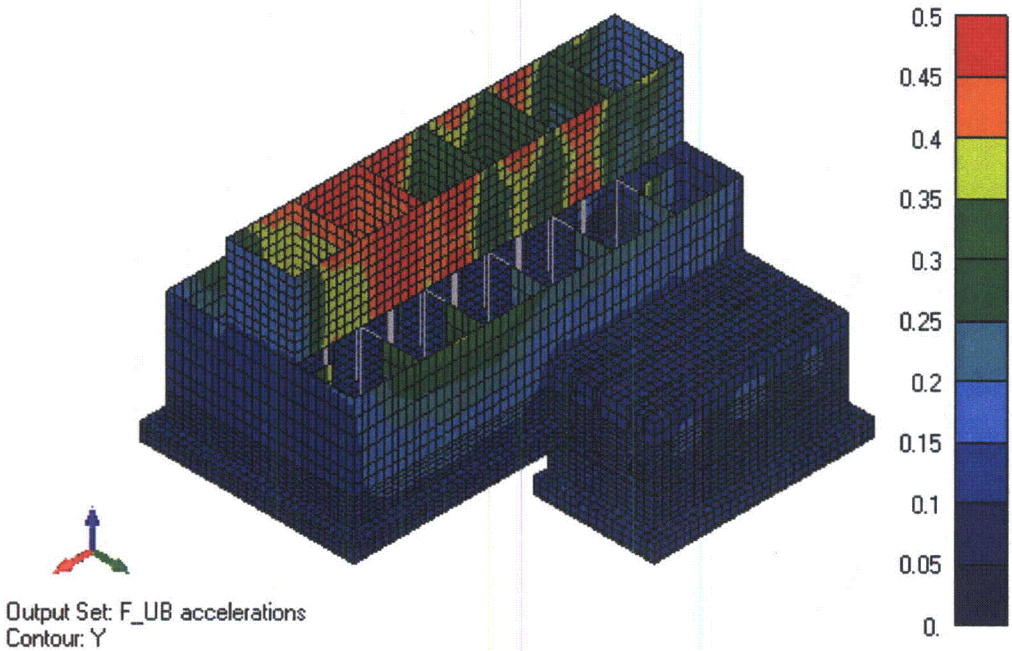

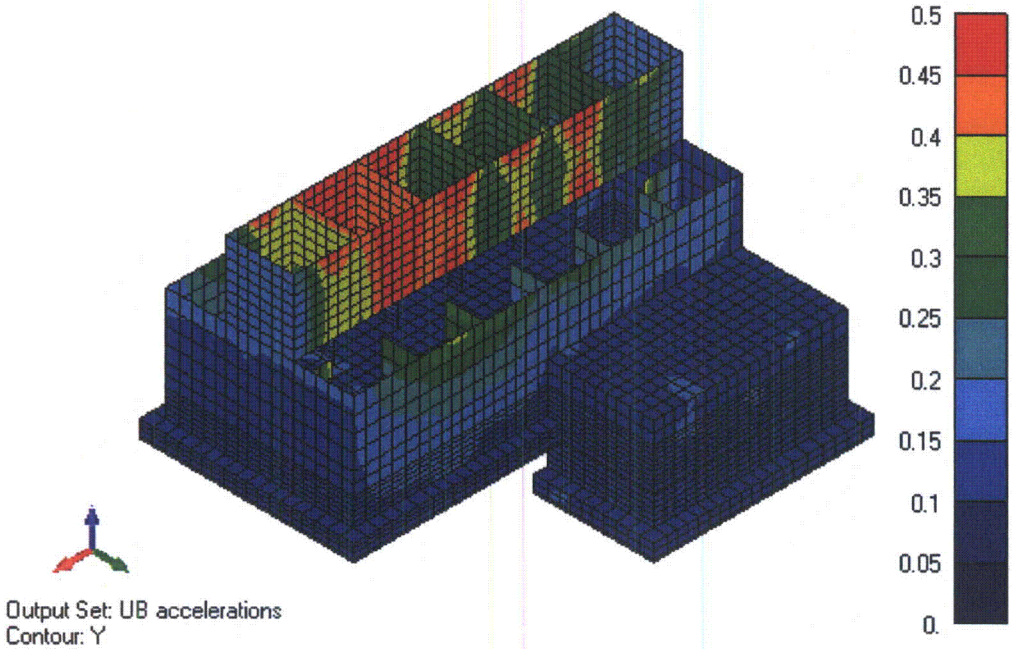

Figure 03.07.02-24.141: Acceleration contour plots of Refined Mesh Model (top) and Original Mesh Model (bottom) for Y-Direction accelerations from Full Basin Upper Bound Soil Case.

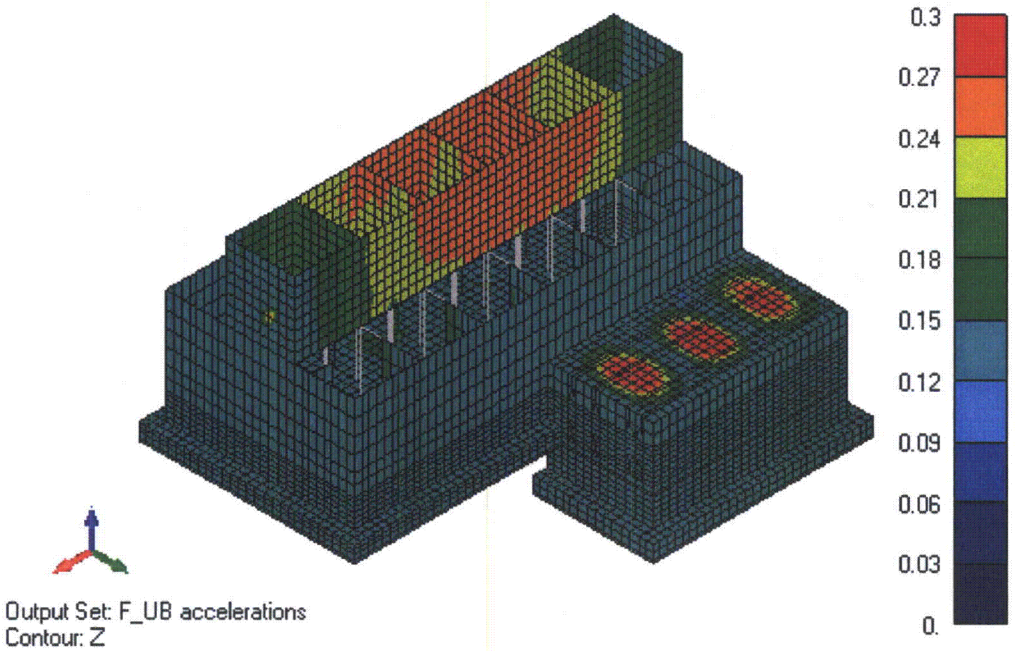

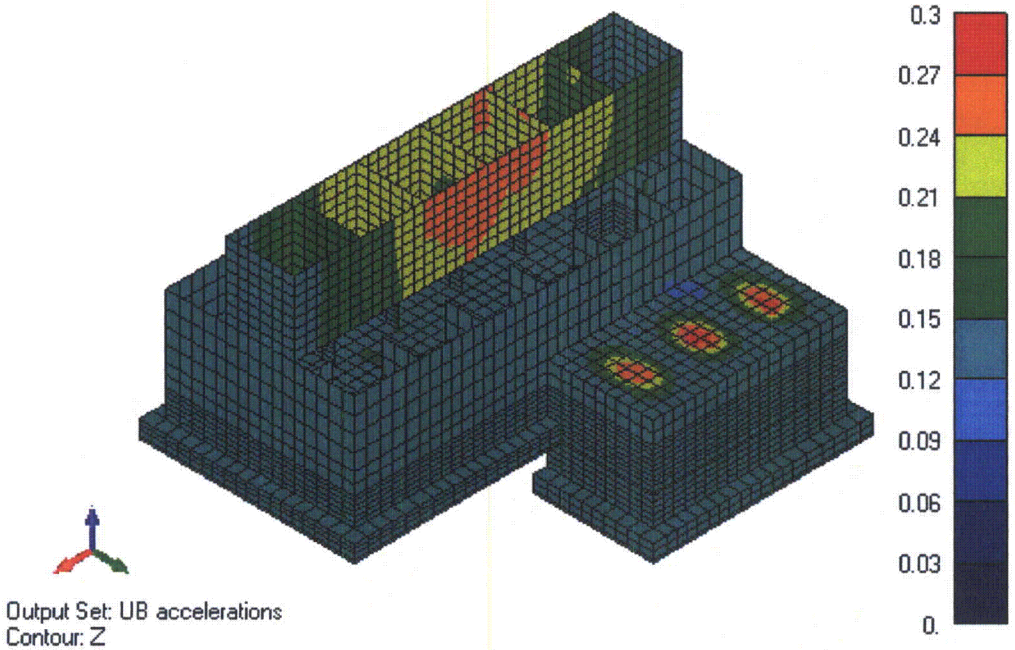

Figure 03.07.02-24.142: Acceleration contour plots of Refined Mesh Model (top) and Original Mesh Model (bottom) for Z-Direction accelerations from Full Basin Upper Bound Soil Case.

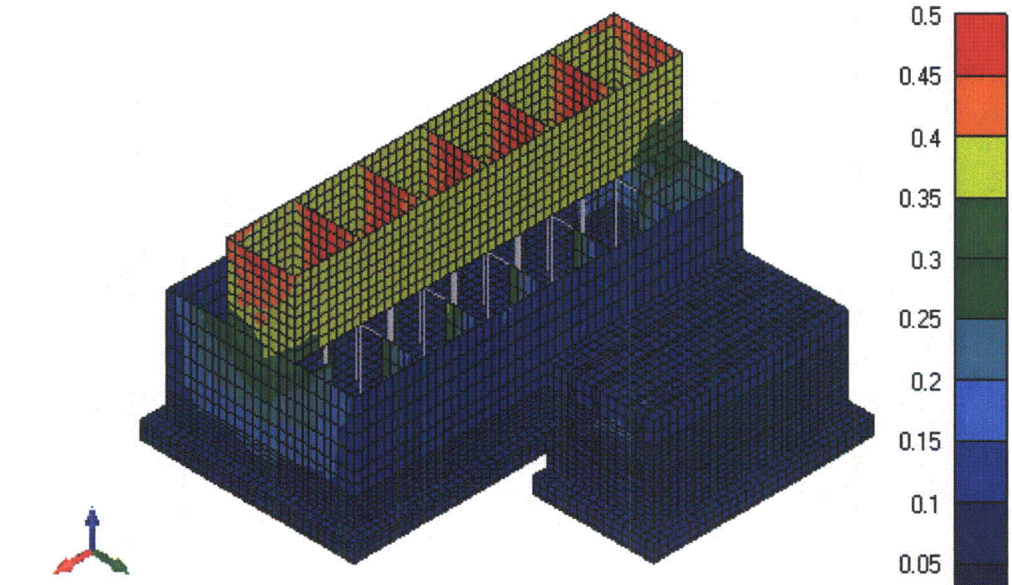

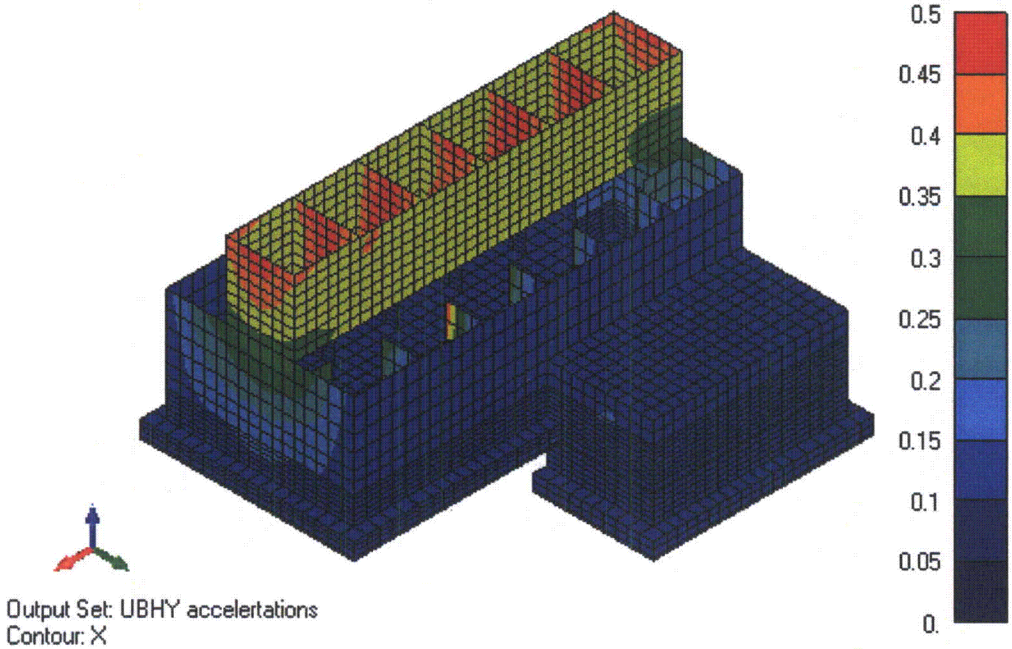

Figure 03.07.02-24.143: Acceleration contour plots of Refined Mesh Model (top) and Original Mesh Model (bottom) for X-Direction accelerations from Empty Basin Upper Bound Soil Case.

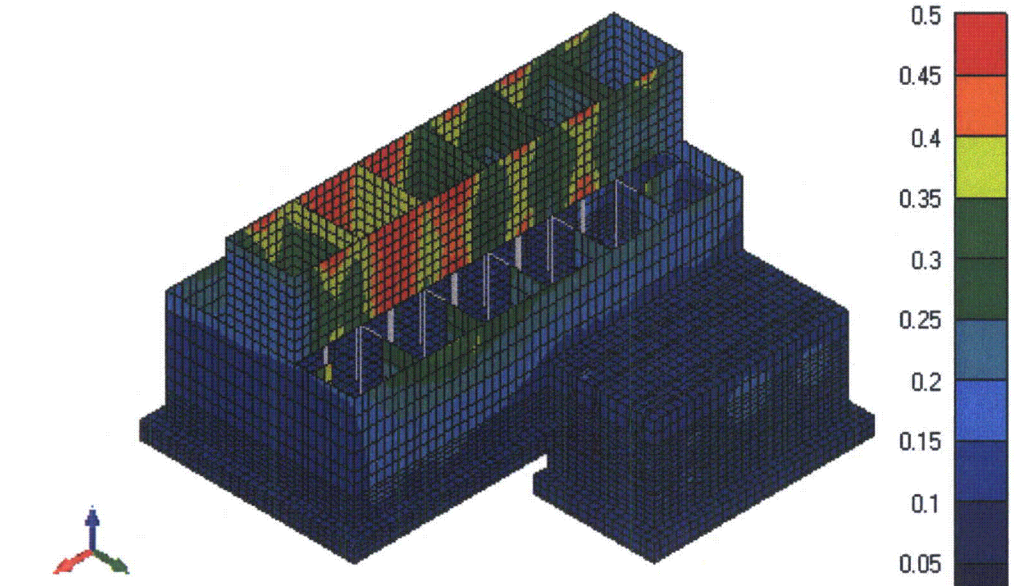

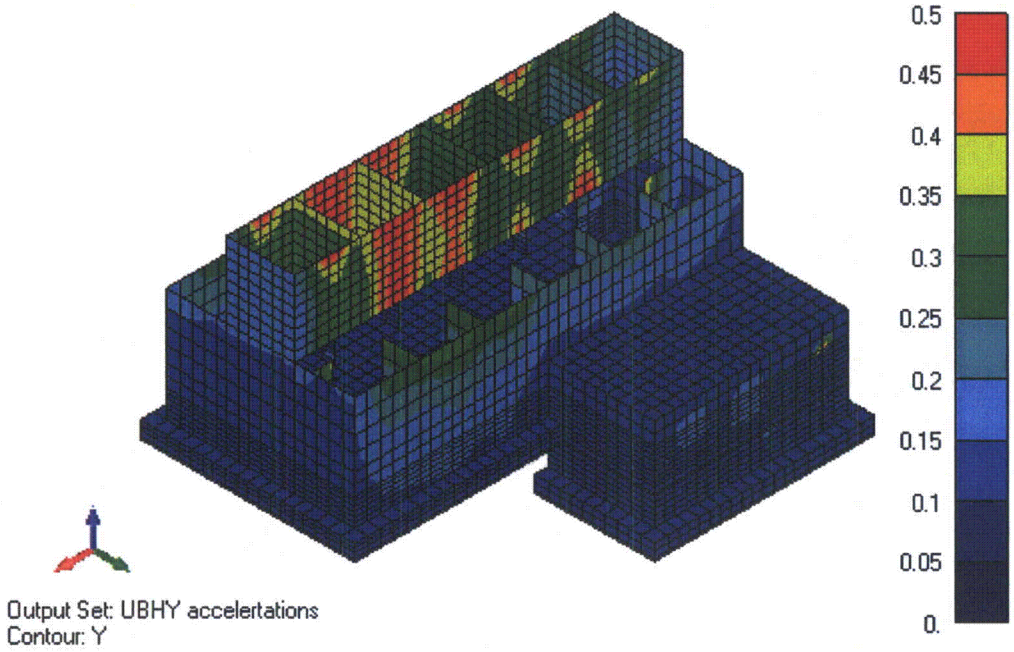

Figure 03.07.02-24.144: Acceleration contour plots of Refined Mesh Model (top) and Original Mesh Model (bottom) for Y-Direction accelerations from Empty Basin Upper Bound Soil Case.

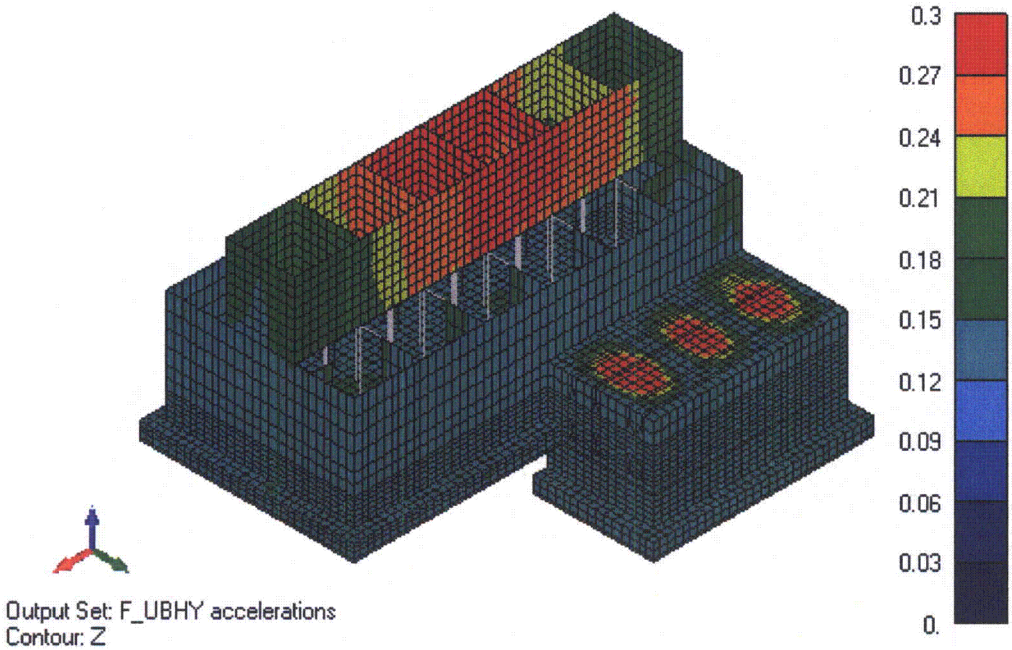

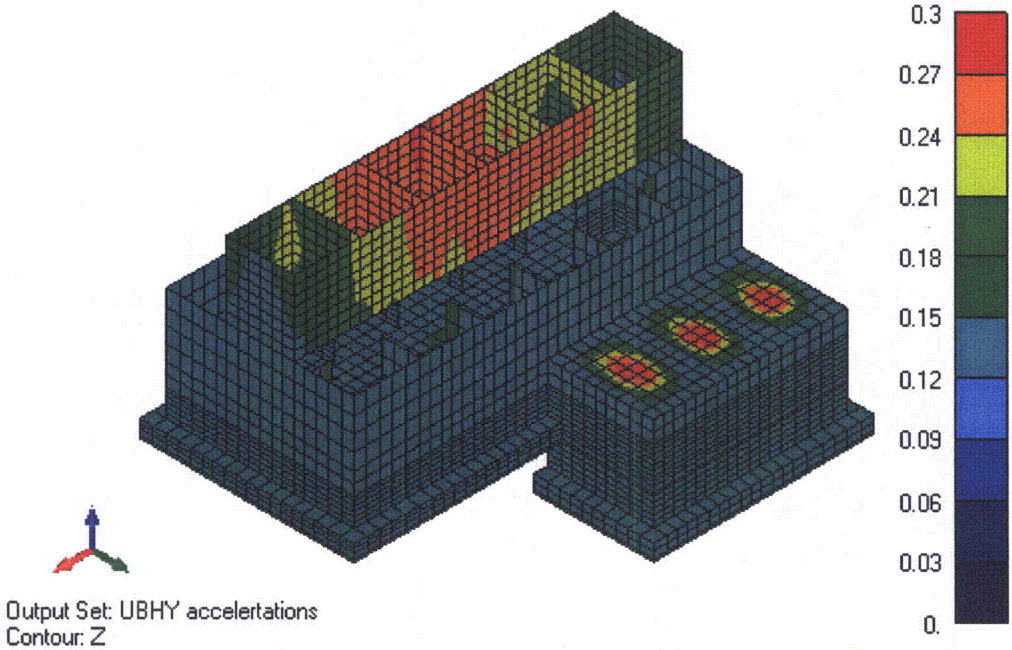

Figure 03.07.02-24.145: Acceleration contour plots of Refined Mesh Model (top) and Original Mesh Model (bottom) for Z-Direction accelerations from Empty Basin Upper Bound Soil Case.

Enclosure 1
Revision to COLA Section 3H.6

3H.6.5.1.2 Percentage of Critical Damping Values

The percentages of critical damping values considered in the seismic analysis for site- specific seismic Category I structures and associated systems and components are the same as listed in DCD Table 3.7-1. The damping values are the same as in Regulatory Guides 1.61 and 1.84, except for the cable trays and conduits, as explained in DCD Section 3.7.1.3. In all cases the OBE level structural damping values, as given in Regulatory Guide 1.61, were used for the generation of in-structure response spectra (ISRS) except for the cracked concrete case where SSE level structural damping was used.

3H.6.5.2.3 Procedures for Analytical Modeling

The seismic analysis of the UHS basin and enclosed cooling tower as well as RSW pump house for each unit was performed using a three-dimensional finite element model presented in Figure 3H.6-40. The material properties for concrete elements of the model are presented in Section 3H.6.4.4.1. Uncracked concrete section was used for member stiffness. Another case with cracked concrete section properties was analyzed. The section modulus of the cracked concrete was based on 50% of the uncracked section modulus. For structural steel elements the Young's Modulus of $29x10^6$ psi and Poisson's ratio of 0.3 was used. The model consists primarily of plate elements that represent the reinforced concrete walls, buttresses, and foundation as well as the walls and slabs of the basin, cooling towers, and pump house. Beam elements were used to represent concrete columns and beams. Finally, solid elements were used to represent the basin and pump houses house basemat. The floor and wall flexibility was modeled in the finite element model. The structural model mesh size is detailed enough to model the principal features of the structure and transmit frequencies of at least 33 Hz. The analysis was performed in the frequency domain as described in DCD Appendix 3A. The input time histories were defined at a time step of 0.005 seconds. The same time step was used for generation of the in-structure response spectra.

3H.6.5.2.4 Soil-Structure Interaction

The following describes the soil-structure-interaction (SSI) analysis for the UHS/RSW Pump House.

~~Soil-structure interaction (SSI)~~ effects were accounted for by the use of the SASSI2000 computer program using subtraction method of analysis, in conjunction with time histories described in Subsection 3H.6.5.1.1.2 and the structural model described in Subsection 3H.6.5.2.3 and shown in Figure 3H.6-15. The input ground motion time histories described in Section 3H.6.5.1.1.2 were applied at the finished grade in the free field. SASSI2000 implicitly considers transmitting boundaries in the formulation of impedance calculation. SASSI2000 sub-structuring method was used and no boundary condition besides the standard SASSI2000 elastic half space at the bottom of the site soil layering was used. The SASSI2000

analysis addresses the embedment of the structure, groundwater effects, the layering of the soil, and variations of the strain-dependent soil properties. A separate SSI analysis for effects of side soil-wall separation during the seismic event was performed for mean in-situ soil profile using the method in Section 3.3.1.9 of ASCE 4-98. Results of this analysis were enveloped with other SSI analyses.

The strain-compatible soil shear wave velocity and damping values for the SSI analysis were obtained from the same site response analysis which was used to develop the GMRS, as described in Section 2.5S.2.5. The seismic site response analysis was conducted using P-SHAKE computer program, which also provided the strain- compatible soil properties for the SSI analysis. A set of mean strain-compatible shear wave velocity and damping profiles along with the associated standard deviations was calculated. The calculated mean properties and associated standard deviations were used to develop the best estimate (BE), upper bound (UB), and lower bound (LB) profiles. While the BE profile is the mean profile, the UB and LB profiles are the median +/- one standard deviation, respectively, maintaining the minimum variation of 1.5 on soil shear modulus, per the guidance provided in SRP 3.7.2. The corresponding compression wave velocity profiles were calculated using the shear wave velocity and the Poisson's ratio. The resulting strain-compatible properties for the three profiles, which were used in the SSI analysis, are presented in Table 3H.6-1. The soil layer thicknesses used in the SSI model were sufficiently small to transmit frequencies up to 33 Hz for mean soil properties in the vertical direction (i.e. SASSI2000 interaction nodes spacing in the vertical direction).

The layer thicknesses used for both in-situ soil and back fill soil, in the SSI model, were modified from those shown in Tables 3H.6-1 and 3H.6-2 to have thicknesses sufficiently small enough to conservatively transmit frequencies up to 33 Hz in the vertical direction for the corresponding mean soil properties. Tables 3H.6-1a, b, and c provide the actual layer thicknesses, along with the strain-compatible soil properties data and passing frequency values for the three in-situ soil profiles, i.e., mean, upper bound, and lower bound, respectively. Similar data for the backfill are provided in Tables 3H.6-2a, b, and c. The layer thicknesses, H, were computed using the following equation:

$$H = V_s / (5 * F_{t-s})$$

where V_s is the shear wave velocity and F_{t-s} is the transmittal frequency.

In the SSI model, the layer thicknesses used for the mean soil case were also used for the lower bound in-situ and back fill soil. Based on the above equation, the transmittal frequencies for the lower bound soil layers are 26 Hz or higher in the vertical direction. ASCE 4-98, Section 3.3.3.5 recommends that "The cutoff frequency may be taken as twice the highest dominant frequency of the coupled soil-structure system for the direction under consideration, but not less than 10 Hz." The dominant frequency of coupled soil- structure system has been calculated using the procedure recommended in ASCE 4-98, Section 3.3.3.5.

Based on this calculation the highest frequency of the coupled soil-structure system is less than 6 Hz. Thus, the cutoff frequency is required to be at least 12 Hz. The lower bound soil model's lowest transmittal frequency of 26 Hz is larger than the required 12 Hz, and therefore is acceptable.

3H.6.5.2.4.1 Soil-Structure Interaction Analysis for Empty UHS Basin

Section 3H.6.5.2.4 describes the SSI analysis for the full UHS basin case. An additional SSI analysis was performed for the empty UHS basin case. This analysis uses the same model and methodology as the analysis described in Section 3H.6.5.2.4 except that analyses for mean and lower bound backfill soil cases were excluded because their properties are bounded by the lower and upper bound in-situ soil cases. Also Poisson's ratio limit was set at 0.495 for calculation of compression wave velocity for soil layers below the ground water table. Results of this analysis and the analysis for the full basin case were enveloped.

3H.6.5.2.4.2 Additional Sensitivity Analysis for Refined Mesh

Additional SSI analyses were performed using a refined mesh for the soil and structural model. These analyses are described below.

Two additional UHS/RSW Pump House SSI analyses were performed for the upper bound soil profile case (UB soil case) considering both full and empty UHS basin, with a refined model shown in Figure 3H.6-15h.

The refined SSI model used for these analyses has the following passing frequency capability (passing frequency, $f = V_s / 5\,h$, where V_s is the shear wave velocity of the soil layer and h is the vertical or horizontal distance between the adjacent interaction nodes):

Vertical direction: 40.4 Hz
Horizontal direction: 23.5 Hz

For soil layers below groundwater level, the Poisson's ratio was capped at 0.495 for determining the compression wave velocity. A cut-off frequency of 33 Hz was used in these analyses for transfer function calculation.

The passing frequency of about 24 Hz in the horizontal direction was selected since the site has a deep soil profile and the SSI frequencies are below 6 Hz. Also, as noted in SRP 3.7.1 Revision 3, Appendix A, the energy content of the earthquake time histories above 24 Hz is inconsequential.

Based on the results of the above refined SSI analyses, and additional structural mesh sensitivity analyses, the following in-structure response spectra obtained from the SSI analyses described in Section 3H.6.5.2.4 and 3H.6.5.2.4.1 were modified by multiplying them with the modification factors shown in Table 3H.6.16. Then, the results of the full and empty basin analyses were enveloped.

- Vertical direction spectra at the center of the Pump House Roof
- Vertical direction spectra at the center of the Pump House Operating Floor
- Vertical direction spectra of the Cooling Tower Walls
- Out-of-plane horizontal spectra of the Basin Walls

The final in-structure response spectra are shown in Figures 3H.6-16 through 3H.6-39.

Table 3H.6-16: Response Spectra Modification Factors

Location	Direction	20% Damping		15% Damping		10% Damping		7% Damping		5% Damping	
		1-30 Hz	30-33 Hz	1-30 Hz	30-33 Hz	1-30 Hz	30-33 Hz	1-30 Hz	30-33 Hz	1-30 Hz	30-33 Hz
Pump House Roof	Vertical	1.444	1.331	1.495	1.346	1.577	1.372	1.629	1.409	1.667	1.463
Pump House Operating Floor	Vertical	1.223	1.190	1.243	1.194	1.294	1.198	1.362	1.202	1.469	1.204
Mid-Level of Basin Walls	Horizontal	1.310	1.113	1.338	1.110	1.404	1.112	1.461	1.117	1.458	1.129
CTSS Walls	Vertical	1.405	1.197	1.441	1.191	1.433	1.205	1.450	1.231	1.478	1.264

Location	Direction	4% Damping		3% Damping		2% Damping		1% Damping		0.5% Damping	
		1-30 Hz	30-33 Hz	1-30 Hz	30-33 Hz	1-30 Hz	30-33 Hz	1-30 Hz	30-33 Hz	1-30 Hz	30-33 Hz
Pump House Roof	Vertical	1.686	1.511	1.793	1.588	2.038	1.718	2.682	1.926	2.769	2.165
Pump House Operating Floor	Vertical	1.550	1.206	1.678	1.209	1.914	1.217	2.486	1.241	2.826	1.373
Mid-Level of Basin Walls	Horizontal	1.502	1.153	1.563	1.186	1.835	1.237	2.372	1.326	2.922	1.370
CTSS Walls	Vertical	1.540	1.289	1.585	1.321	1.749	1.364	1.966	1.418	2.593	1.574

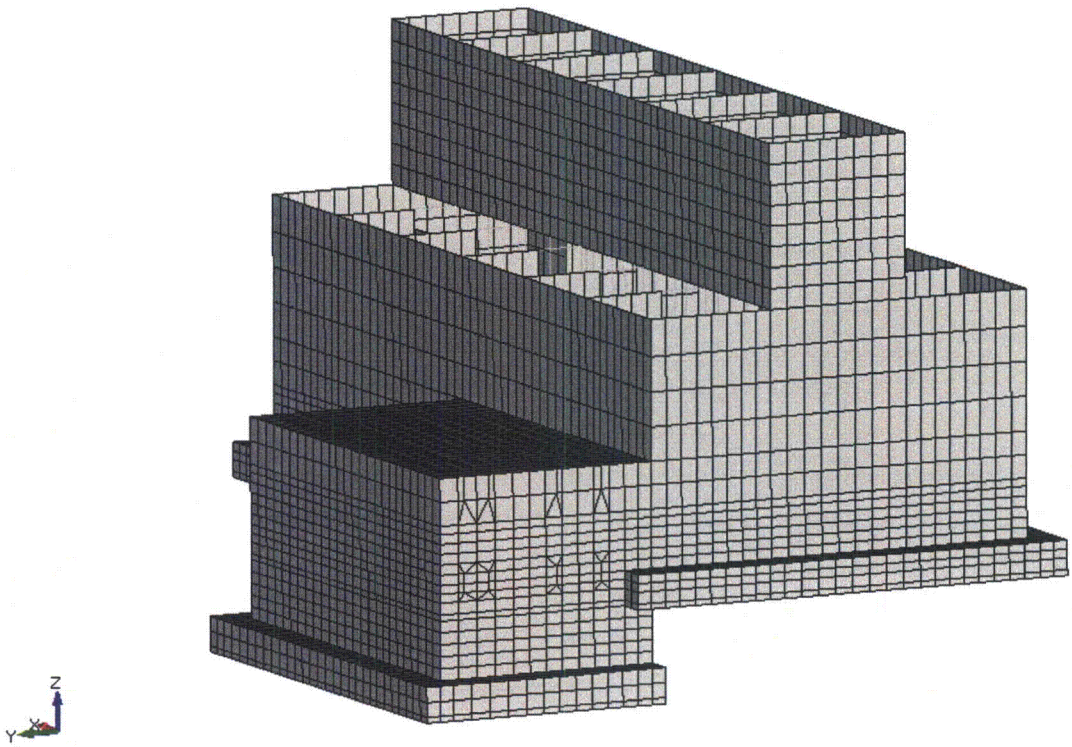

Figure 3H.6-15h: SSI Refined Mesh Model of UHS/RSW Pump House

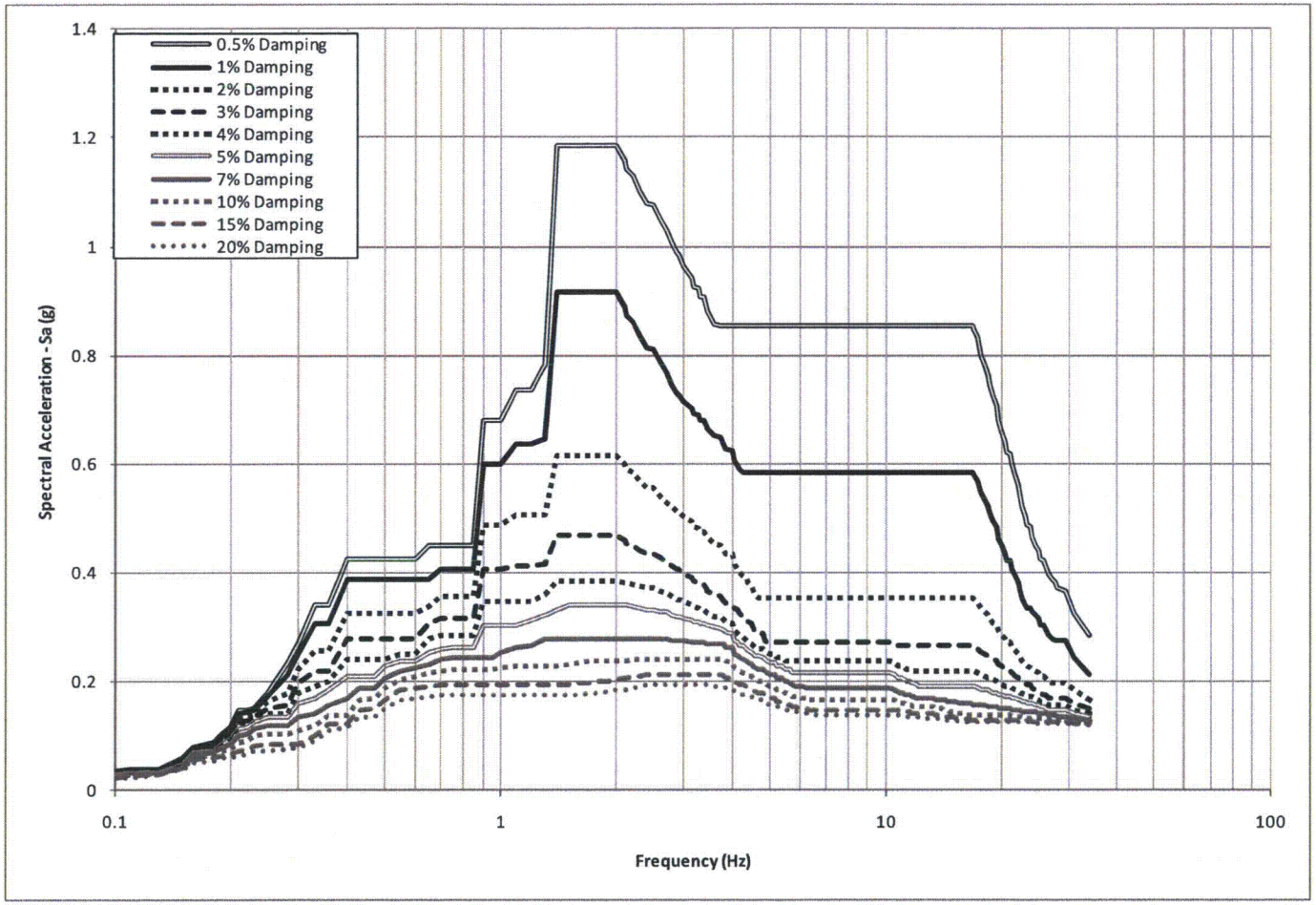

Figure 3H.6-16: Broadened FRS in E-W (X) Direction at the Top of RSW Pump House Mat (Elevation 18 ft MSL)

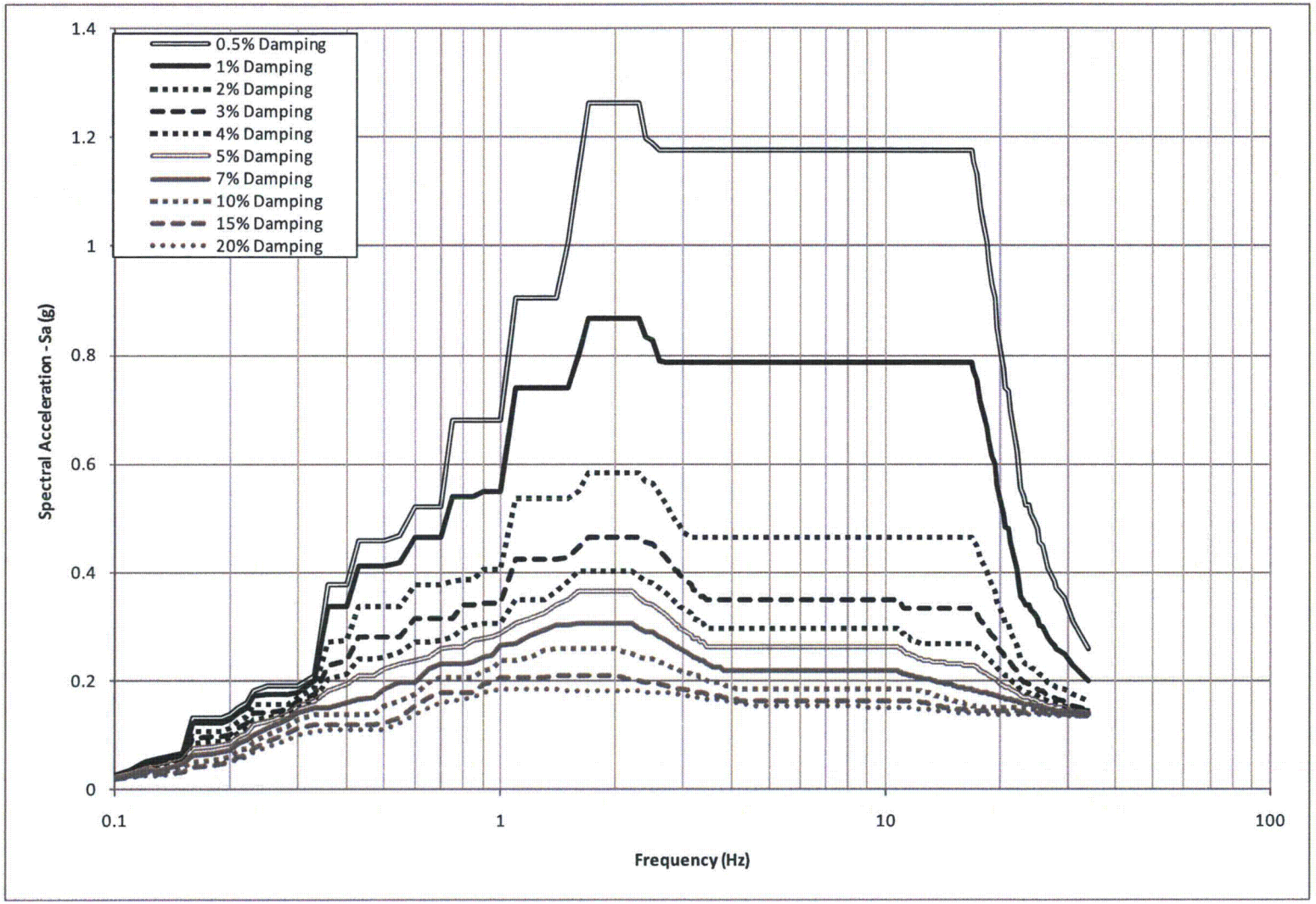

Figure 3H.6-17: Broadened FRS in N-S (Y) Direction at the Top of RSW Pump House Mat (Elevation 18 ft MSL)

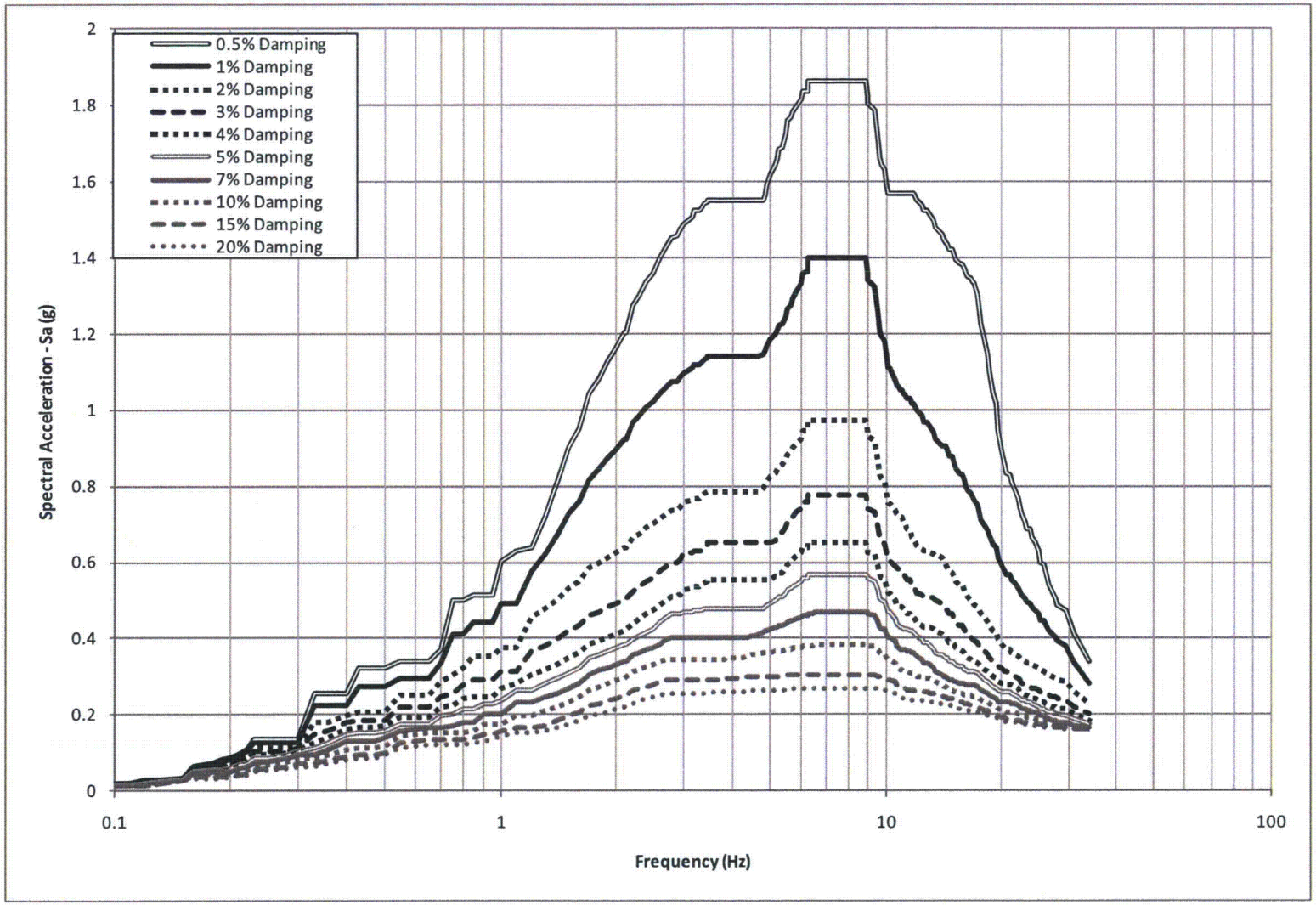

Figure 3H.6-18: Broadened FRS in Vertical (Z) Direction at the Top of RSW Pump House Mat (Elevation 18 ft MSL)

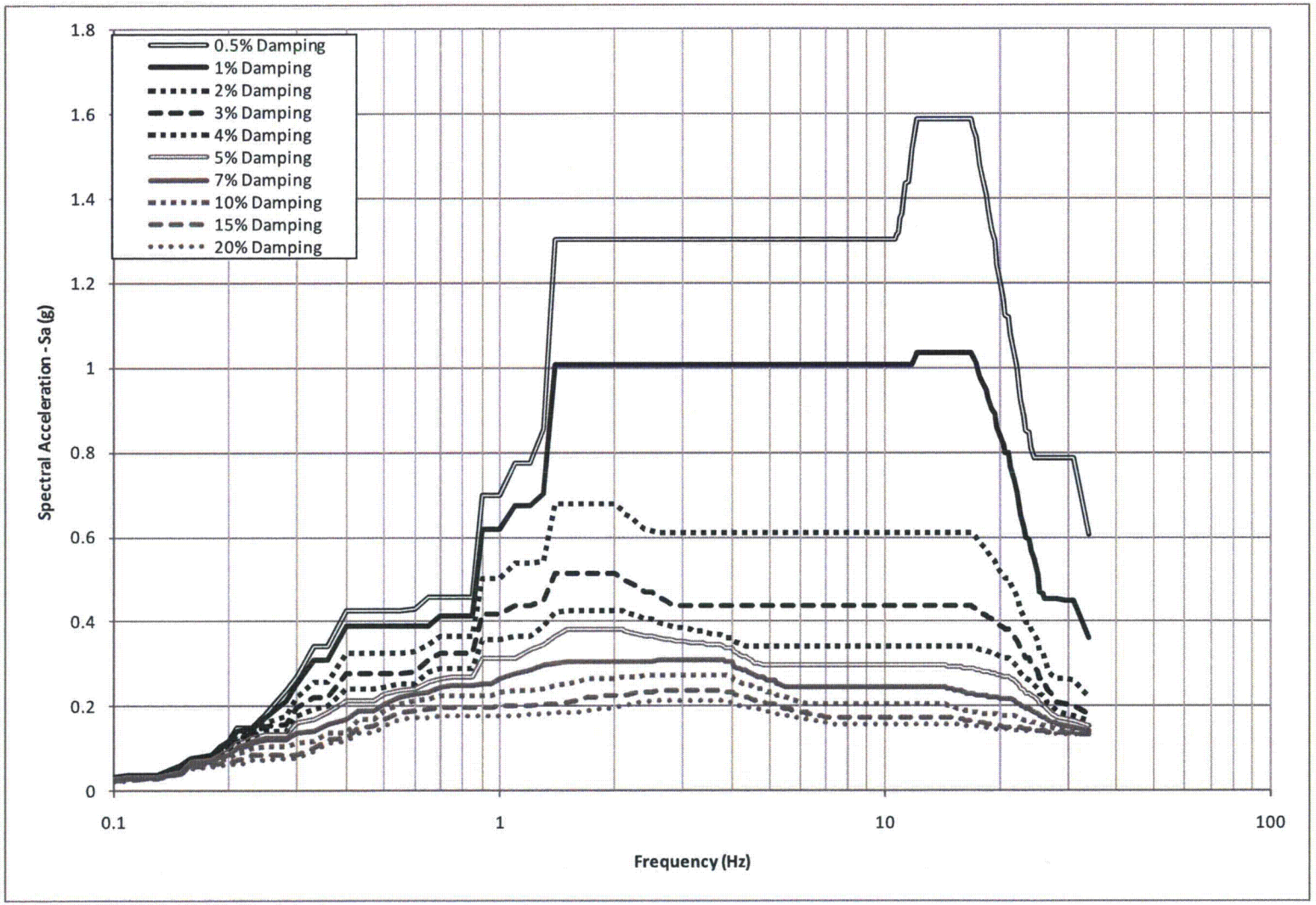

Figure 3H.6-19: Broadened FRS in E-W (X) Direction at the RSW Pump House Operating Floor (Elevation 14 ft MSL)

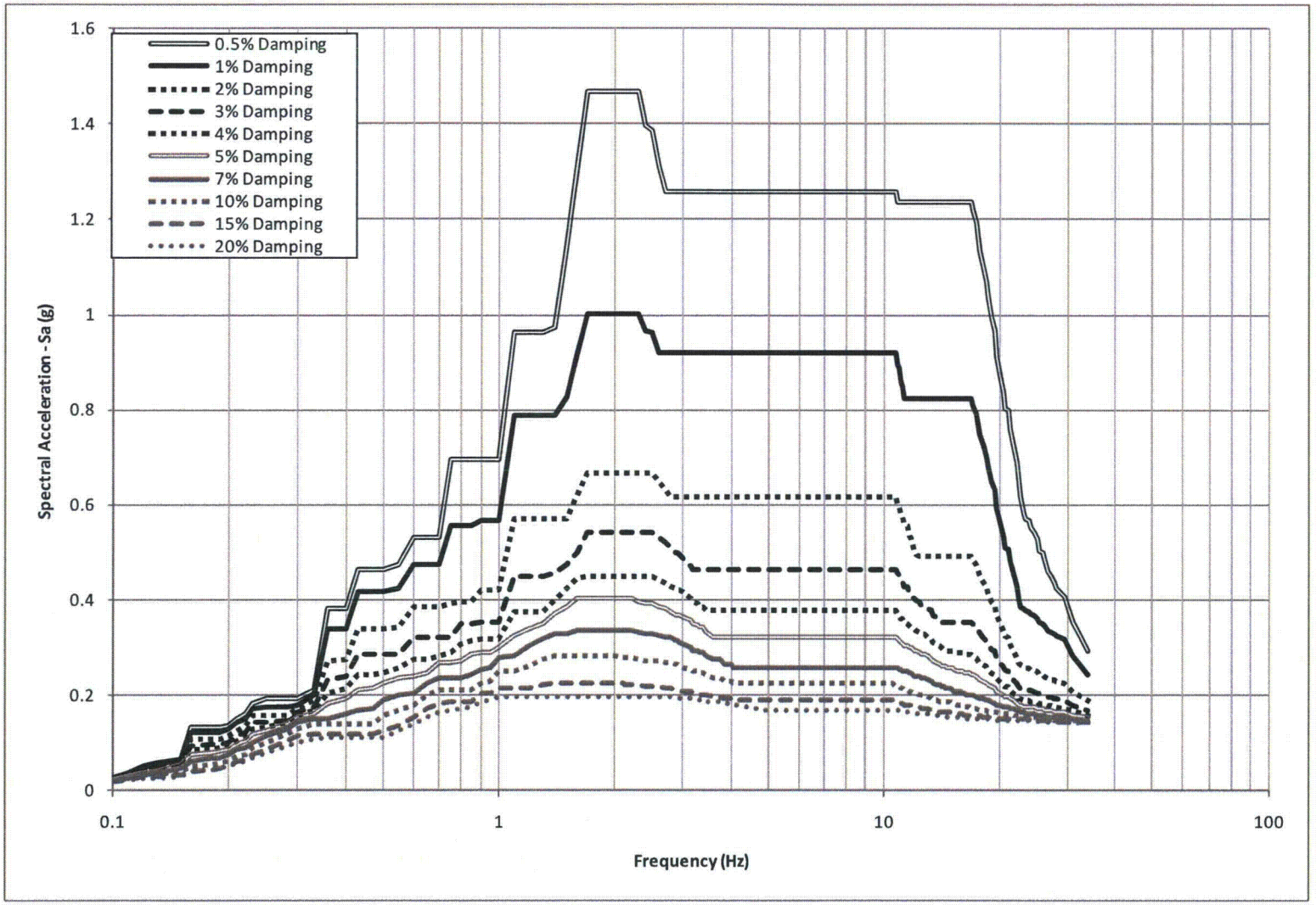

Figure 3H.6-20: Broadened FRS in N-S (Y) Direction at the RSW Pump House Operating Floor (Elevation 14 ft MSL)

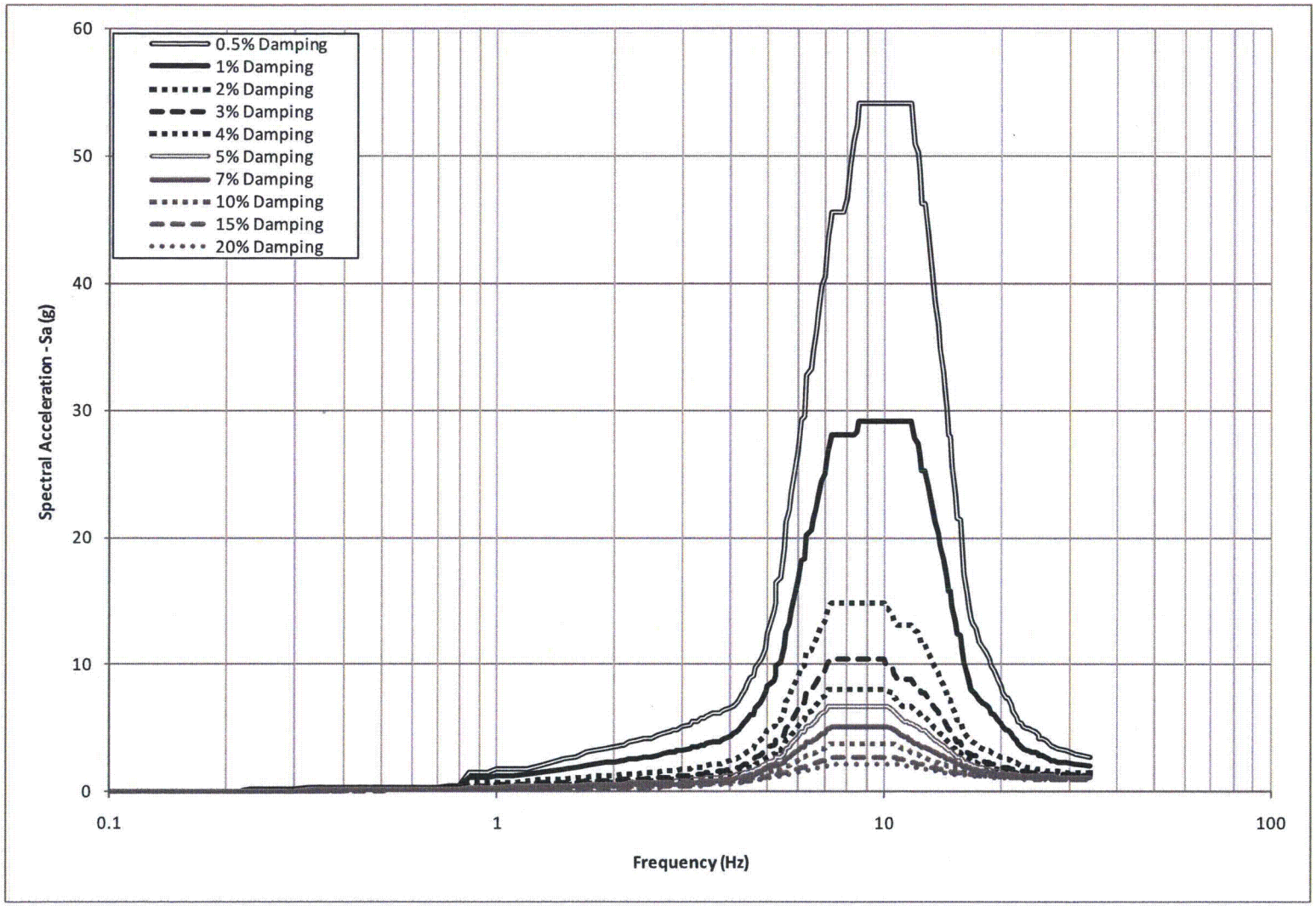

Figure 3H.6-21: Broadened FRS in Vertical (Z) Direction at the RSW Pump House Operating Floor (Elevation 14 ft MSL)

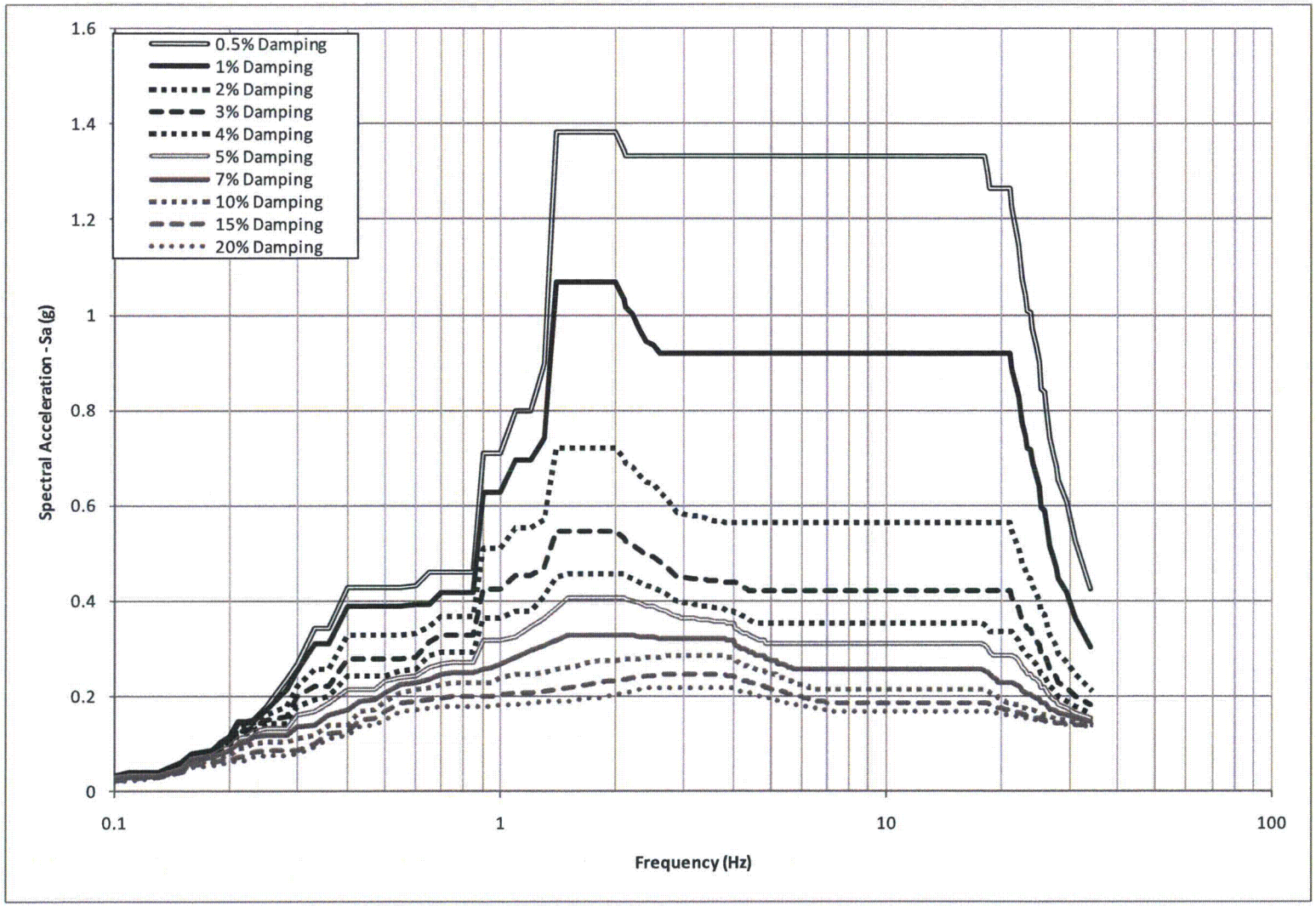

Figure 3H.6-22: Broadened FRS in E-W (X) Direction at the RSW Pump House Roof (Elevation 50 ft MSL)

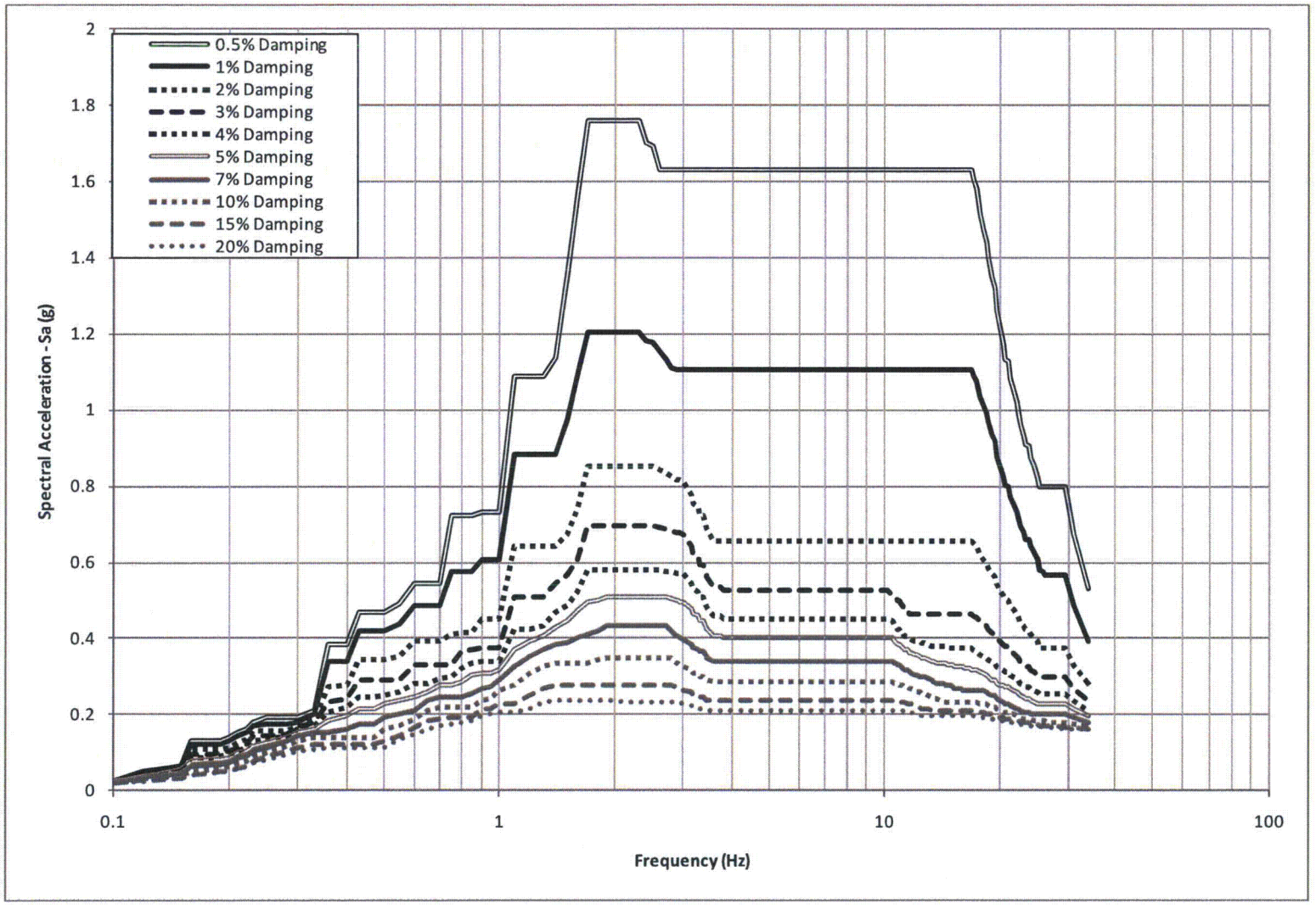

Figure 3H.6-23: Broadened FRS in N-S (Y) Direction at the RSW Pump House Roof (Elevation 50 ft MSL)

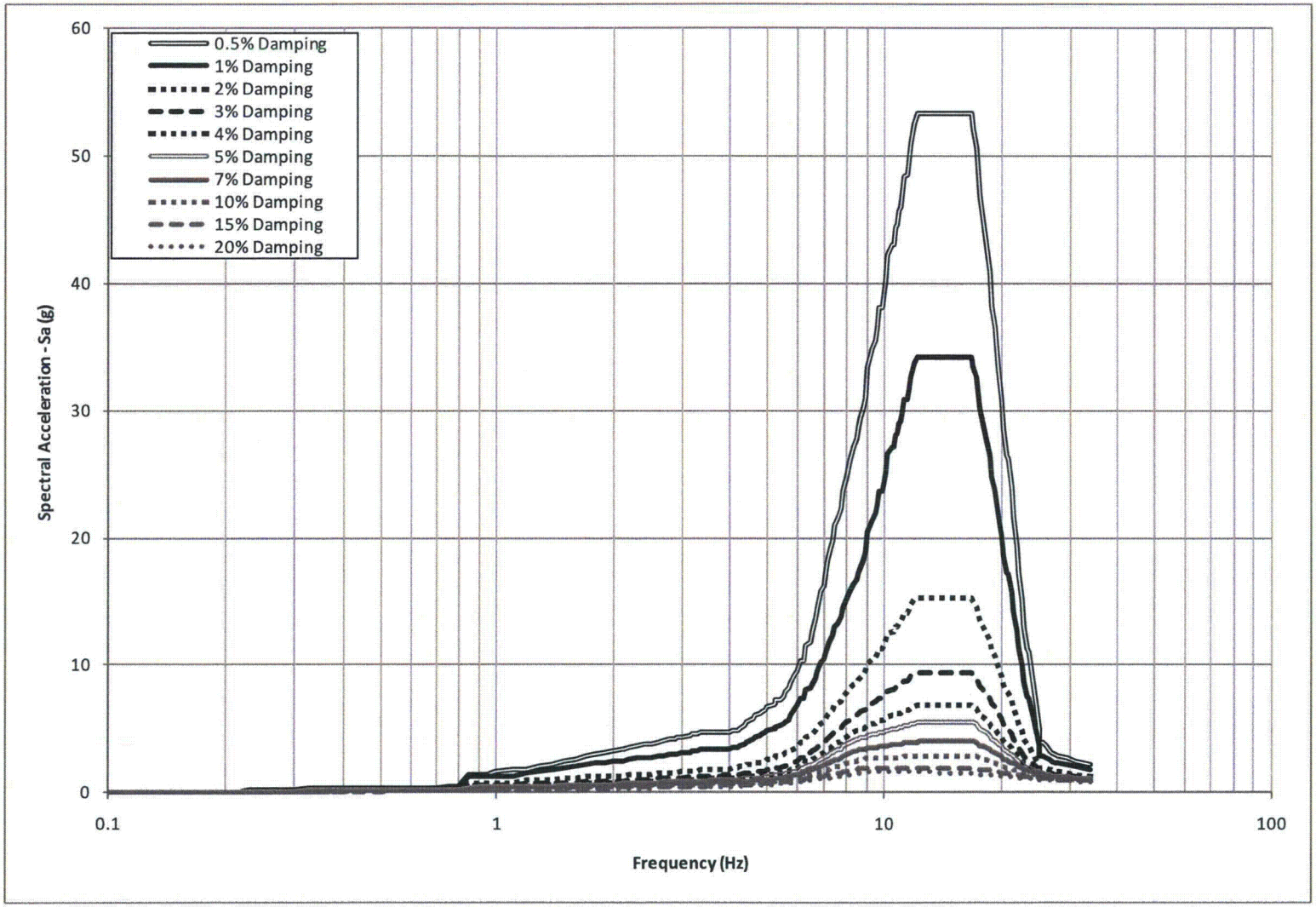

Figure 3H.6-24: Broadened FRS in Vertical (Z) Direction at the RSW Pump House Roof (Elevation 50 ft MSL)

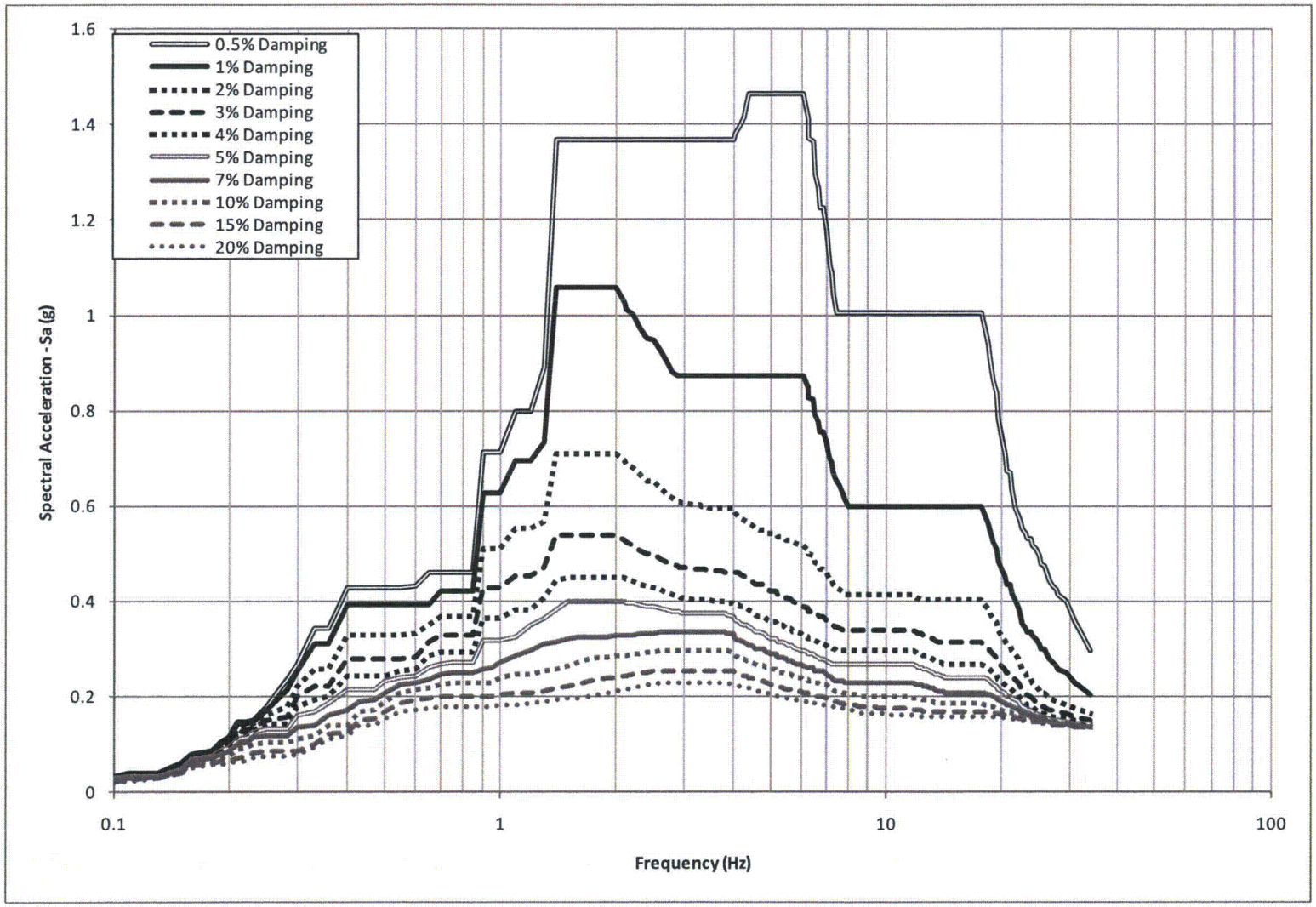

Figure 3H.6-25: Broadened FRS in E-W (X) Direction at the Top of UHS Basin Mat (Elevation 14 ft MSL)

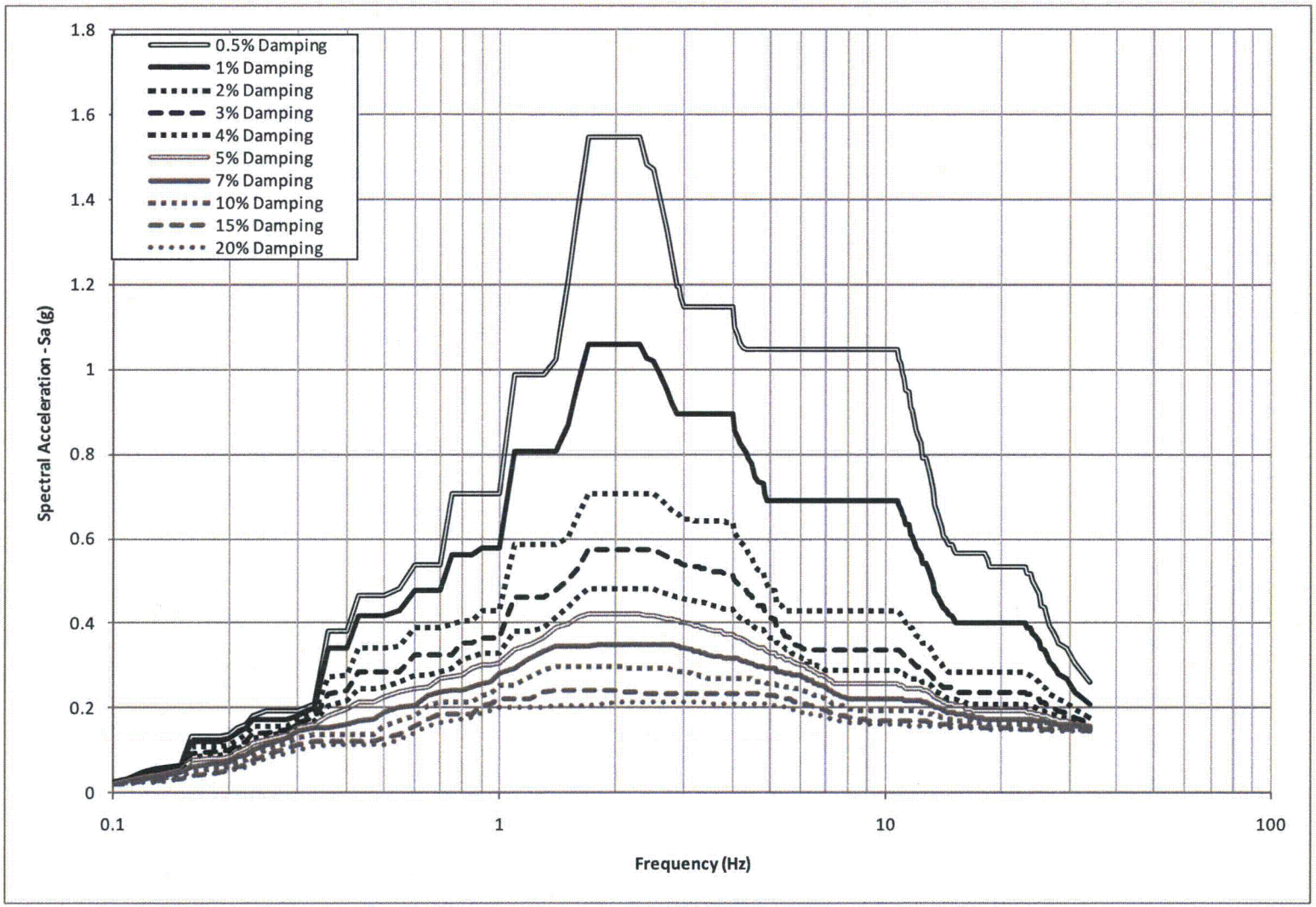

Figure 3H.6-26: Broadened FRS in N-S (Y) Direction at the Top of UHS Basin Mat (Elevation 14 ft MSL)

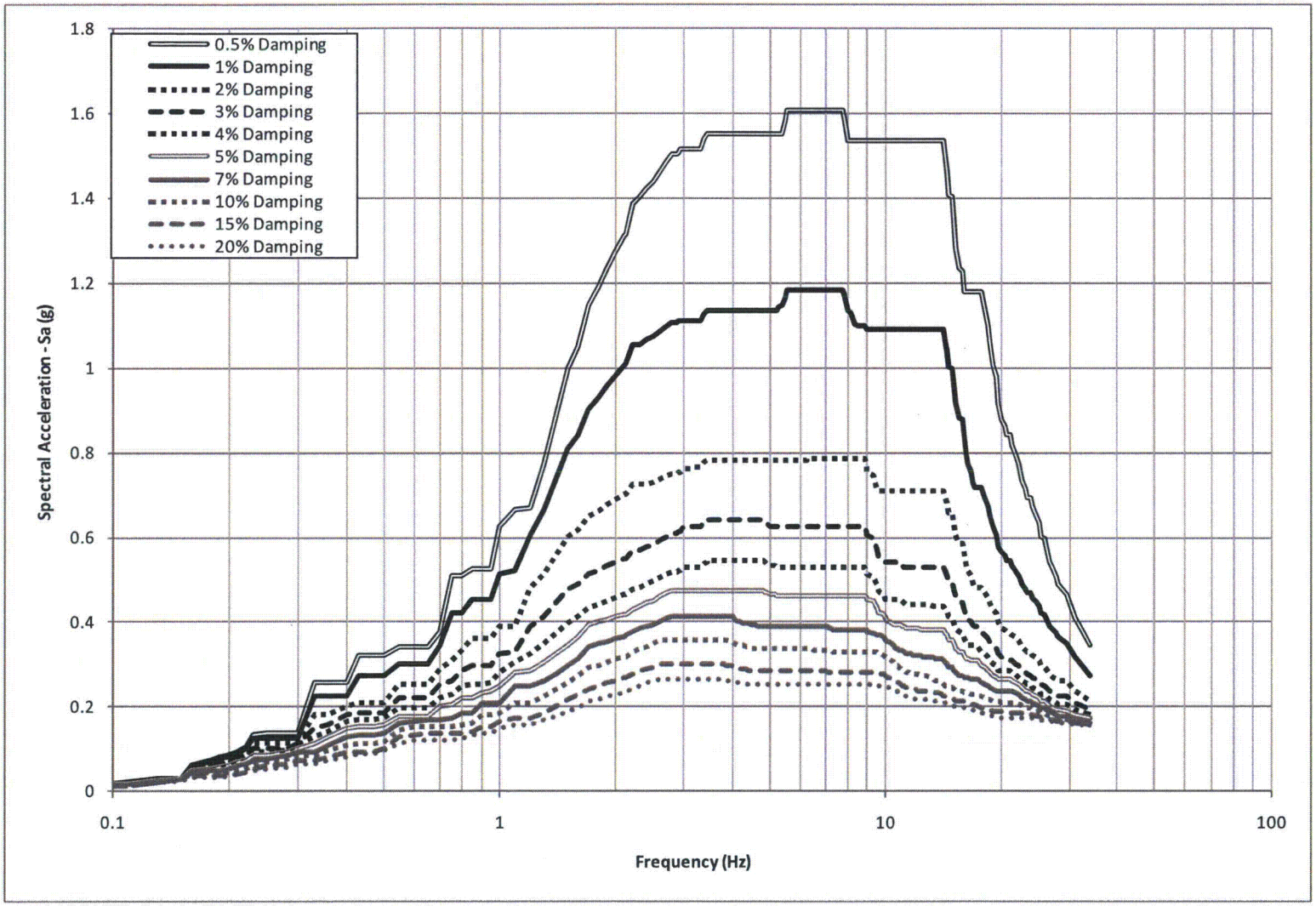

Figure 3H.6-27: Broadened FRS in Vertical (Z) Direction at the Top of UHS Basin Mat (Elevation 14 ft MSL)

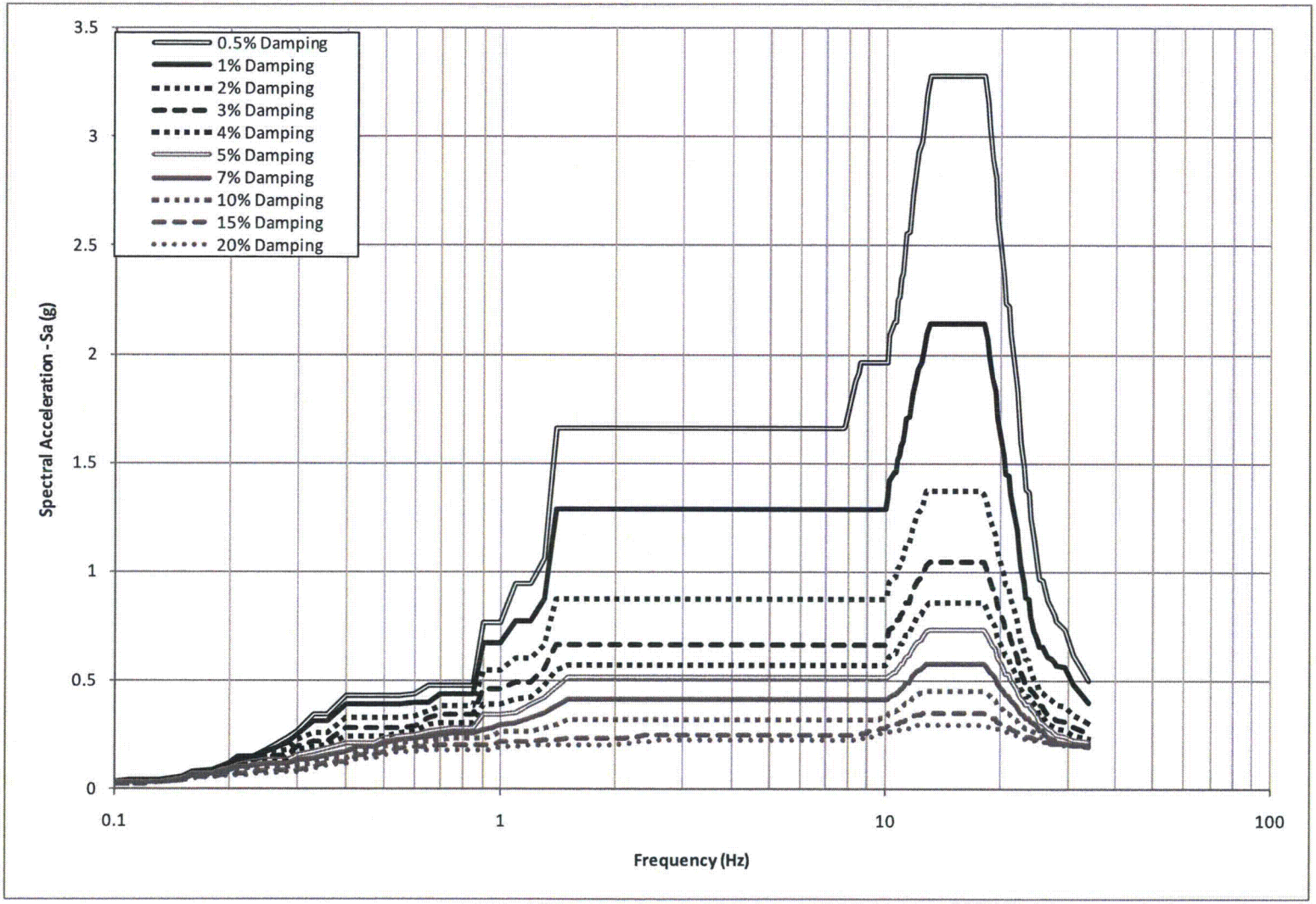

Figure 3H.6-28: Broadened FRS in E-W (X) Direction at the Top of UHS Basin Walls (Elevation 97.5 ft MSL)

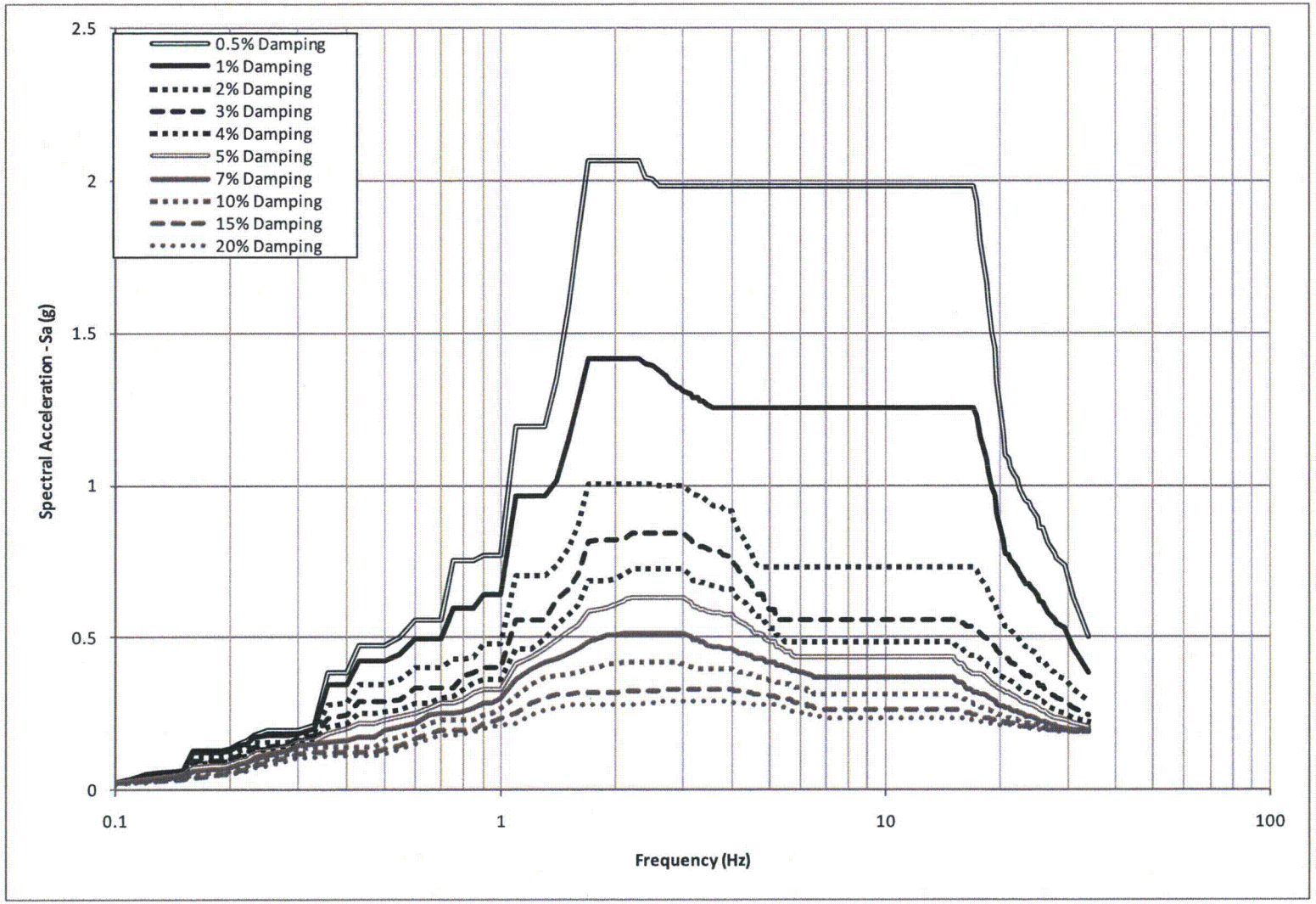

Figure 3H.6-29: Broadened FRS in N-S (Y) Direction at the Top of UHS Basin Walls (Elevation 97.5 ft MSL)

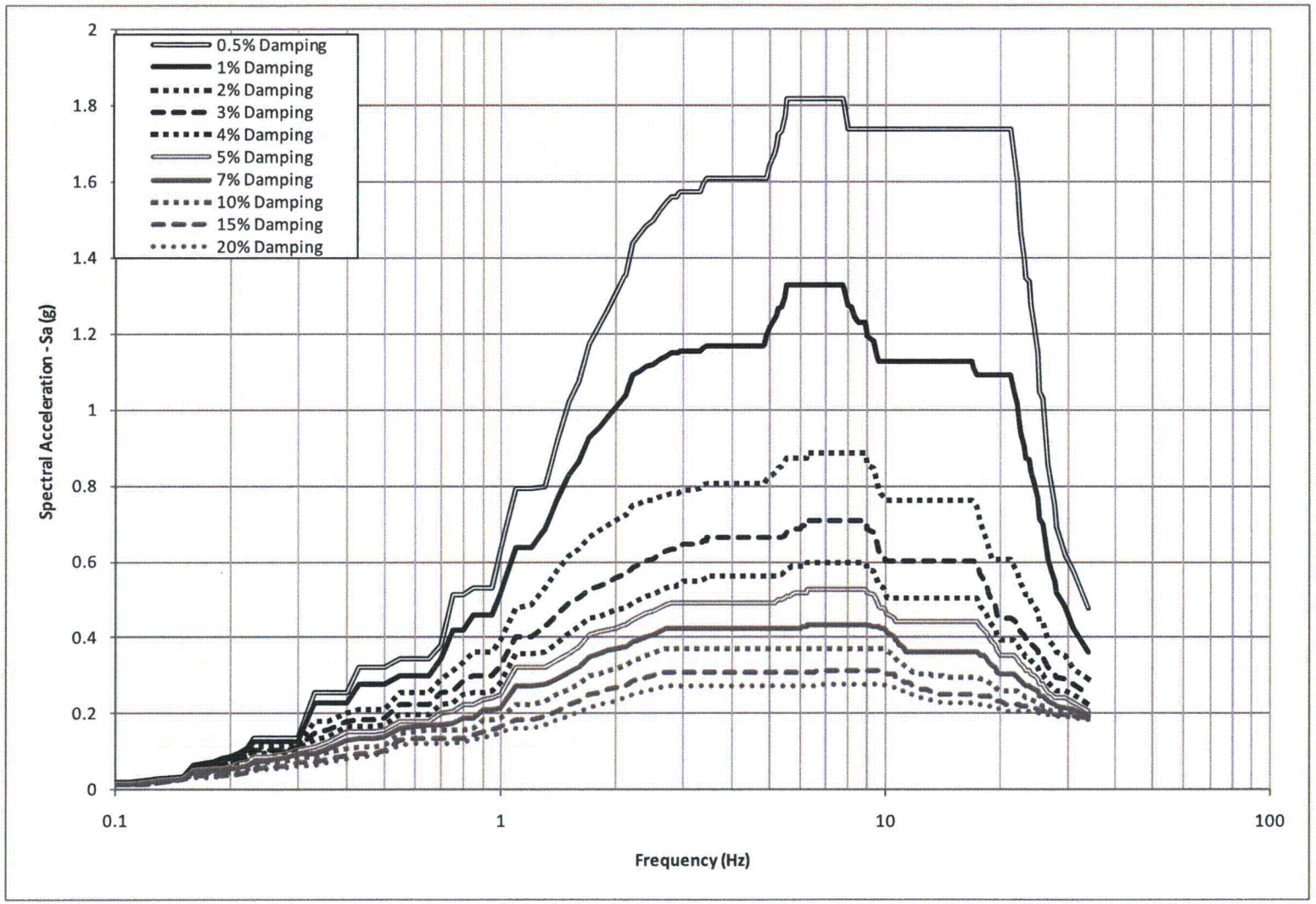

Figure 3H.6-30: Broadened FRS in Vertical (Z) Direction at the Top of UHS Basin Walls (Elevation 97.5 ft MSL)

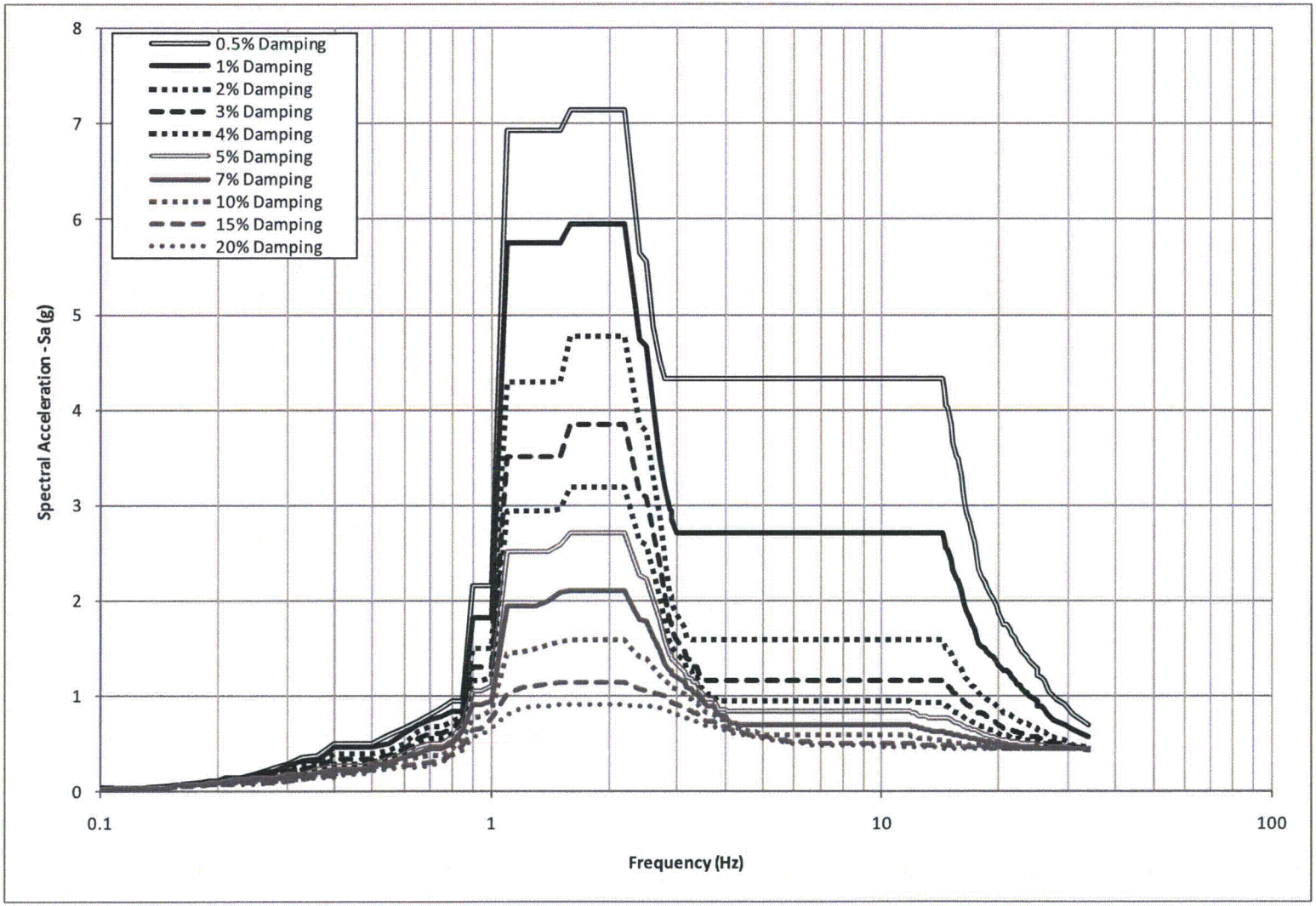

Figure 3H.6-31: Broadened FRS in E-W (X) Direction at the Bottom of Cooling Towers (Elevation 97.5 ft MSL)

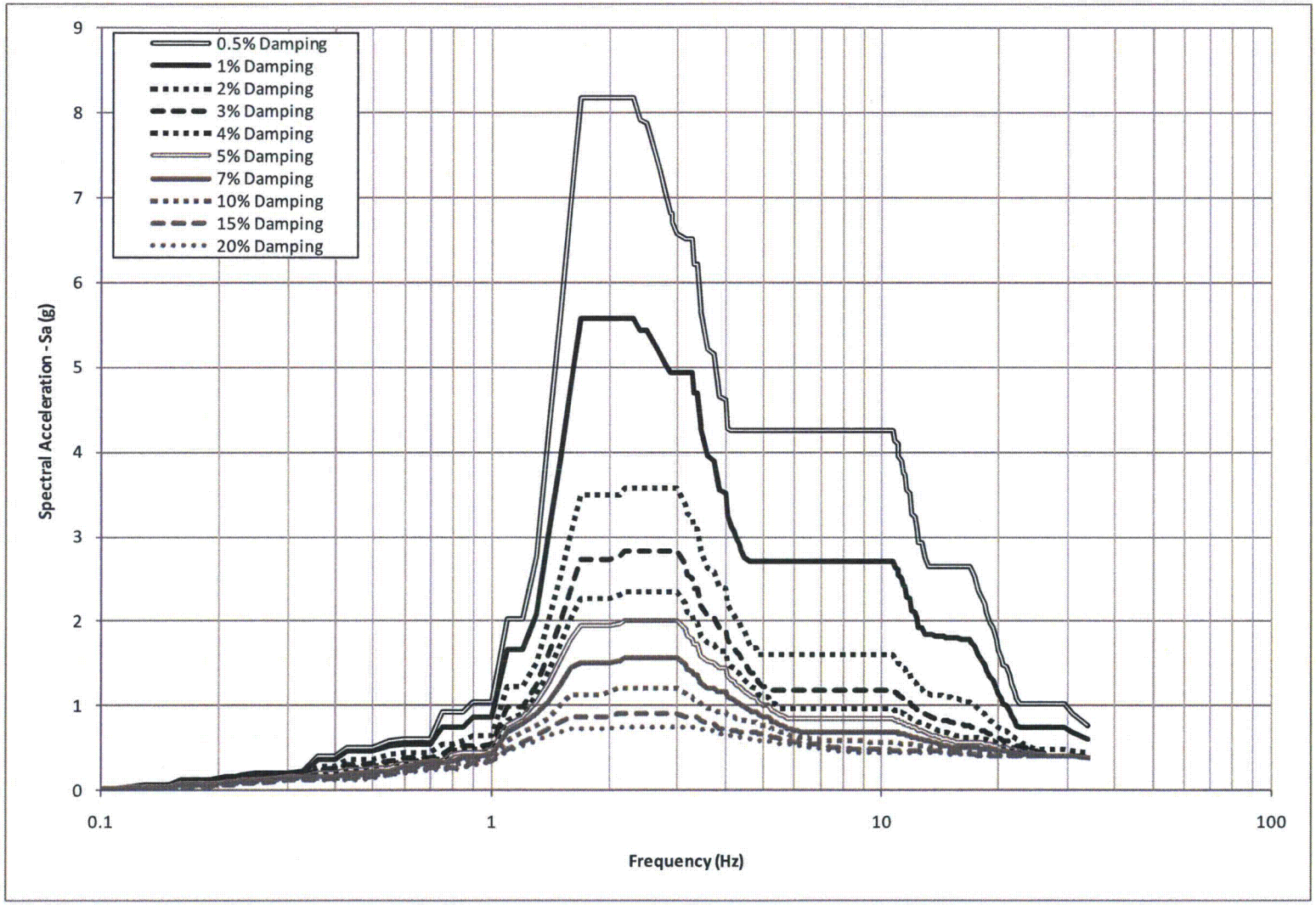

Figure 3H.6-32: Broadened FRS in N-S (Y) Direction at the Bottom of Cooling Towers (Elevation 97.5 ft MSL)

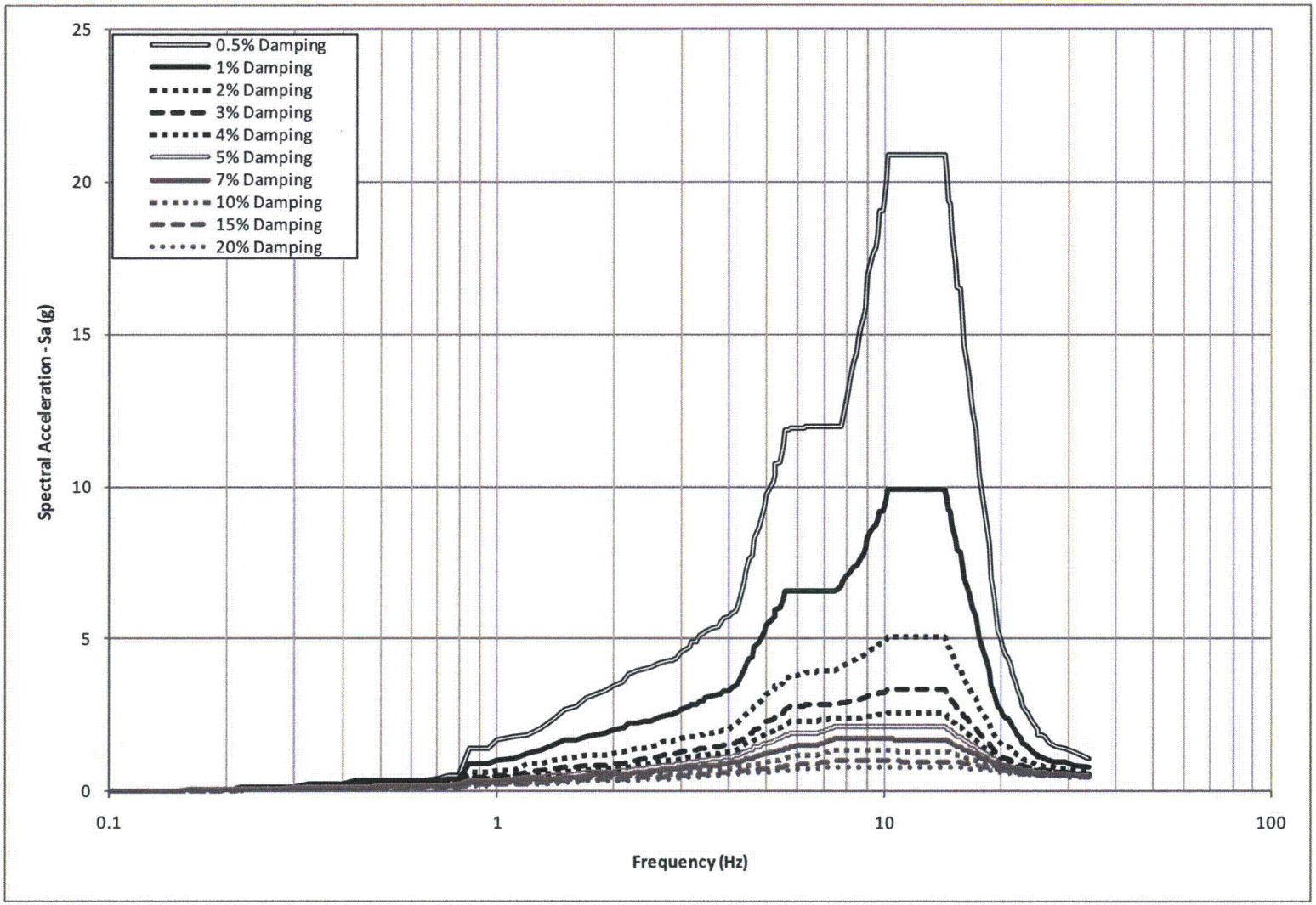

Figure 3H.6-33: Broadened FRS in Vertical (Z) Direction at the Bottom of Cooling Towers (Elevation 97.5 ft MSL)

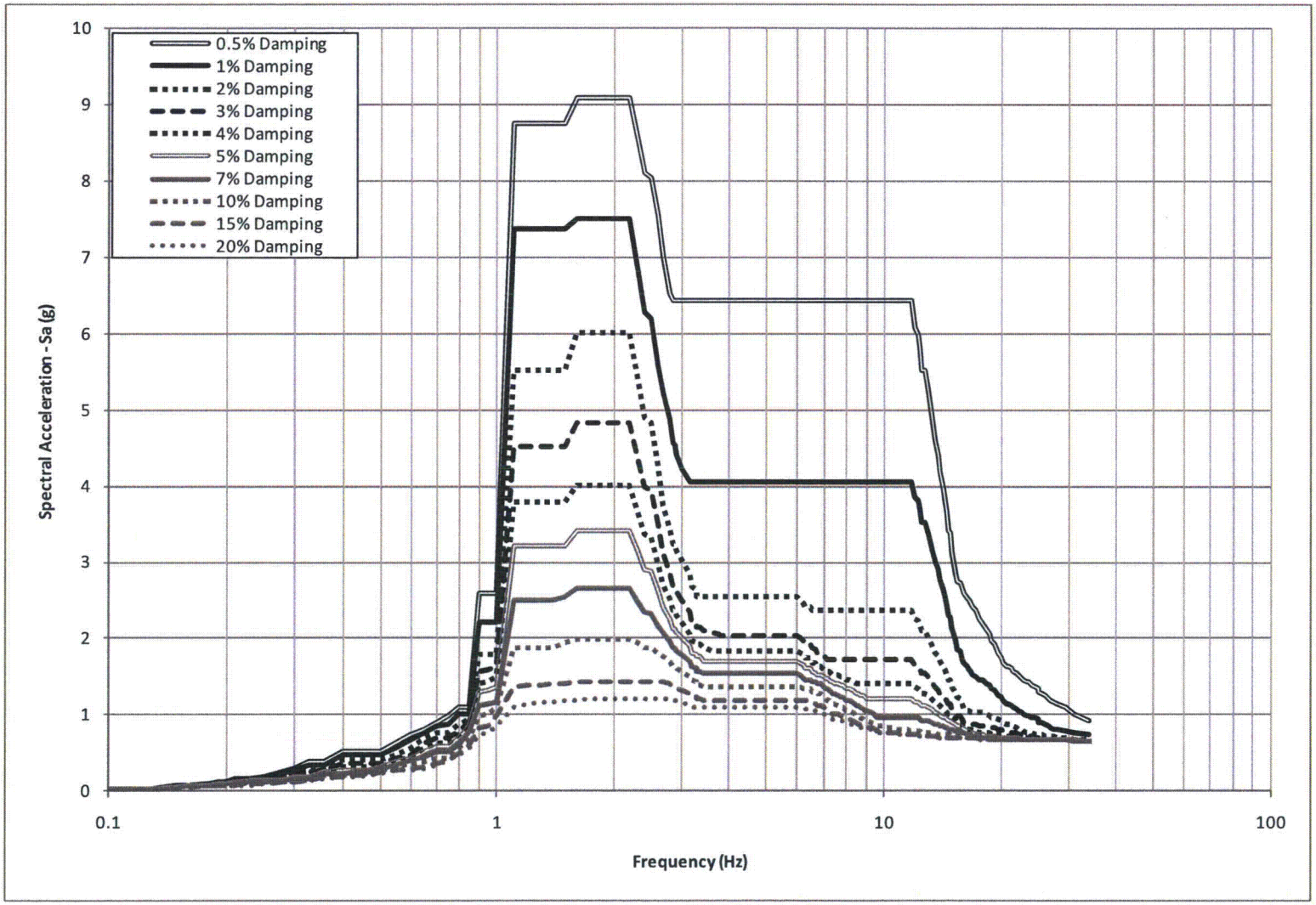

Figure 3H.6-34: Broadened FRS in E-W (X) Direction at the Mid-Level of Cooling Towers (Elevation 125.25 ft MSL)

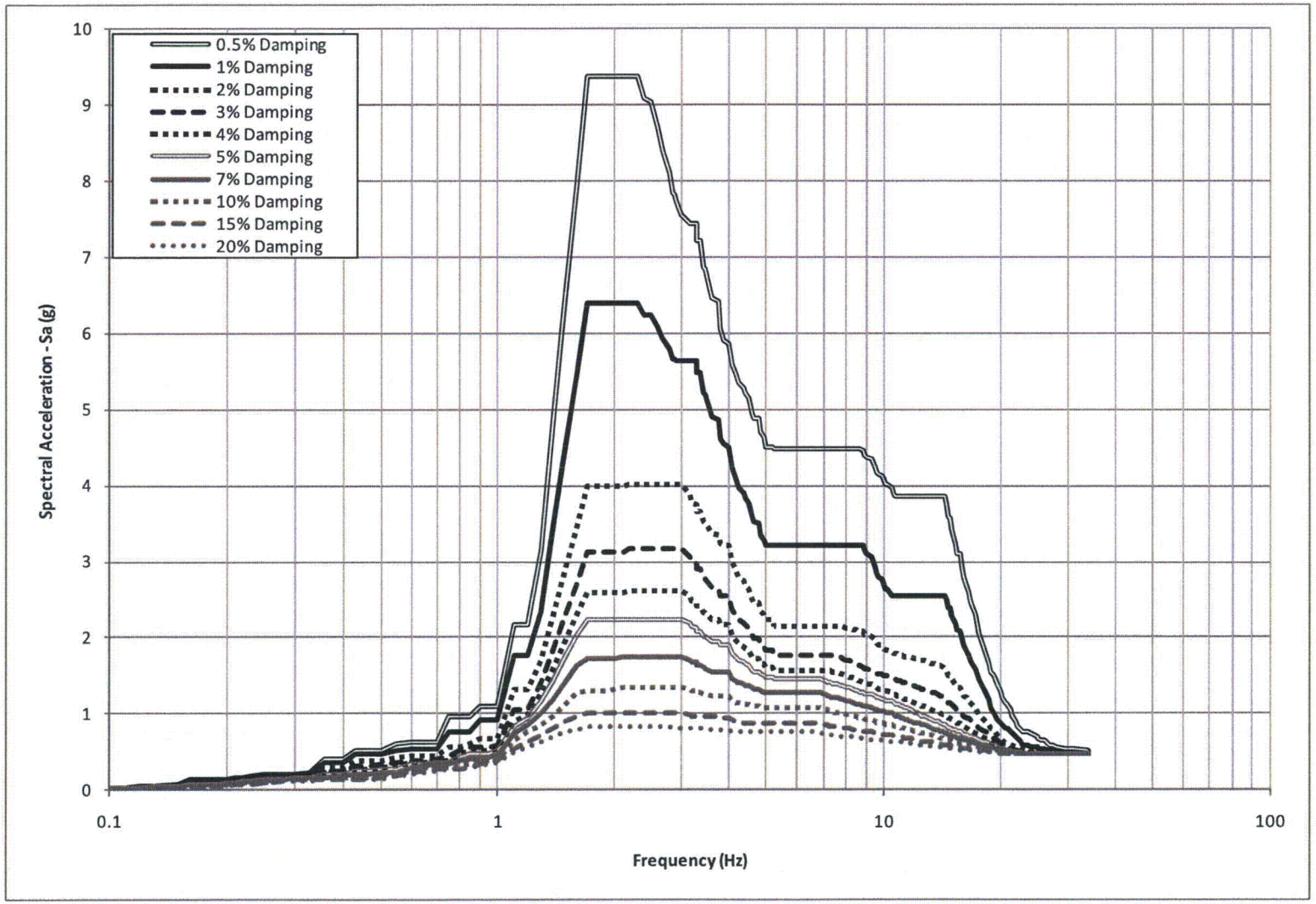

Figure 3H.6-35: Broadened FRS in N-S (Y) Direction at the Mid-Level of Cooling Towers (Elevation 125.25 ft MSL)

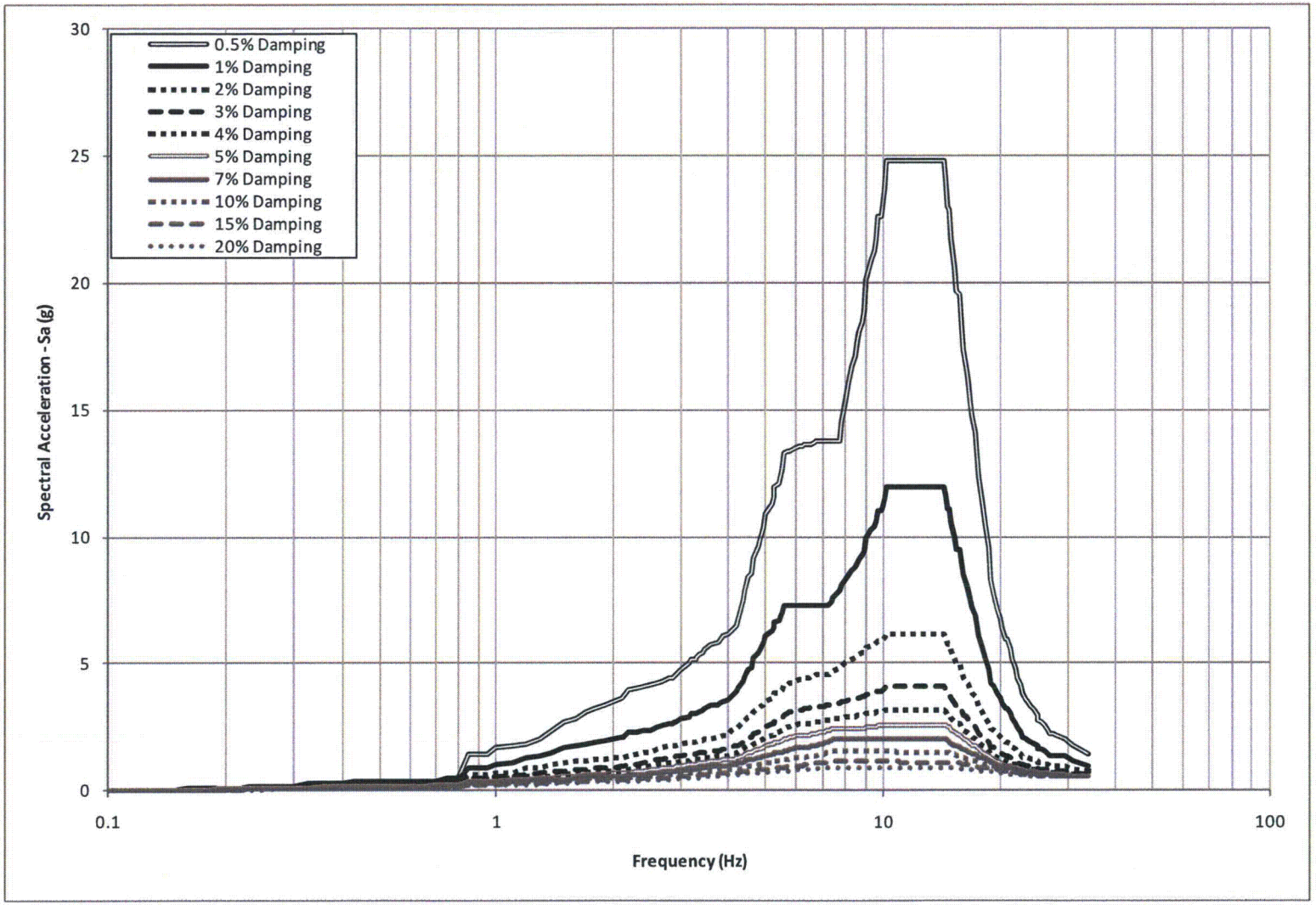

Figure 3H.6-36: Broadened FRS in Vertical (Z) Direction at the Mid-Level of Cooling Towers (Elevation 125.25 ft MSL)

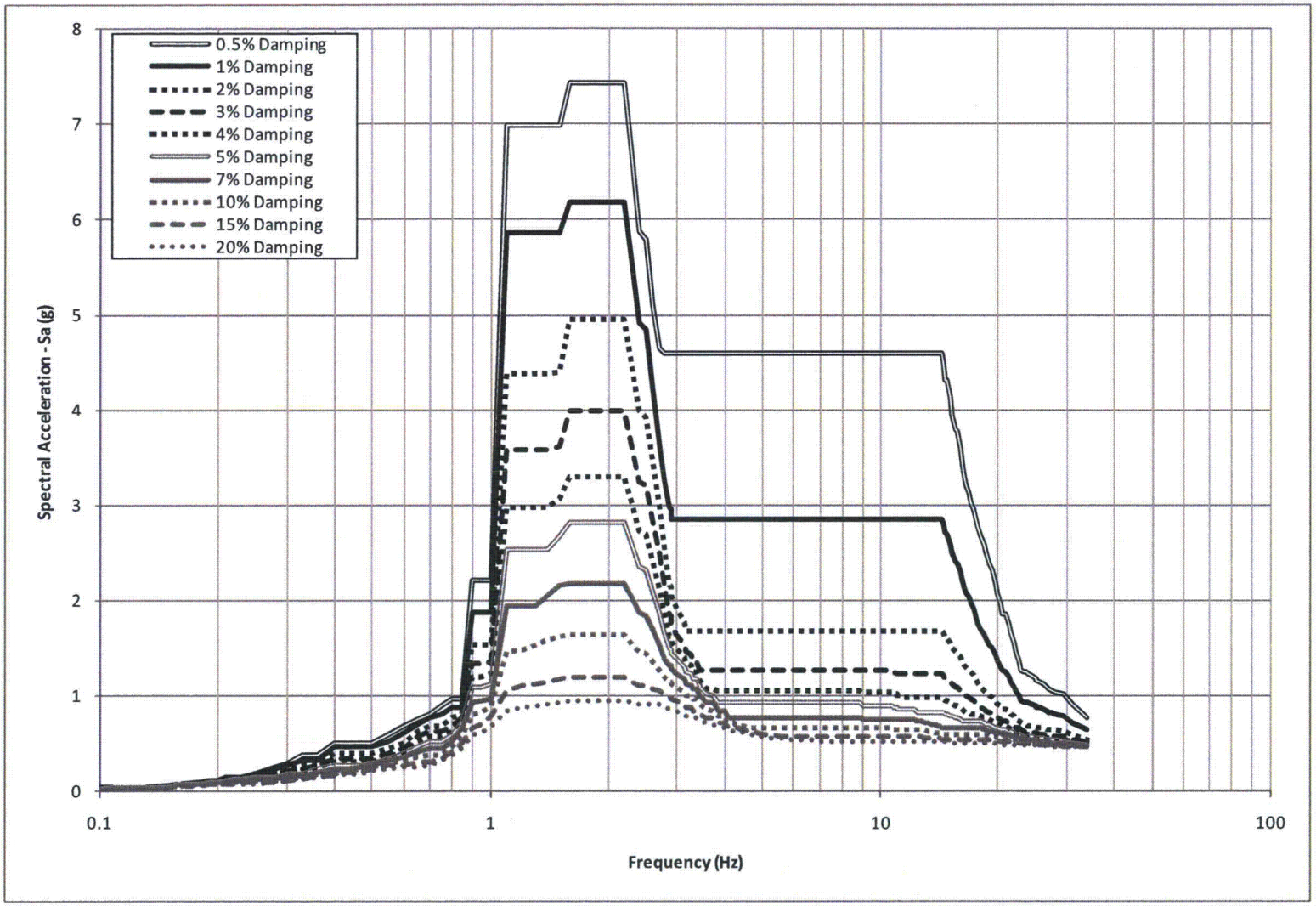

Figure 3H.6-37: Broadened FRS in E-W (X) Direction at the Top of Cooling Towers (Elevation 153 ft MSL)

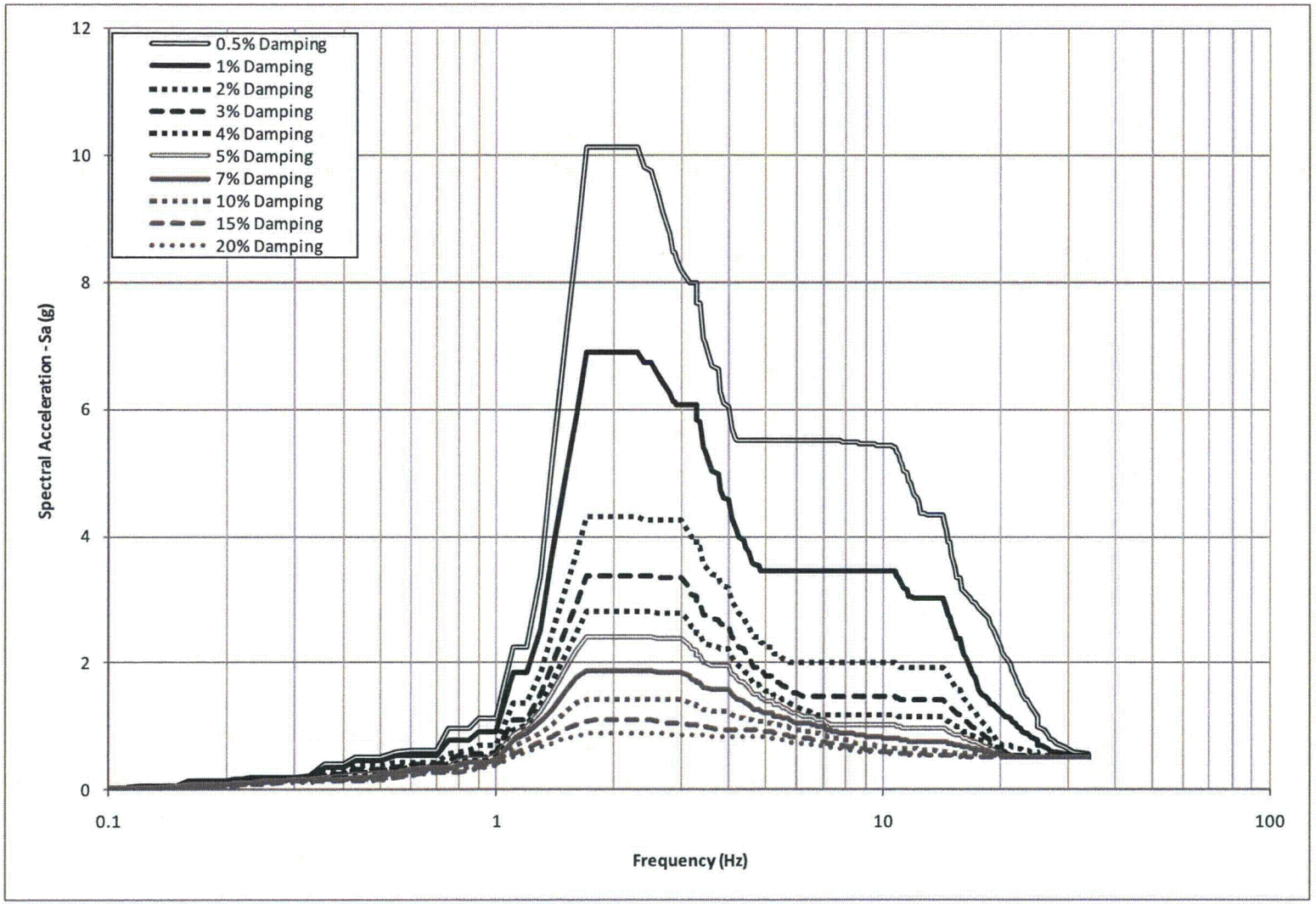

Figure 3H.6-38: Broadened FRS in N-S (Y) Direction at the Top of Cooling Towers (Elevation 153 ft MSL)

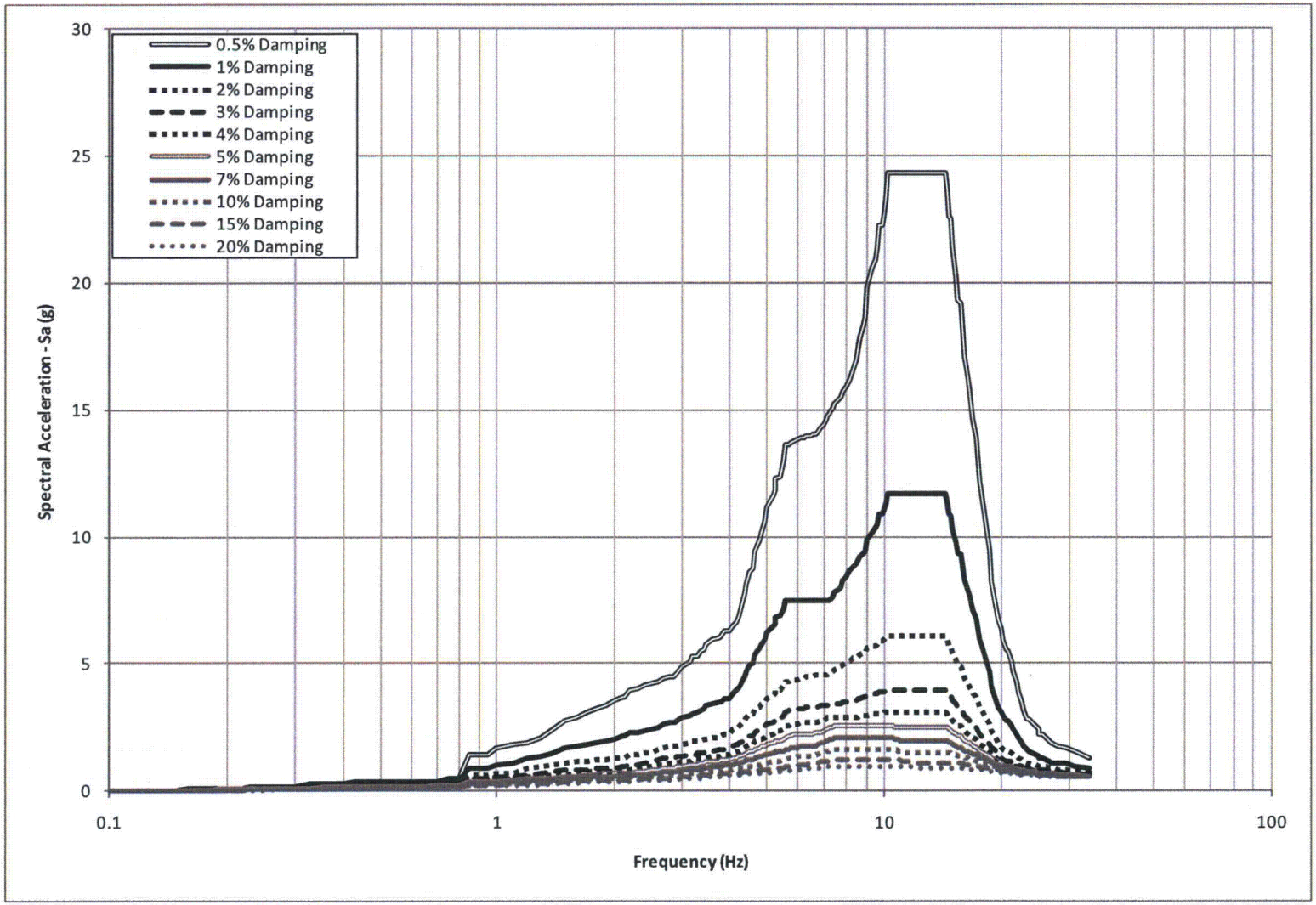

Figure 3H.6-39: Broadened FRS in Vertical (Z) Direction at the Top of Cooling Towers (Elevation 153 ft MSL)

RAI 03.07.02-25

QUESTION:

Follow-up Question to RAI 03.07.02-16 (STP-NRC-100036)

10CFR50, Appendix S requires that evaluation for SSE must take into account soil-structure interaction (SSI) effects. In the response to Item 1 of RAI 03.07.02-16 with regard to the adequacy of the structural mesh size used in the SSI analysis, the applicant has presented comparisons of the first two modes of the fixed-base structure in the E-W direction (f1 = 2.133 and f2 = 2.056 Hz) and N-S direction (f1 = 3.187 and f2 = 3.028 Hz) calculated using the SSI and design meshes. Although the comparisons of the two modes are good, they only represent a mass participation of about 17.1% and 15.4% for the E-W and N-S directions, respectively. In addition, the local modes are not reflected in these comparisons. As such, the applicant is requested to provide comparisons of the higher modes that include the out-of-plane modes of the slabs and walls to ensure the adequacy of the SSI mesh for transmitting frequencies of at least 33 Hz. This should include comparisons of in-structure response spectra of slabs, roofs and wall panels for the fixed-base structure calculated using the coarse SSI and fine design meshes subject to representative horizontal and vertical foundation motions. The staff needs this information to determine that the coarse mesh size (for modeling the structure) used in the SSI analysis is adequate for evaluation of SSI effect.

RESPONSE:

To assess the adequacy of the structural mesh size used in the Ultimate Heat Sink (UHS) and Reactor Service Water (RSW) Pump House Soil-Structure Interaction (SSI) model, the following three (3) fixed-base time history analyses were performed for comparison of in-structure response spectra and maximum accelerations at various locations:

1. Fixed-base time history analysis of the structural model which was used in the original SSI model (called original SSI model hereinafter)

2. Fixed-base time history analysis of the structural model which was used in the refined SSI model (called refined SSI model hereinafter) in the refined SSI analysis described in Supplement 2 response to RAI 03.07.02-24 which is being submitted concurrently with this response.

3. Fixed-base time history analysis of a more refined structural model (called refined structural model hereinafter). In this refined structural model each element of the original SSI model was divided into four (4) elements.

The following provides additional details for the above analyses:

- Figures 03.07.02-25.1 thru 03.07.02-25.3 show original SSI model, refined SSI model, and refined structural model, respectively. Figures 03.07.02-25.6 thru 03.07.02-25.8 show Pump House roof to the same scale from the original SSI model, refined SSI model, and refined structural model, respectively.

  Note that the comparison of the mesh in the above noted figures for the original SSI model, refined SSI model, and refined structural model shows that the mesh refinement of these models is significantly different from each other, with the mesh refinement of the refined SSI model being in between those for the original SSI model and refined structural model.

- The node locations for comparison of in-structure response spectra are shown in Figures 03.07.02-25.1 thru 03.07.02-25.3 for the original SSI model, refined SSI model, and refined structural model, respectively. These locations include the Pump House Operating Floor, Pump House Roof, UHS Basin Walls, and UHS Cooling Tower Walls. The node locations for comparison of maximum accelerations, in addition to those locations for comparison of in-structure response spectra, include those shown in Figures 03.07.02-25.4 and 03.07.02-25.5.

  Note: The node selection for comparison of the in-structure response spectra and maximum accelerations described above is in excess of the nodes selected in the discussions on this topic during the August 4, 2010 NRC public meeting in Rockville, MD.

- Thick shell elements are used to represent the walls, floors, and roofs of the UHS/RSW Pump House. The basemat of the UHS/RSW Pump House is modeled using solid elements.

- Time history analyses were performed using 4% structural damping.

- Modal superposition was used.

- Cut-off frequency of 51 Hz was used resulting in consideration of 890, 890, and 829 modes for the original SSI model, refined SSI model, and refined structural model, respectively.

- Site-specific safe shutdown earthquake (SSE) motions were selected as input motions and the results from the X, Y, and Z excitations were combined using square-root-sum-of-squares (SRSS) method.

In the above analyses, consistent with the SSI analysis and design of the UHS/RSW Pump House, thick shell elements are used because thick shell formulations are more accurate. For shell elements, two thickness formulations are available, thin or thick, with the difference being in the consideration of transverse shear deformations as noted below:

- Thick shell formulation includes the effects of transverse shear deformation
- Thin shell formulation neglects transverse shear deformation

For situations where shear deformations are rather negligible and, therefore, use of thin shell elements may be justified, use of thick shell elements will not introduce any inaccuracy and the results using thick shell elements will be nearly identical (yet more accurate) to those using thin shell elements. To demonstrate this, a 49 ft x 78 ft slab panel (similar to the Pump House roof slab panel), fixed on all four edges as shown in Figure 03.07.02-25.9, was analyzed for slab thicknesses of six inches and six feet, using both thin and thick shell formulations. A time history analysis of these slabs was performed by exciting the models in the out-of-plane direction with the vertical site-specific SSE motion. Comparison of the resulting in-structure response spectra at the center of the six inch thick slab is shown in Figure 03.07.02-25.10. As seen from this comparison, both thick and thin shell element formulations yield nearly identical results, as should be expected. Comparison of the in-structure response spectra for the six feet thick slab is shown in Figure 03.07.02-25.11. This comparison shows, as expected, that the resulting spectra are significantly different showing the significance of the transverse shear deformations.

Figures 03.07.02-25.12 through 03.07.02-25.39 provide comparison of un-widened in-structure response spectra, for 5% damping, from the analyses of the three structural models as described above. Table 03.07.02-25.1 provides a comparison of maximum accelerations from the analyses with original SSI model and refined structural model. Based on these comparisons, it is concluded that there is good agreement between the spectra and maximum accelerations generated from the original SSI model and the refined structural model in all three X, Y, and Z directions with the exception of the following cases:

- Vertical excitation at the center of the Pump House Roof (see Figure 03.07.02-25.20)
- Vertical excitation at the center of the Pump House Operating Floor (see Figure 03.07.02-25.14)
- Vertical excitation of the Cooling Tower Walls (see Figure 03.07.02-25.36)
- Out-of-plane excitation of the UHS Basin Walls (see Figures 03.07.02-25.24 and 03.07.02-25.25)

The above results indicate that a more refined mesh for Pump House Roof, Pump House Operating Floor, UHS Basin Walls, and Cooling Tower Walls results in higher spectra and/or maximum accelerations.

Comparison of the response spectra shown in Figures 03.07.02-25.12 through 03.07.02-25.39 also shows that the structural mesh of the refined SSI model used for the refined SSI analysis described in Supplement 2 response to RAI 03.07.02-24 (being submitted concurrently with this response) have converged, since the changes between the results from the refined SSI model and refined structural model are in general insignificant. In a few cases where the differences are more pronounced, the results from the refined structural model are lower than the results from refined SSI model signifying that further refinement is not required.

For resolution of the above findings and the COLA revisions, please see the response to RAI 03.07.02-24, Supplement 2 which is being submitted concurrently with this response.

No additional COLA revision is required as a result of this response.

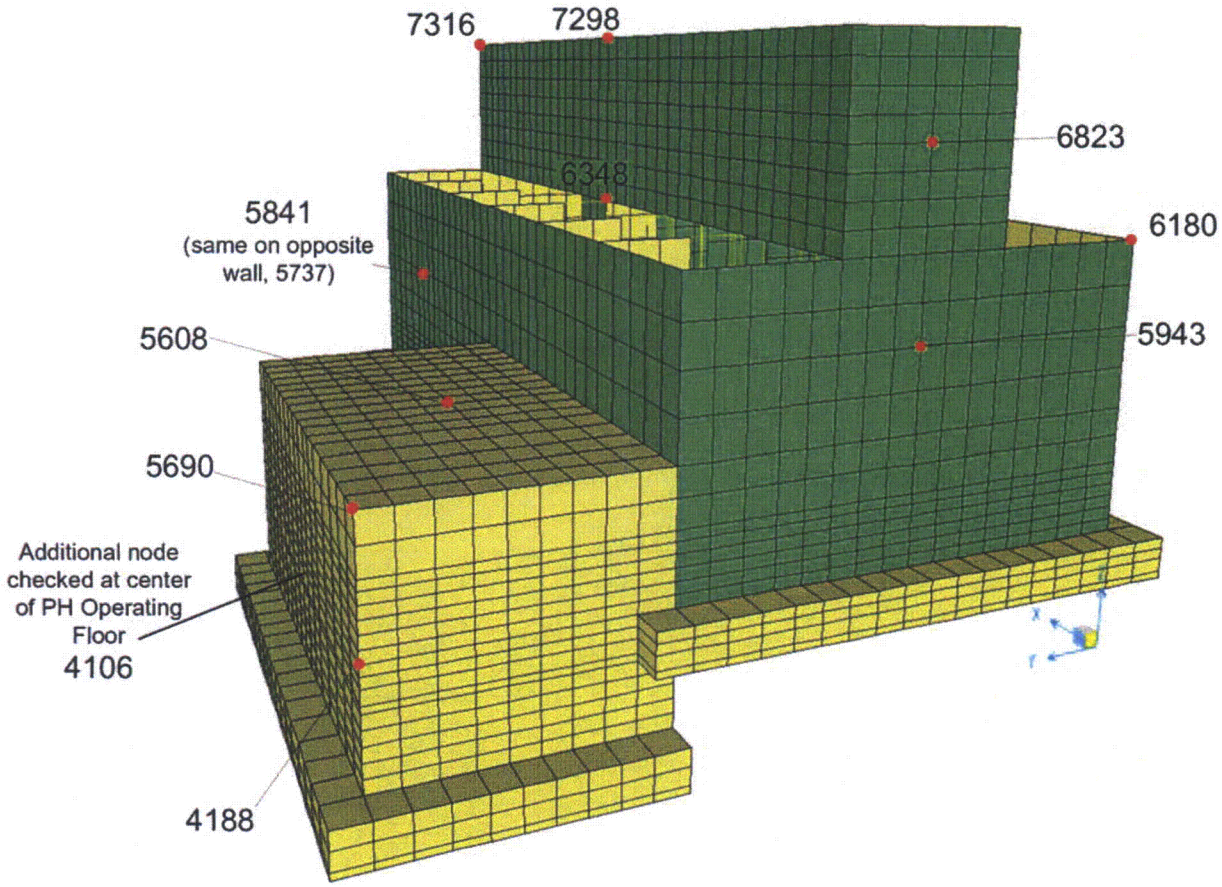

Figure 03.07.02-25.1: Node locations for spectra comparison on Original SSI Model (North is along Y-Axis)

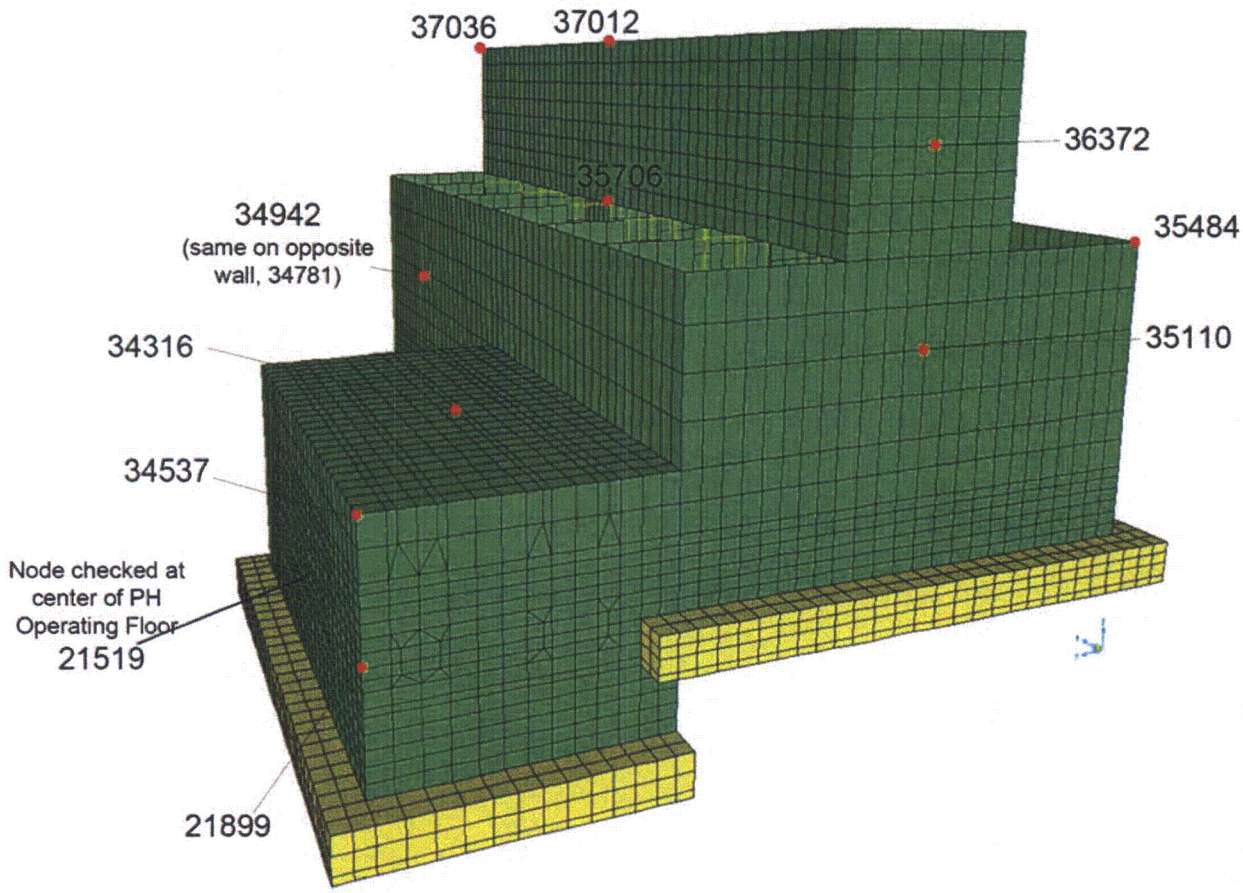

Figure 03.07.02-25.2: Node locations for spectra comparison on Refined SSI Model (North is along Y-axis)

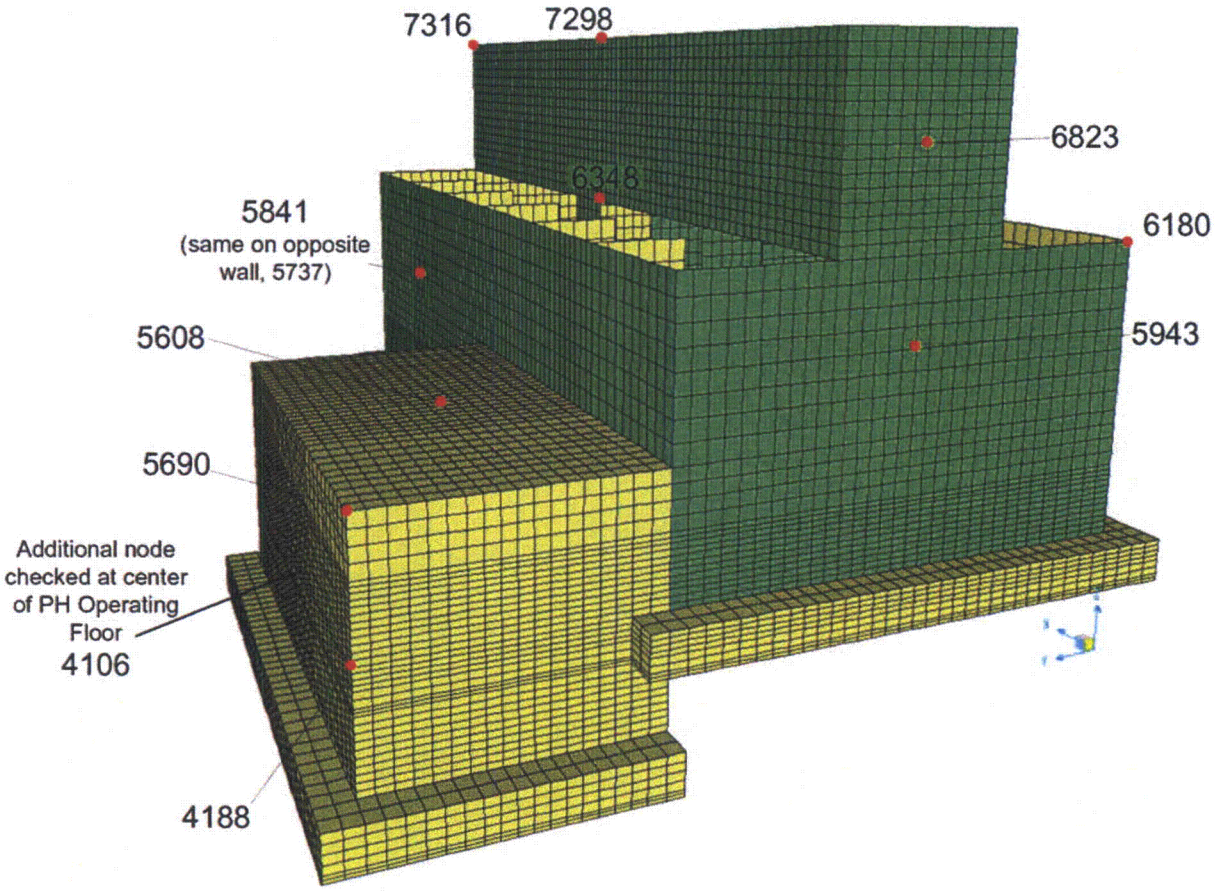

Figure 03.07.02-25.3: Node locations for spectra comparison on the Refined Structural Model (North is along Y-axis)

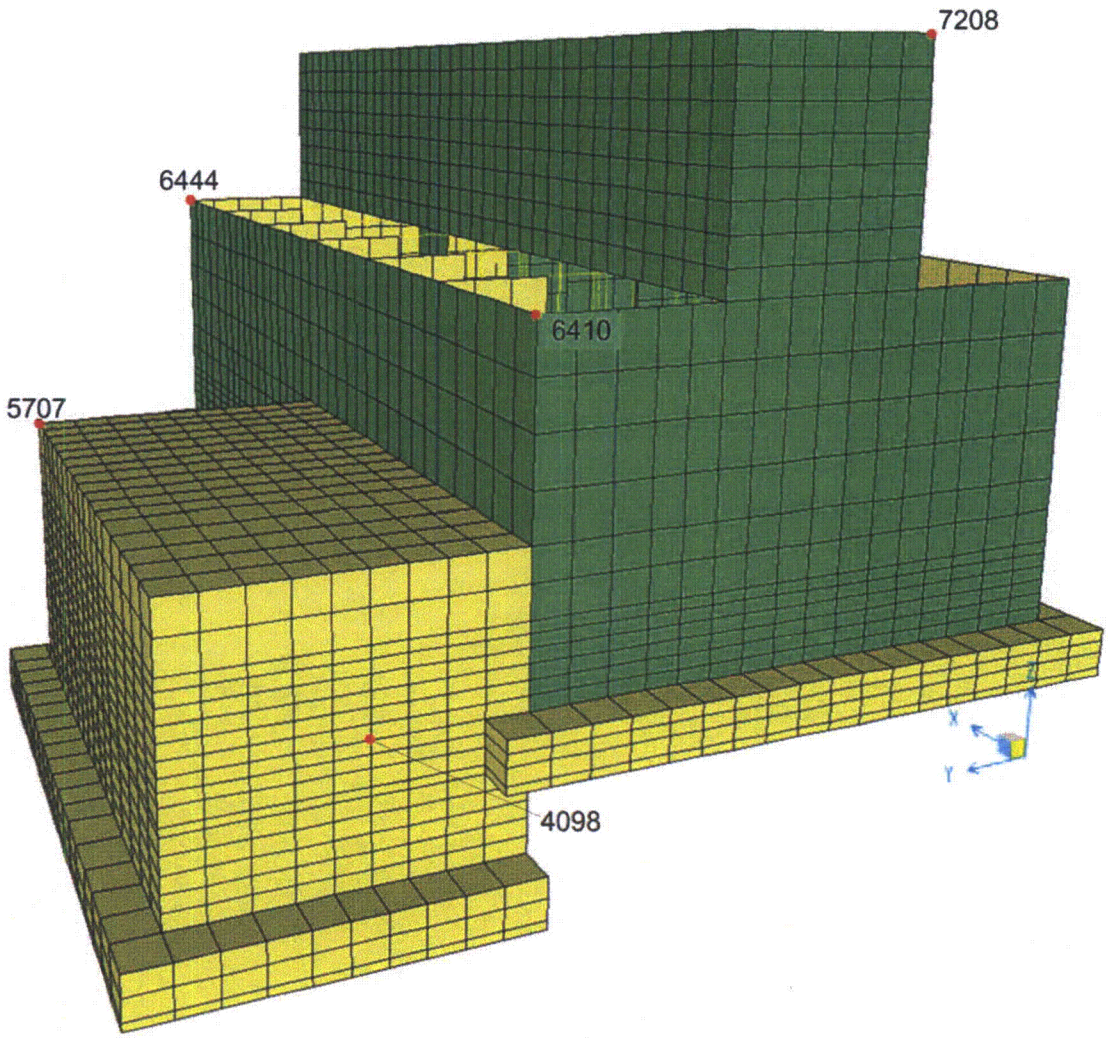

Figure 03.07.02-25.4: Additional node locations for acceleration comparison on the Original SSI Model (North is along Y-axis)

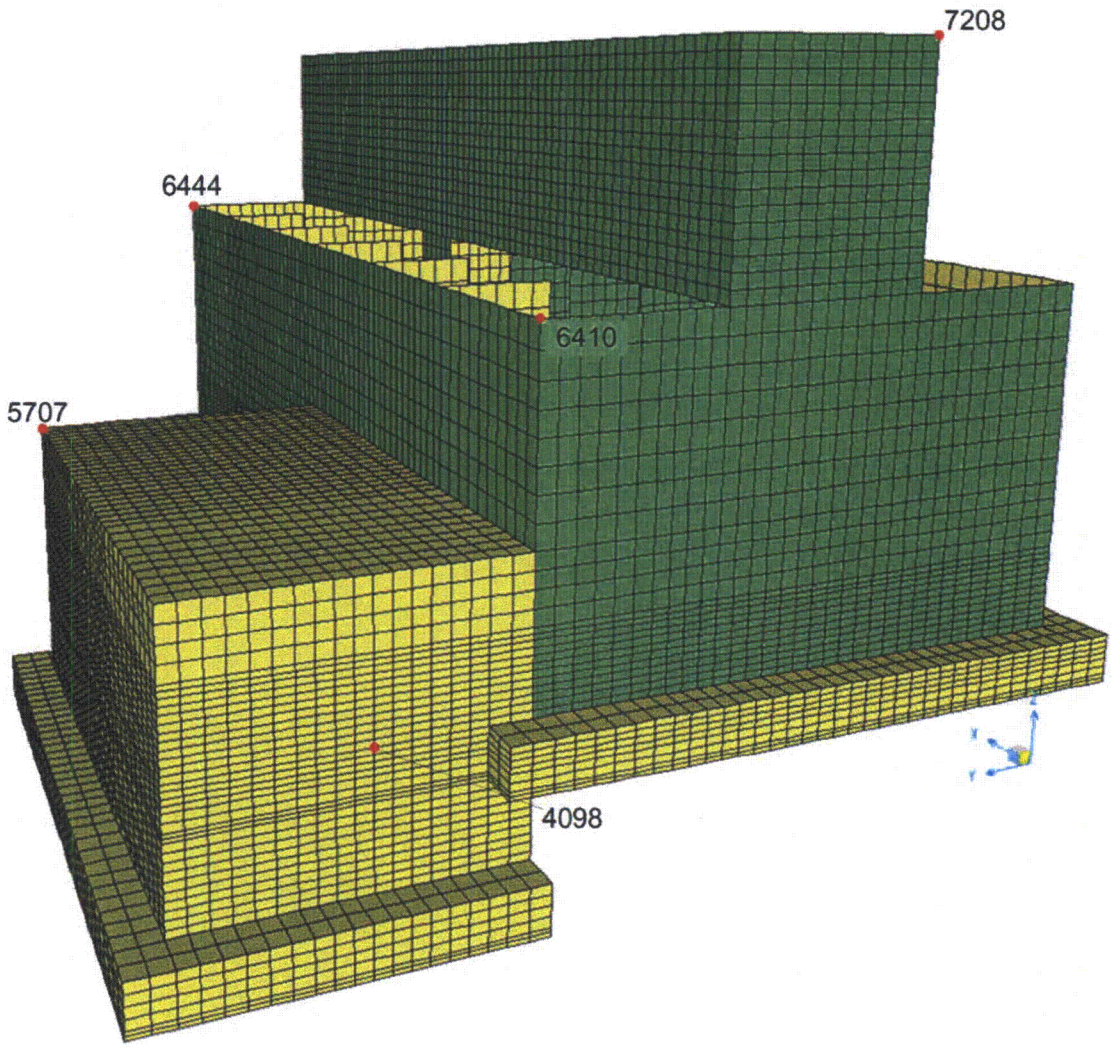

Figure 03.07.02-25.5: Additional node locations for acceleration comparison on the Refined Structural Model (North is along Y-axis)

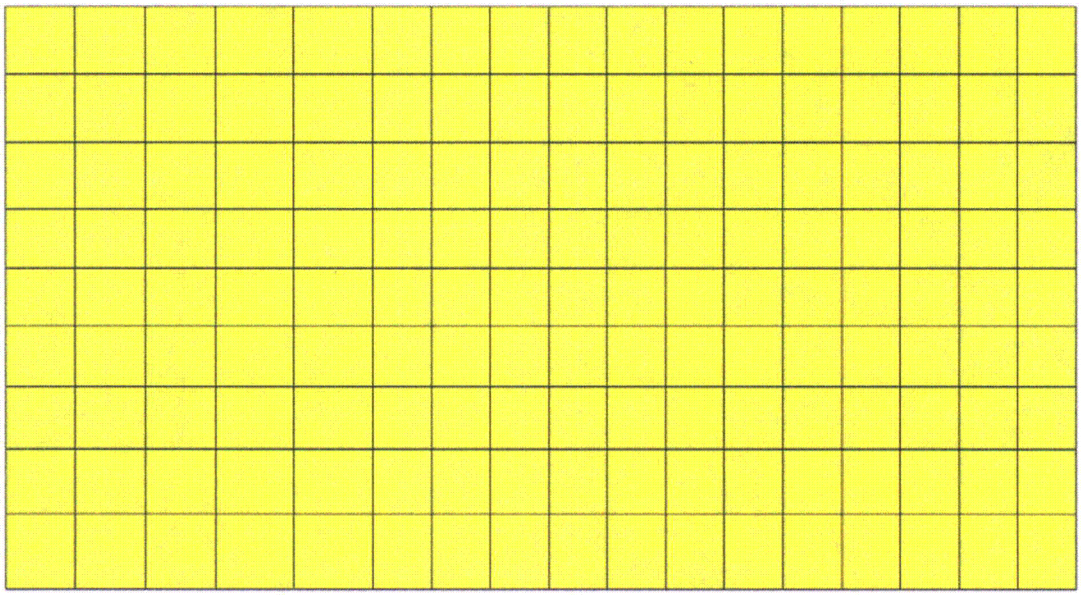

Figure 03.07.02-25.6: Sample mesh (Pump House Roof) from Original SSI Model.

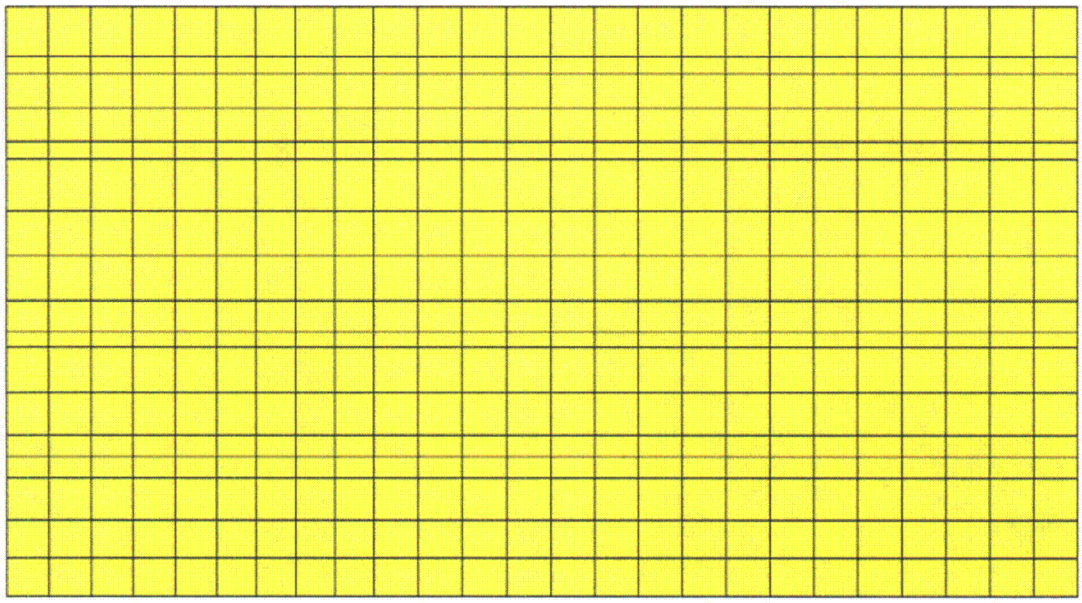

Figure 03.07.02-25.7: Sample mesh (Pump House Roof) from Refined SSI Model.

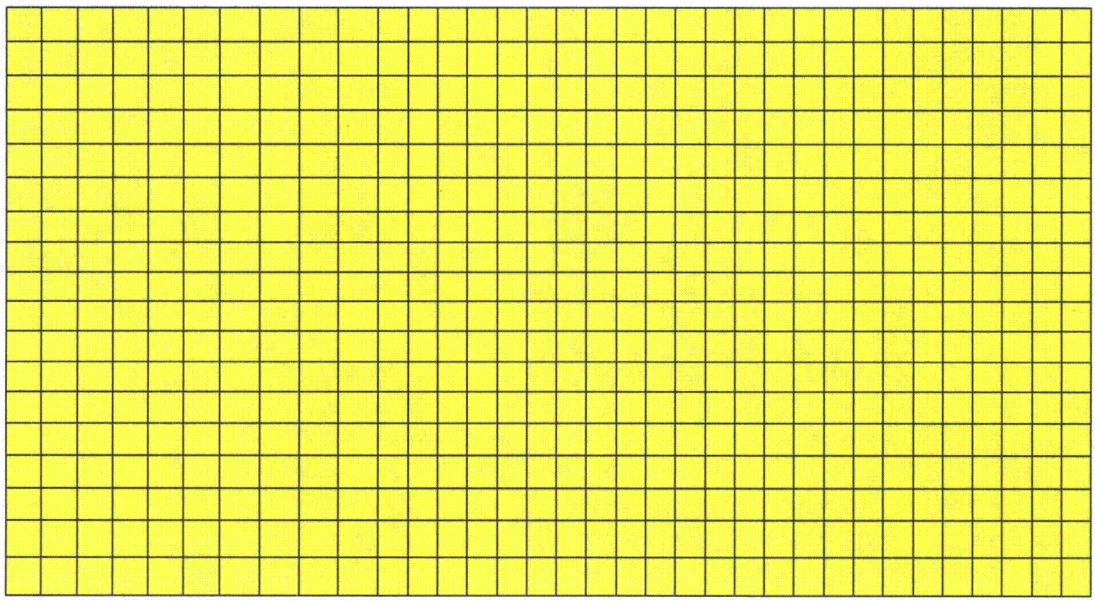

Figure 03.07.02-25.8: Sample mesh (Pump House Roof) from Refined Structural Model.

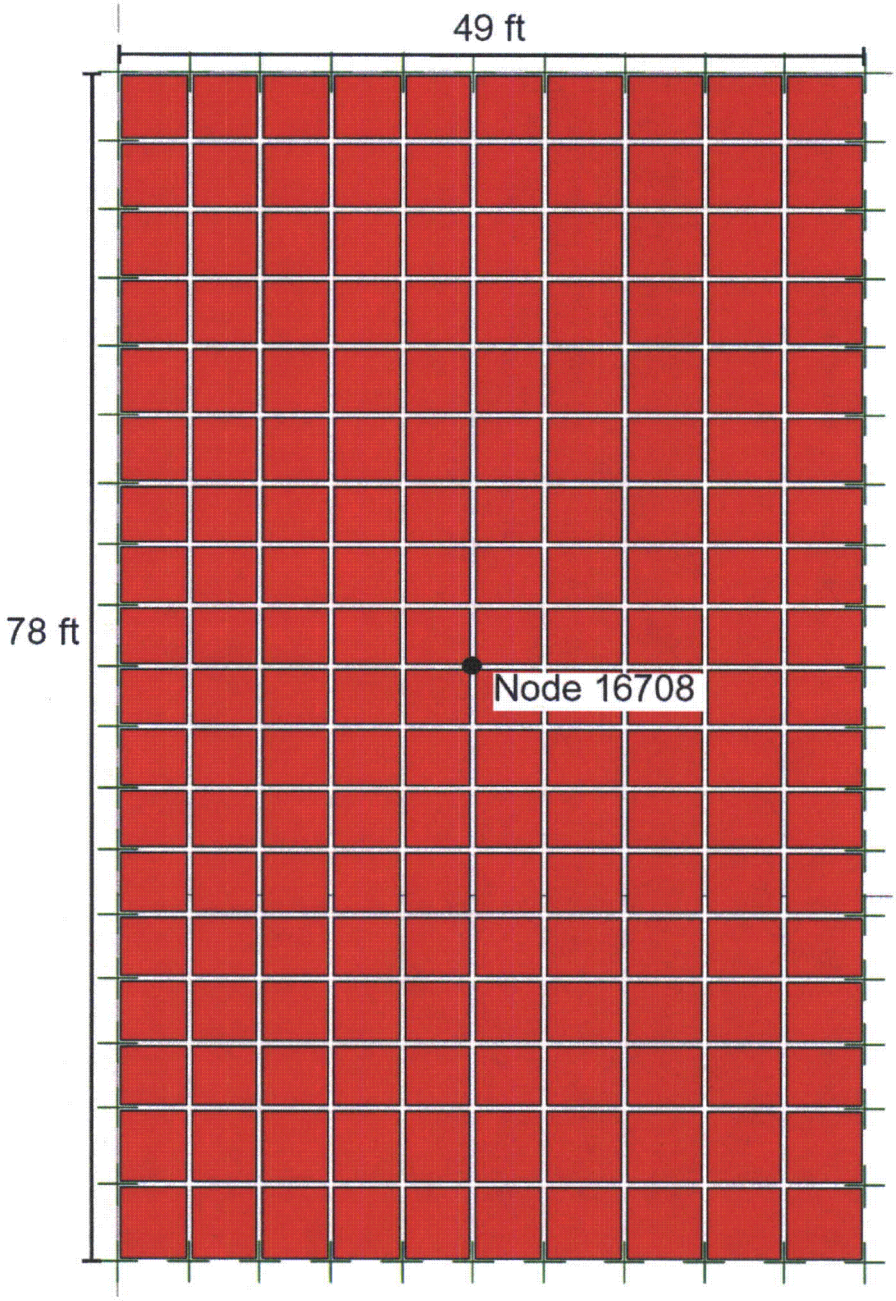

Figure 03.07.02-25.9: Slab model (dimensions equal to one bay of Pump House Roof).

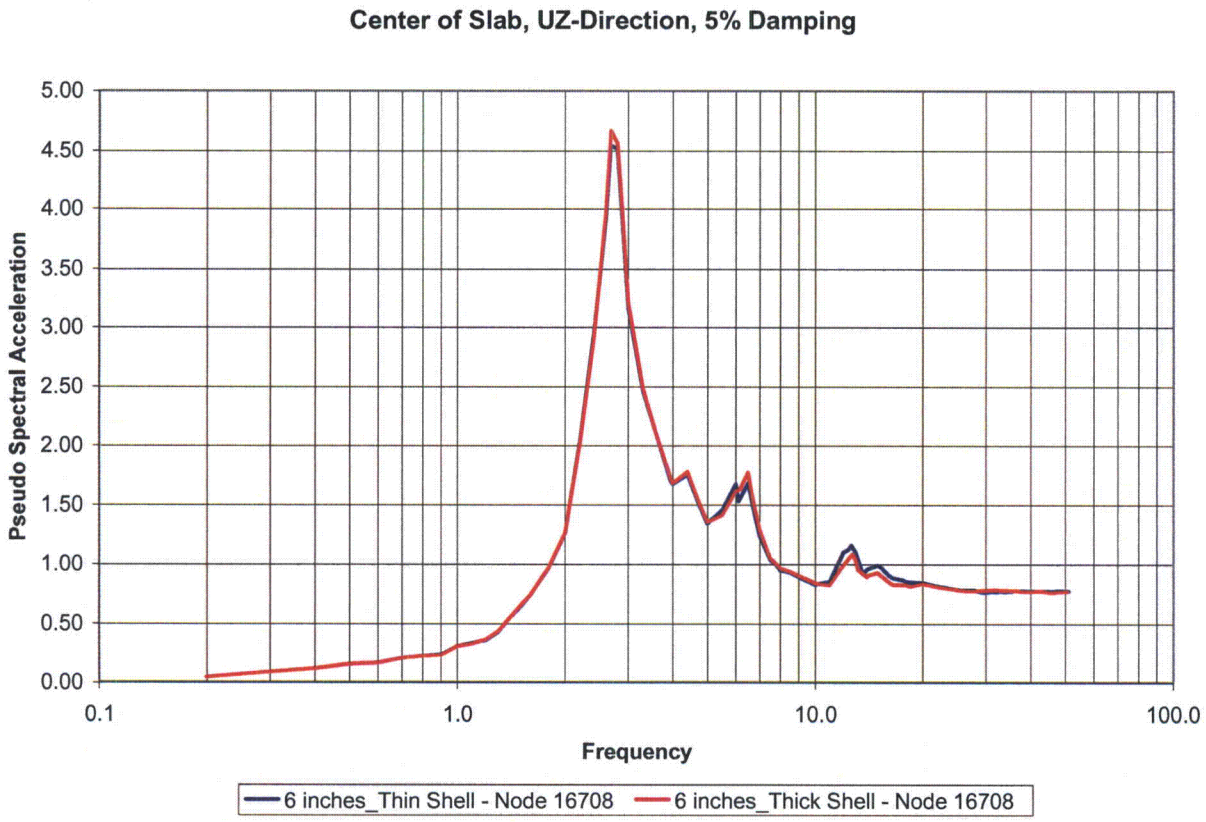

Figure 03.07.02-25.10: Spectra comparison at center of 6 inch slab with thin and thick shell elements.

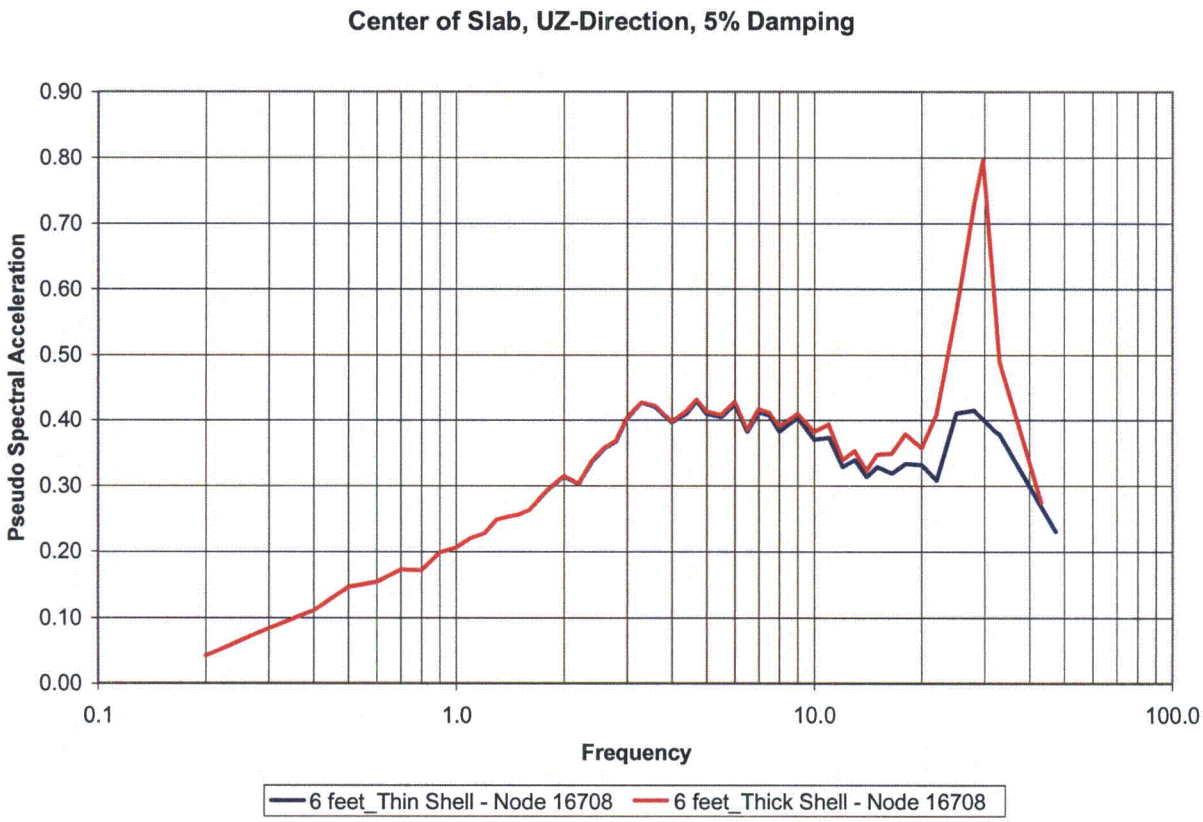

Figure 03.07.02-25.11: Spectra comparison at center of 6 foot slab with thin and thick shell elements.

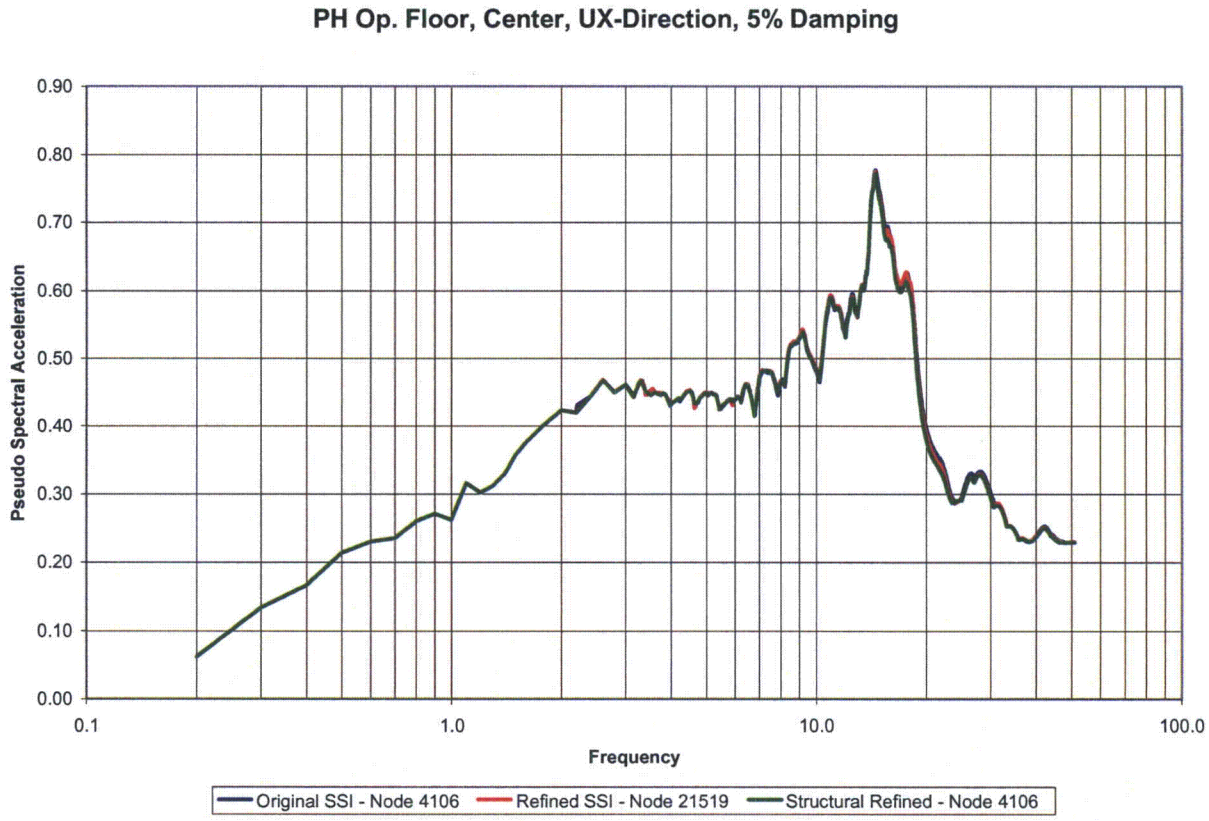

Figure 03.07.02-25.12: Center of Pump House Operating Floor, X-direction, 5% Damping

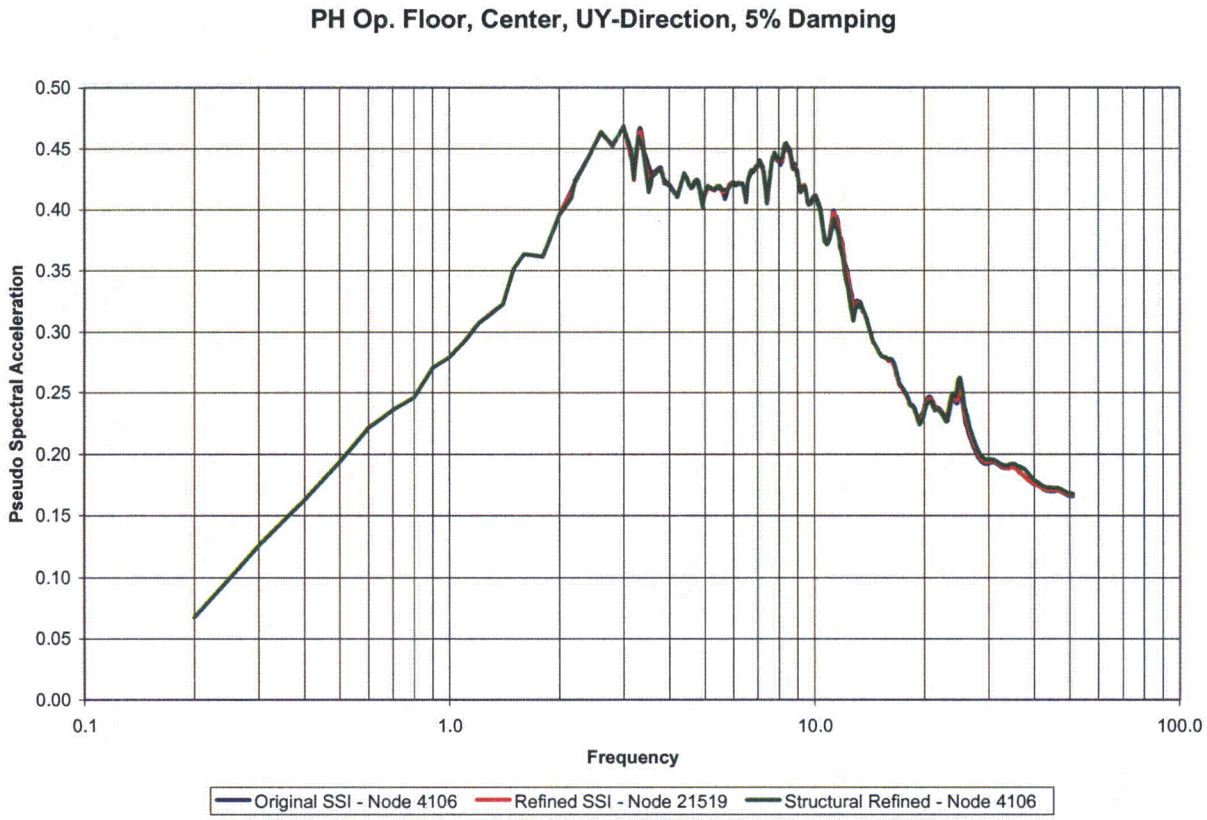

Figure 03.07.02-25.13: Center of Pump House Operating Floor, Y-direction, 5% Damping

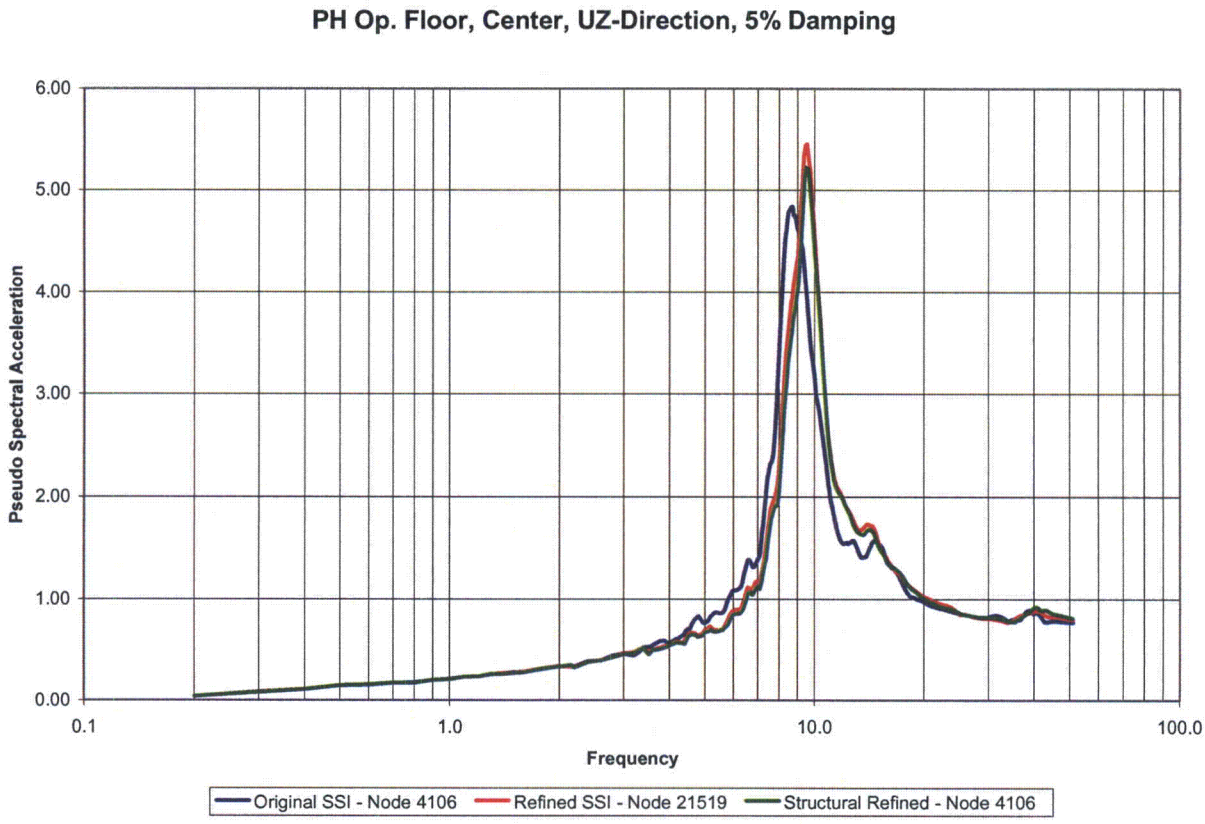

Figure 03.07.02-25.14: Center of Pump House Operating Floor, Z-direction, 5% Damping

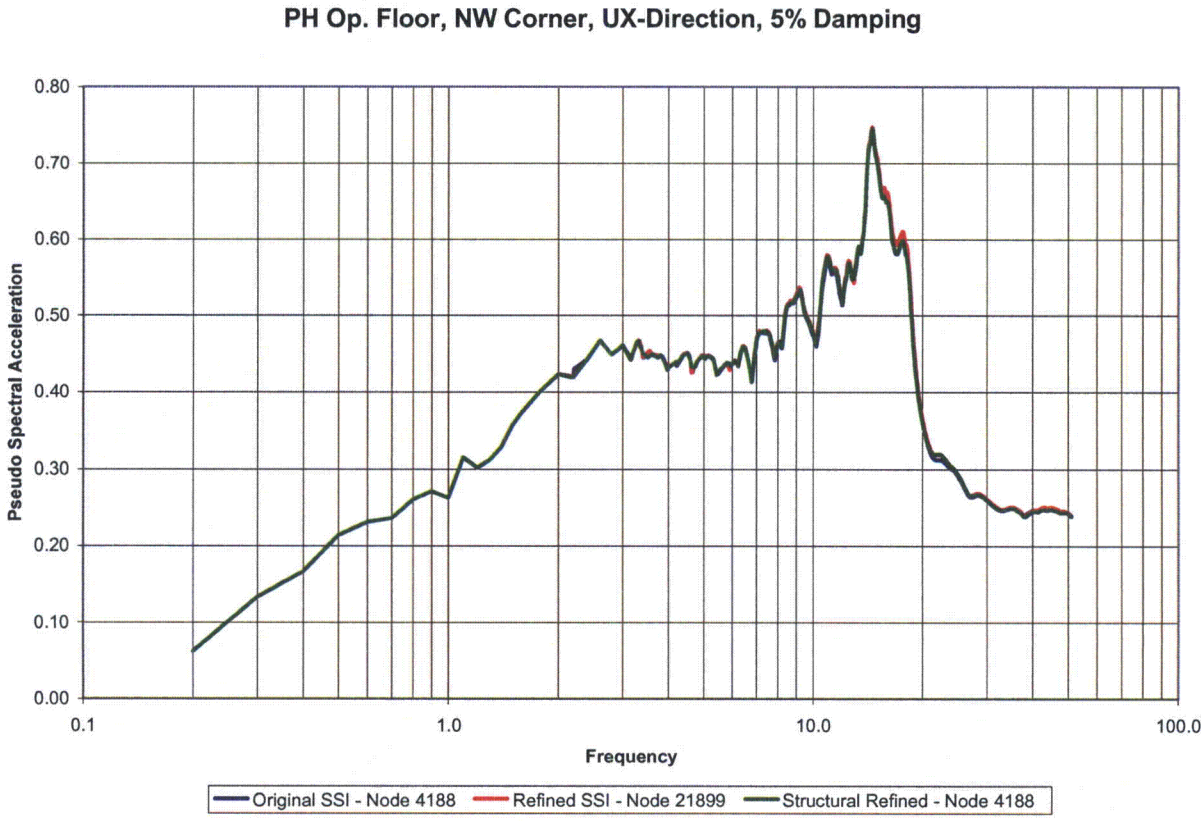

Figure 03.07.02-25.15: Pump House Operating Floor, NW Corner, X-direction, 5% Damping

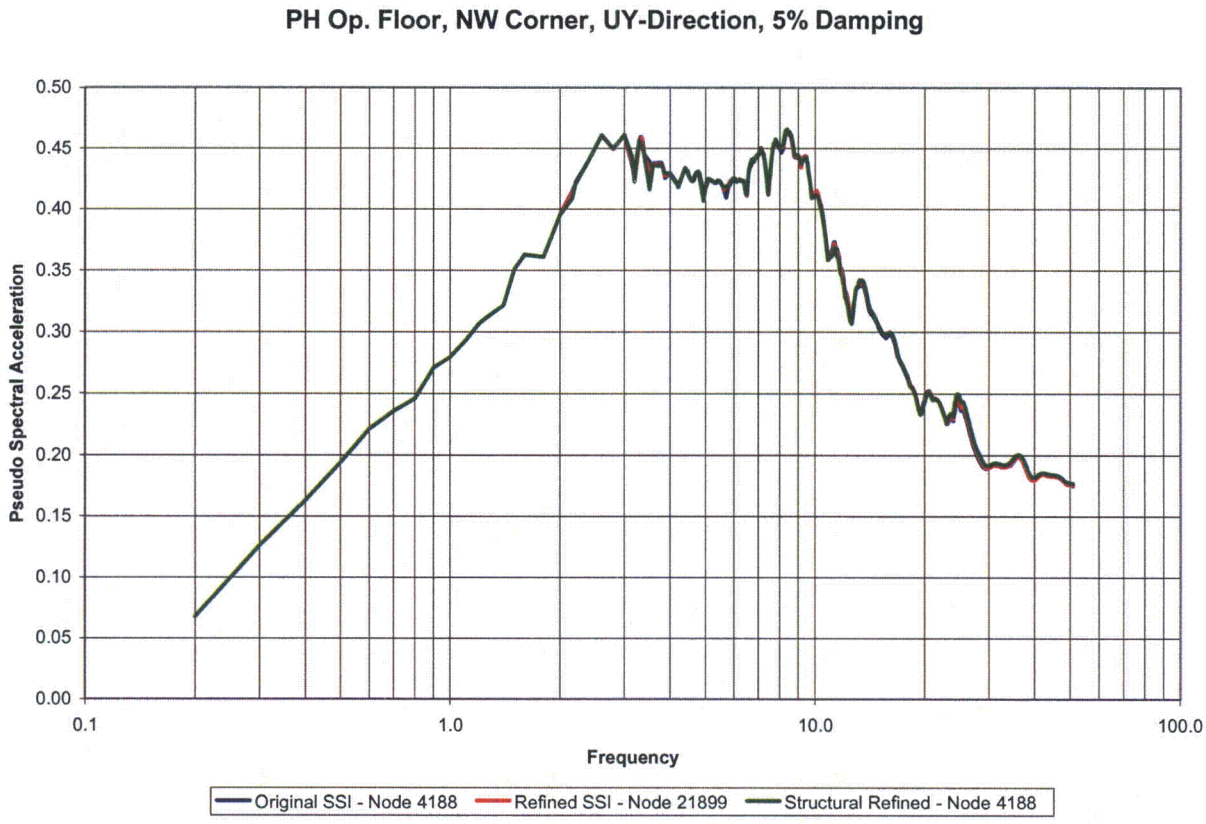

Figure 03.07.02-25.16: Pump House Operating Floor, NW Corner, Y-direction, 5% Damping

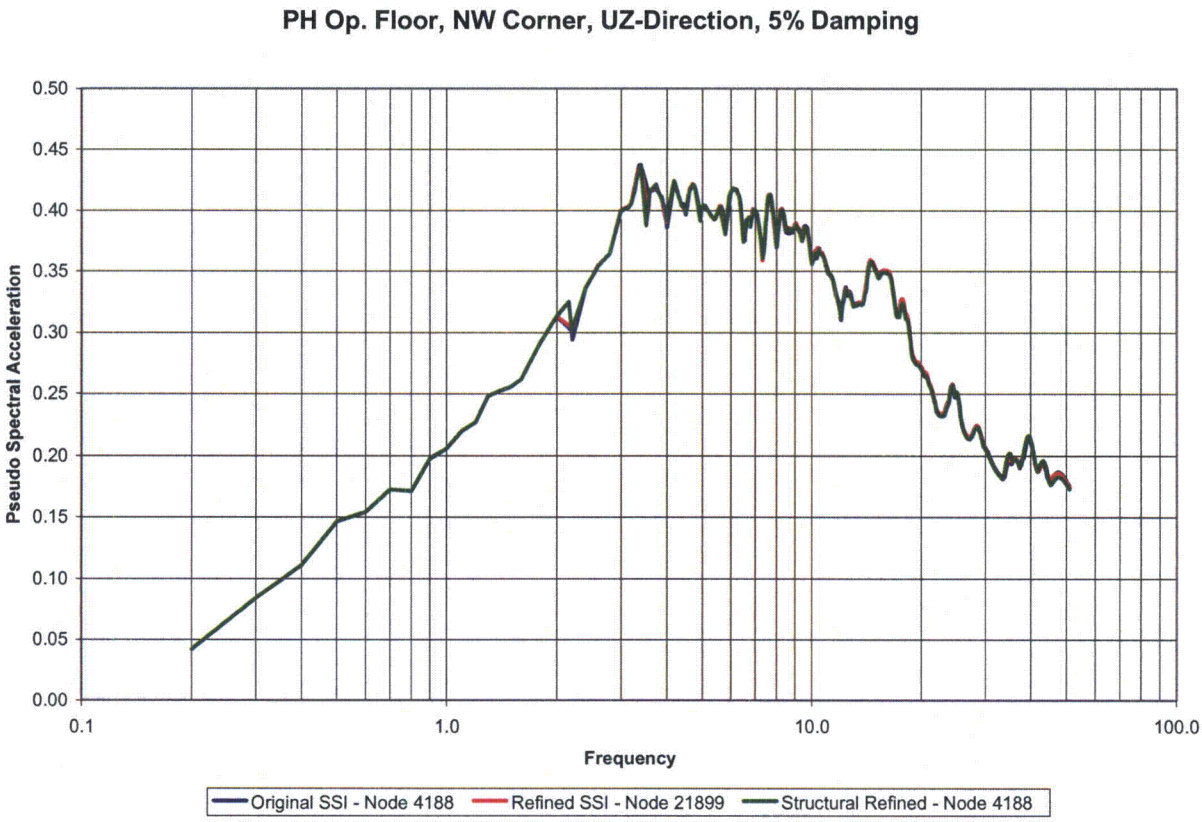

Figure 03.07.02-25.17: Pump House Operating Floor, NW Corner, Z-direction, 5% Damping

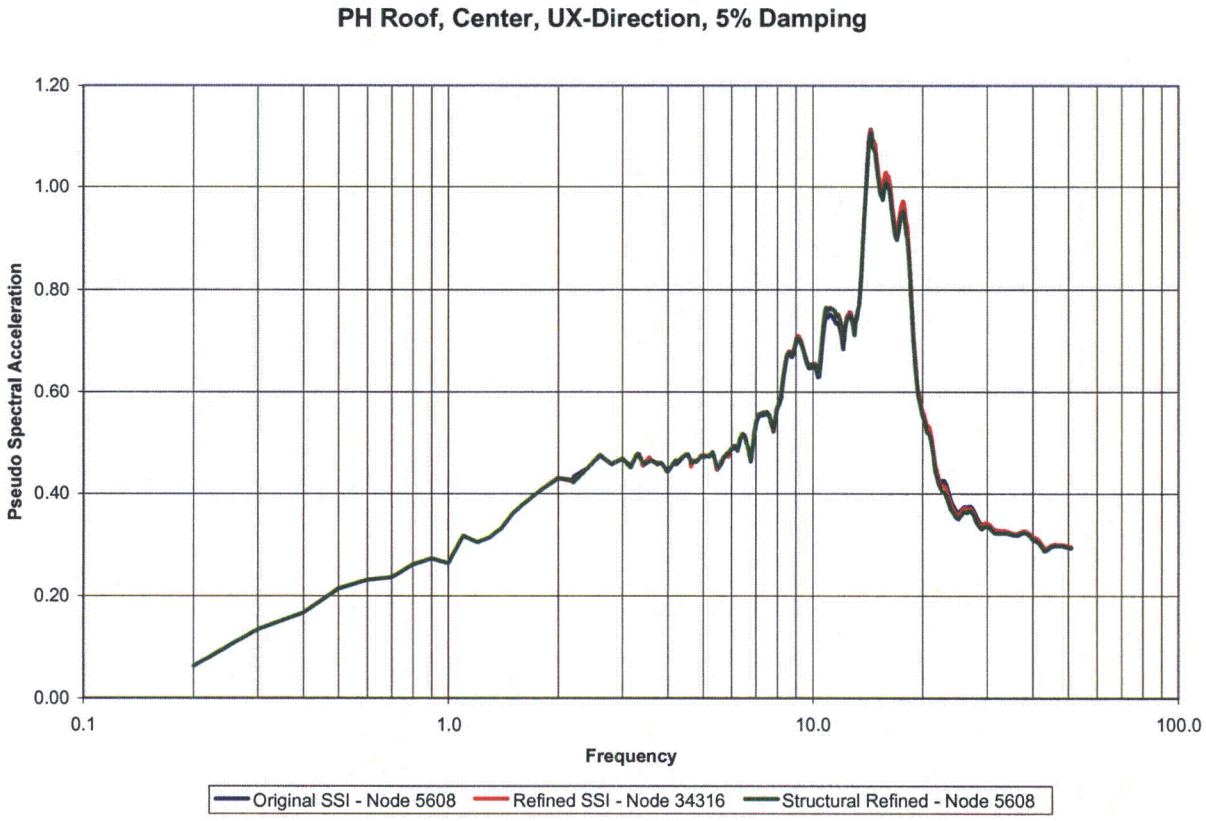

Figure 03.07.02-25.18: Center of Pump House Roof, X-direction, 5% Damping

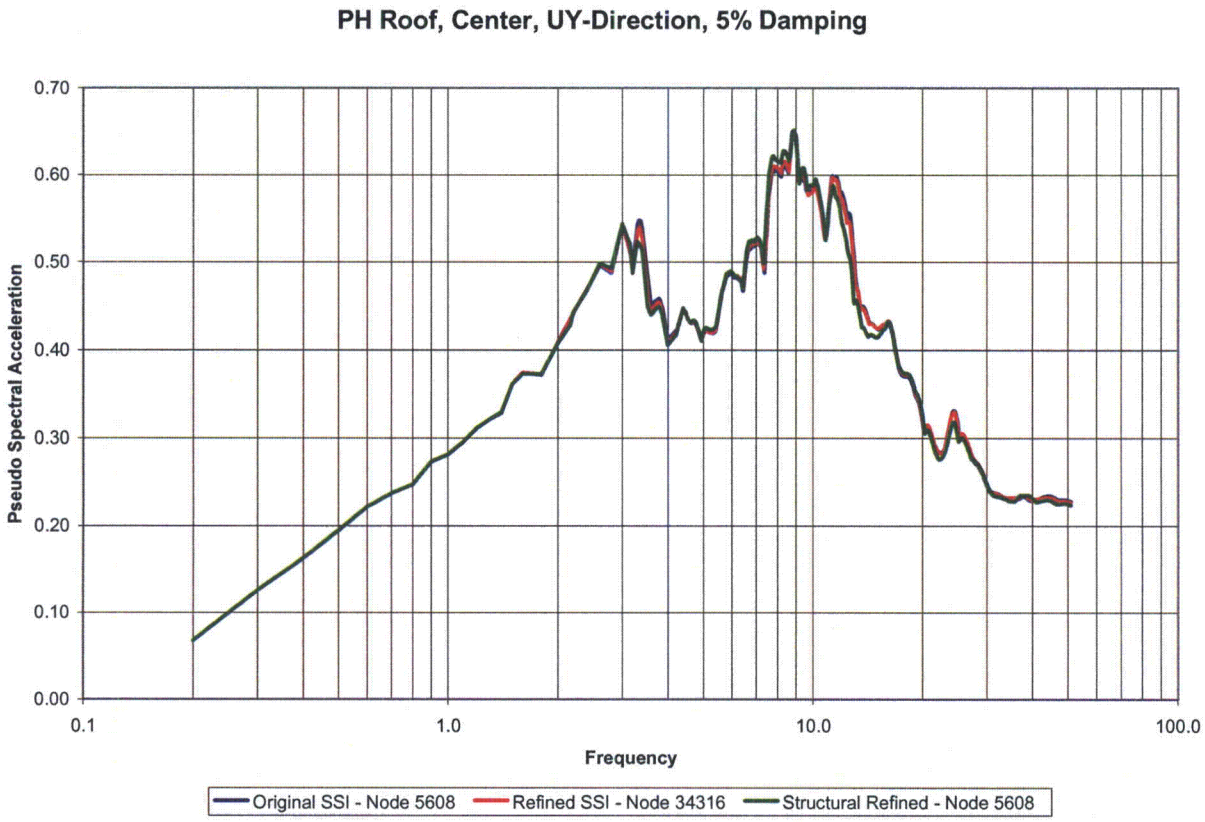

Figure 03.07.02-25.19: Center of Pump House Roof, Y-direction, 5% Damping

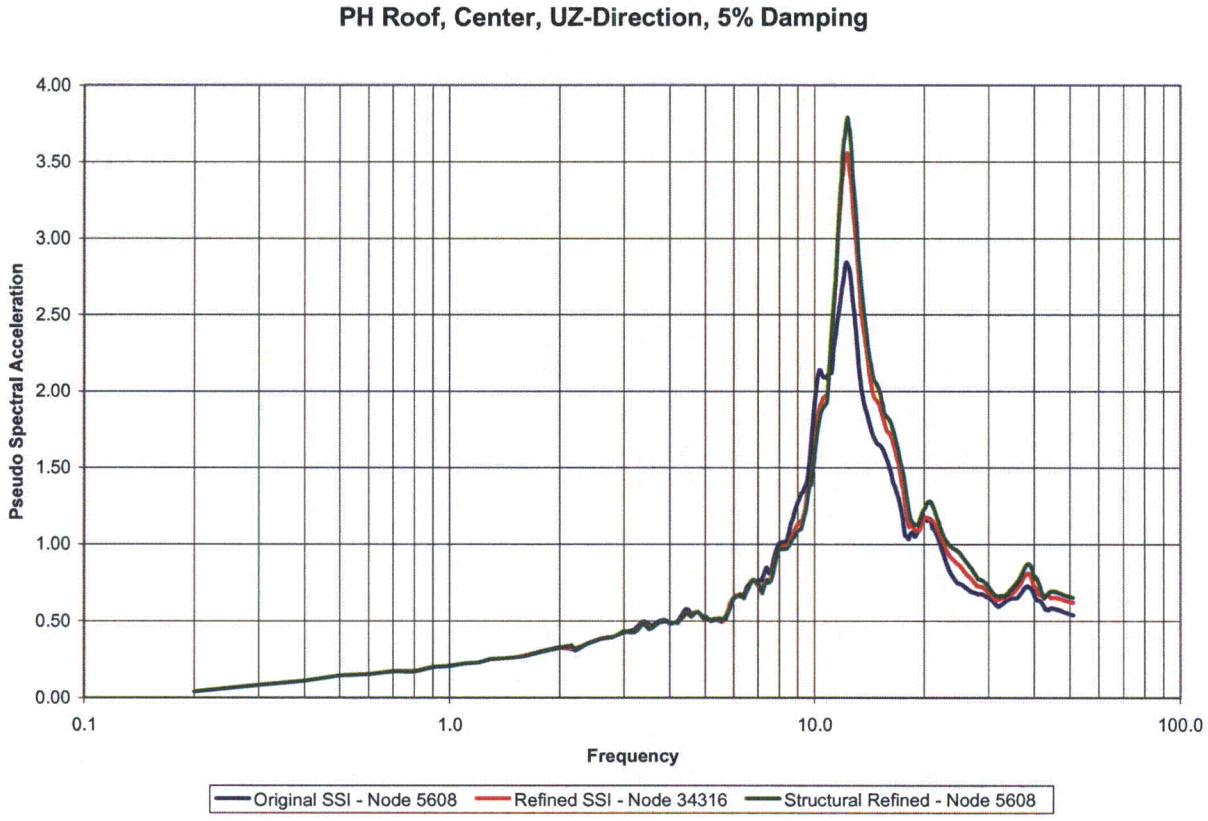

Figure 03.07.02-25.20: Center of Pump House Roof, Z-direction, 5% Damping

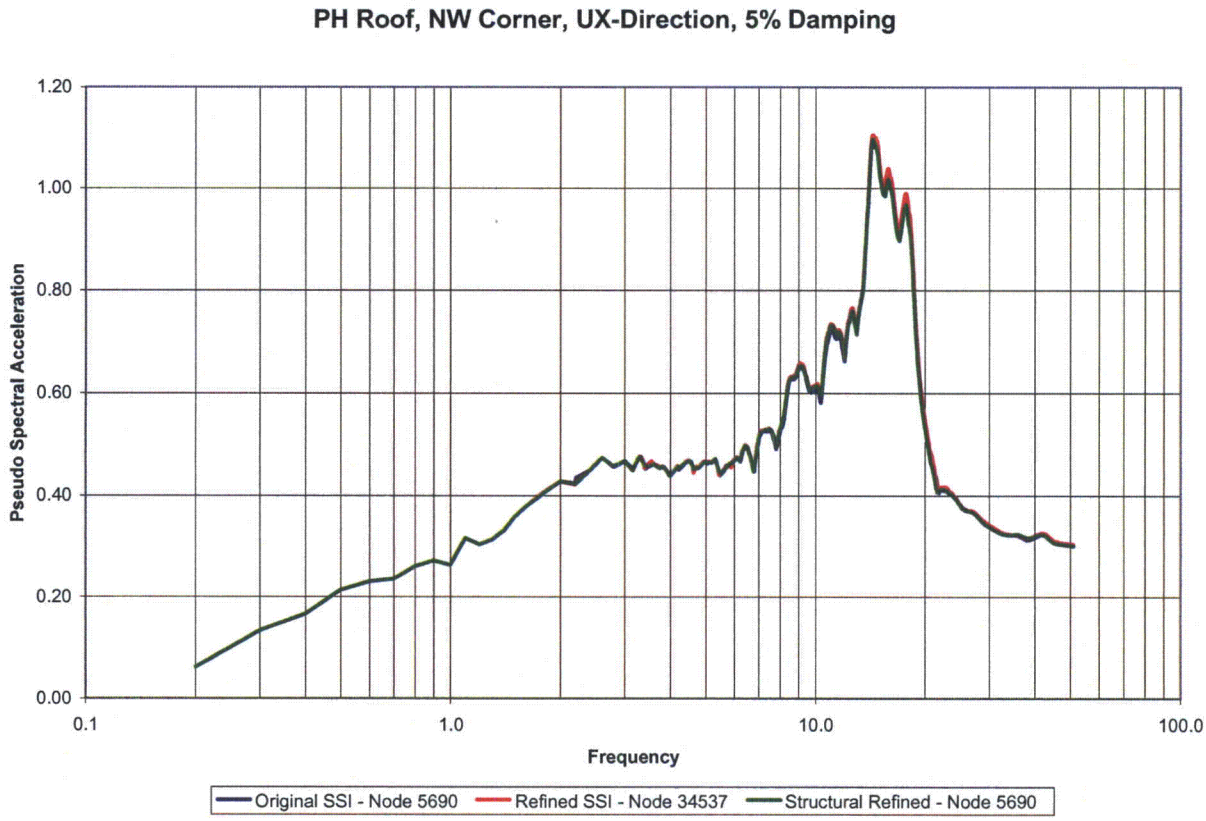

Figure 03.07.02-25.21: Pump House Roof, NW Corner, X-direction, 5% Damping

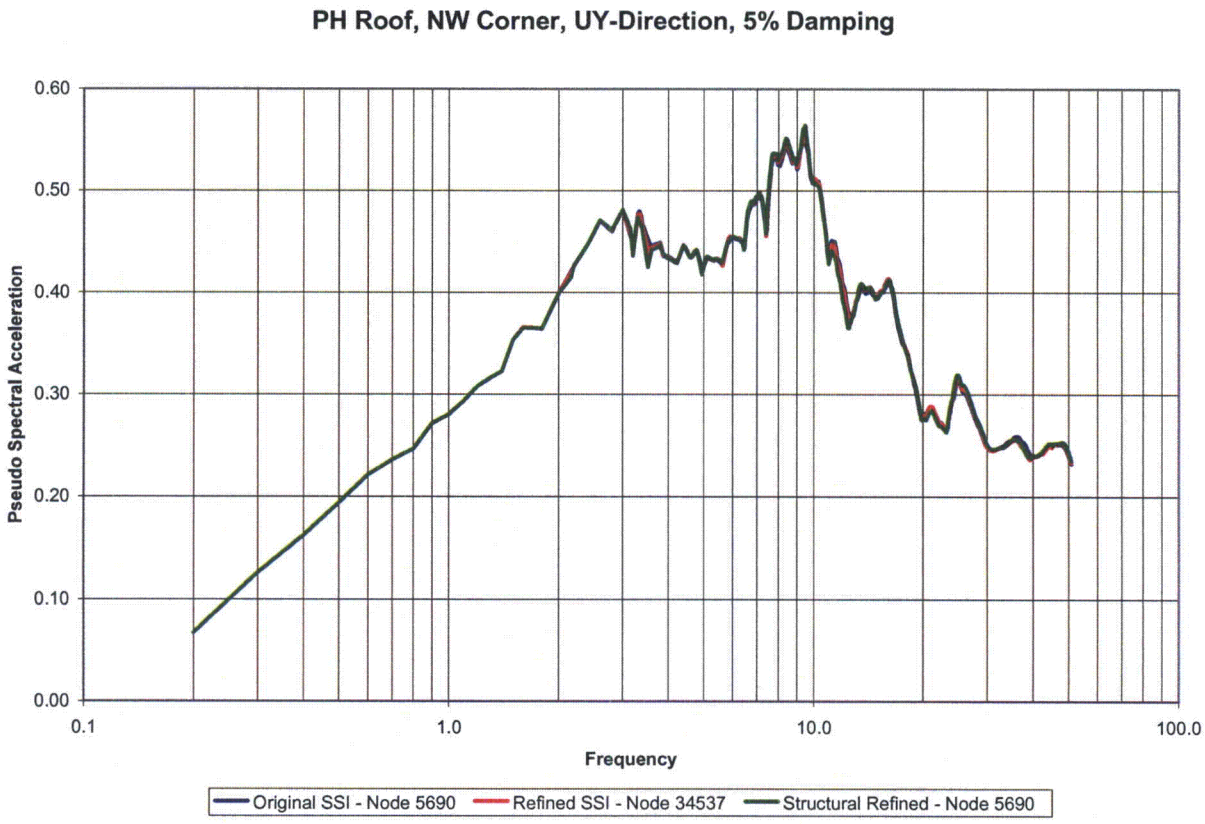

Figure 03.07.02-25.22: Pump House Roof, NW Corner, Y-direction, 5% Damping

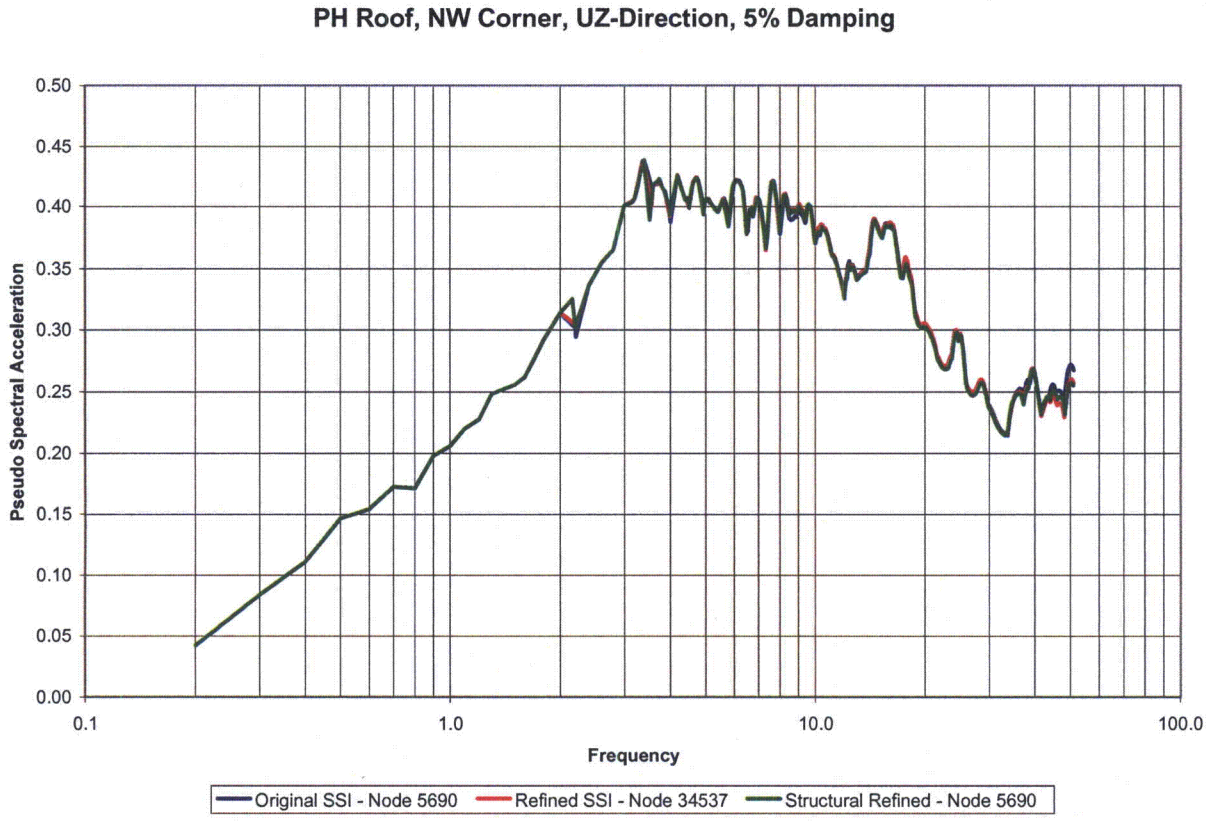

Figure 03.07.02-25.23: Pump House Roof, NW Corner, Z-direction, 5% Damping

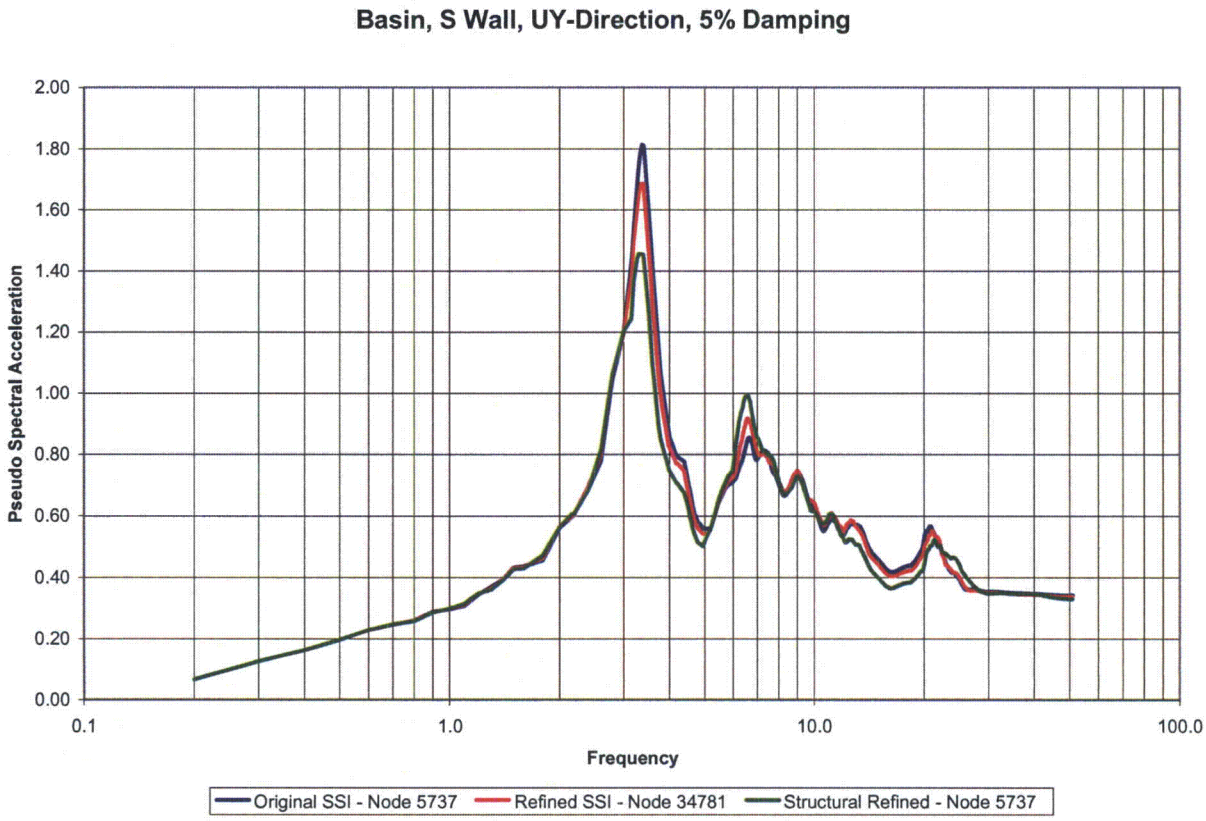

Figure 03.07.02-25.24: Basin South Wall, Y-direction, 5% Damping

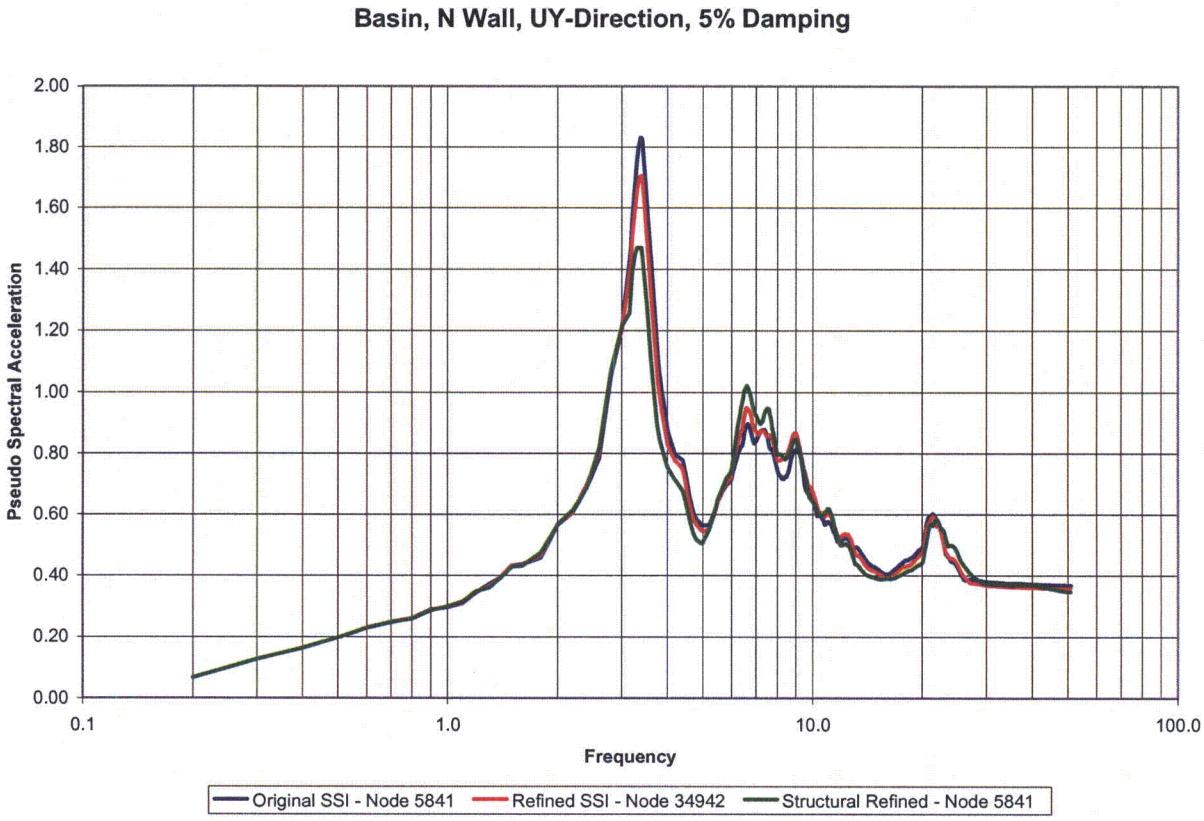

Figure 03.07.02-25.25: Basin North Wall, Y-direction, 5% Damping

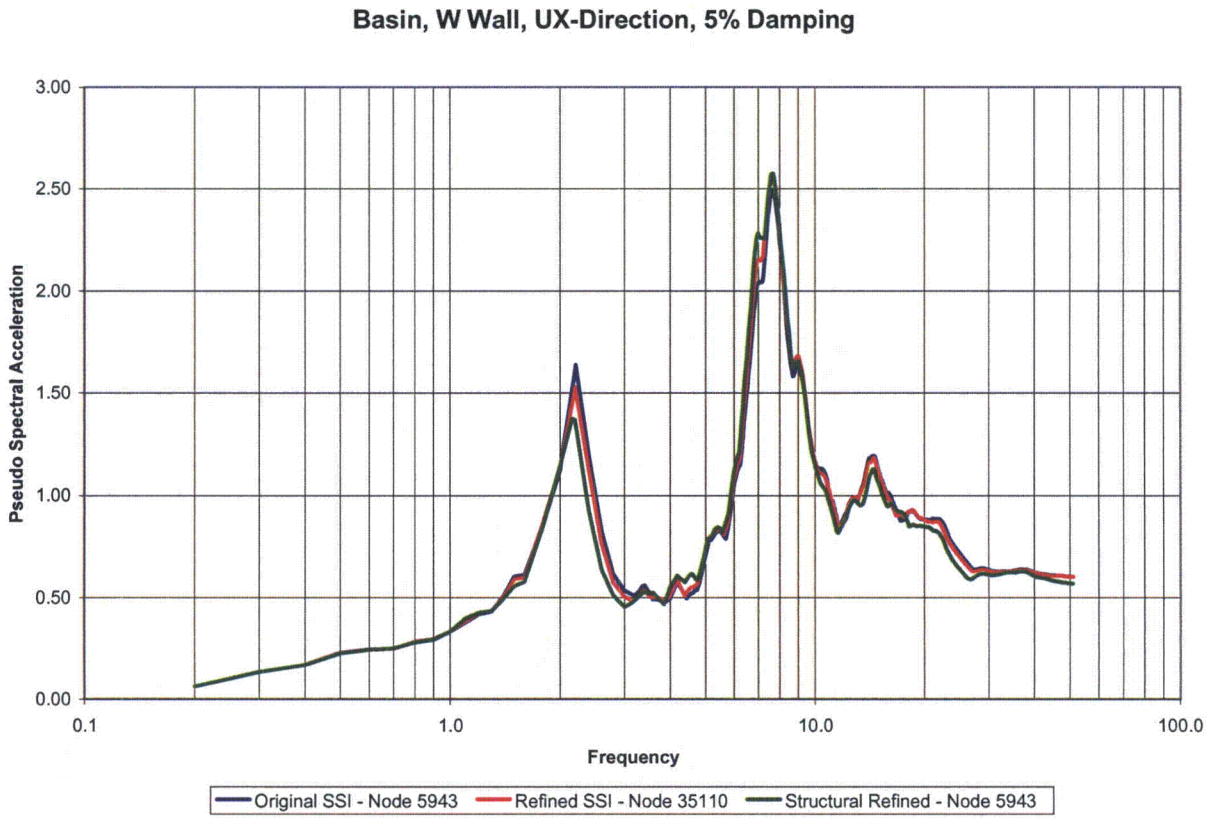

Figure 03.07.02-25.26: Basin West Wall, X-direction, 5% Damping

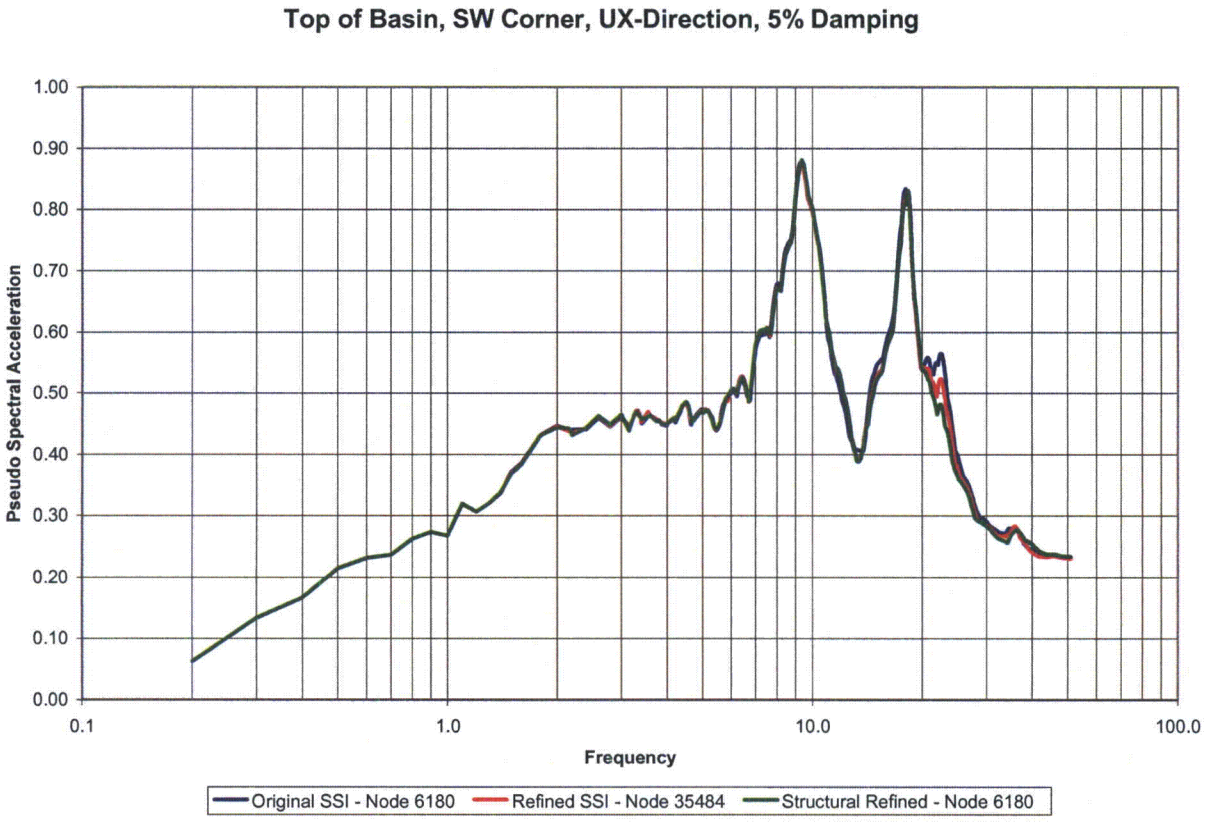

Figure 03.07.02-25.27: Top of Basin, SW Corner, X-direction, 5% Damping

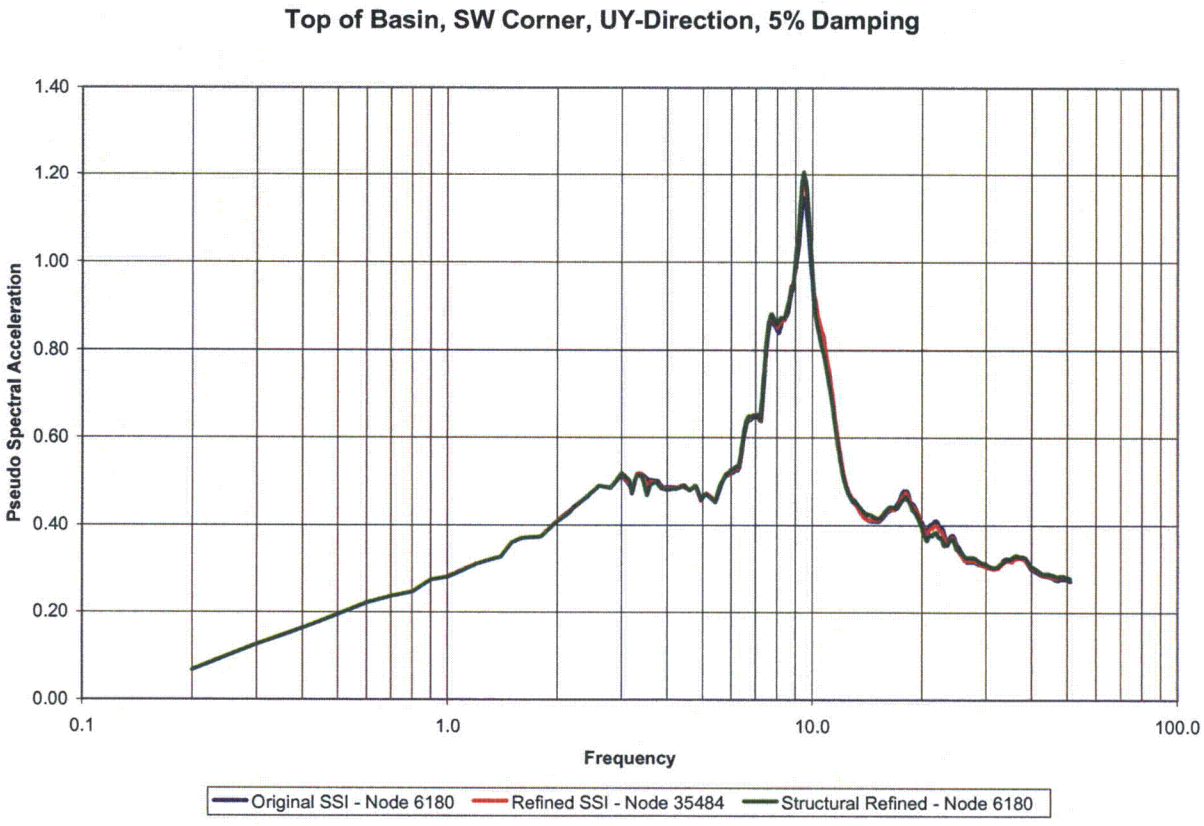

Figure 03.07.02-25.28: Top of Basin, SW Corner, Y-direction, 5% Damping

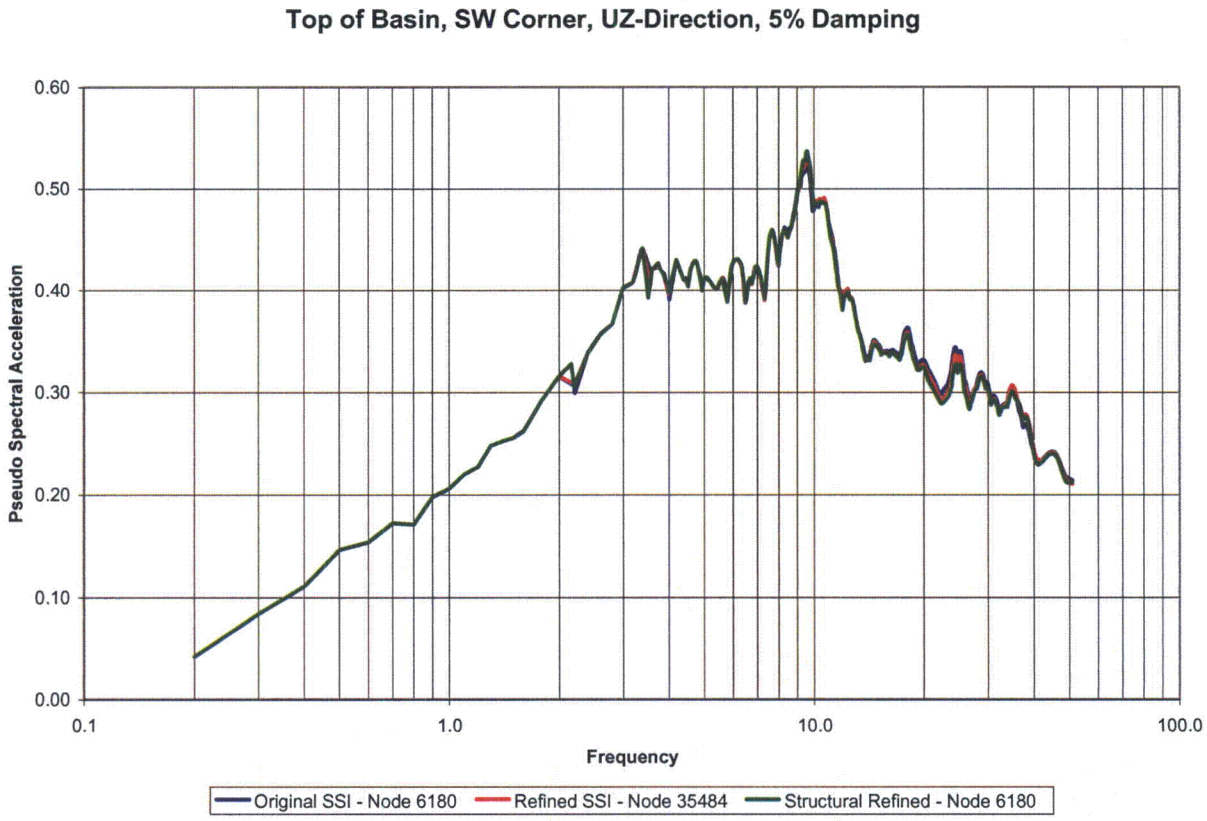

Figure 03.07.02-25.29: Top of Basin, SW Corner, Z-direction, 5% Damping

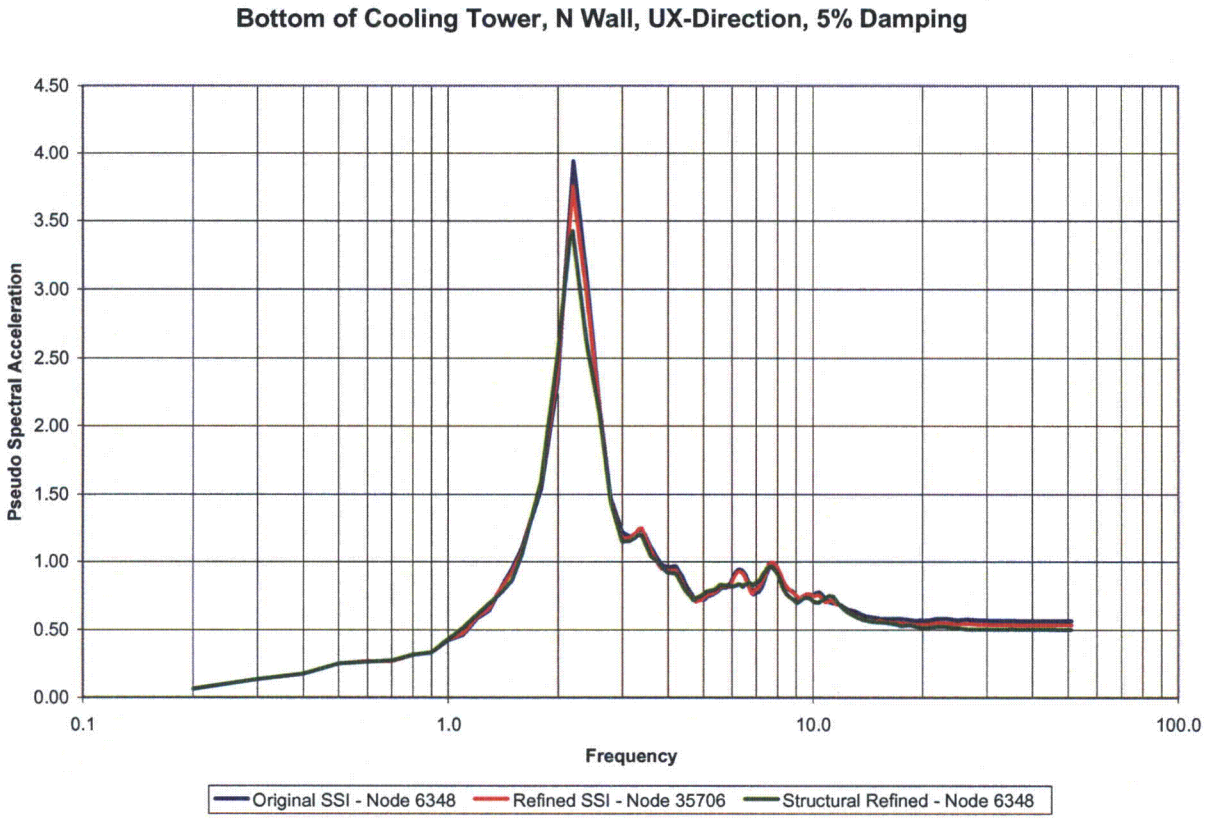

Figure 03.07.02-25.30: Bottom of Cooling Tower North Wall, X-direction, 5% Damping

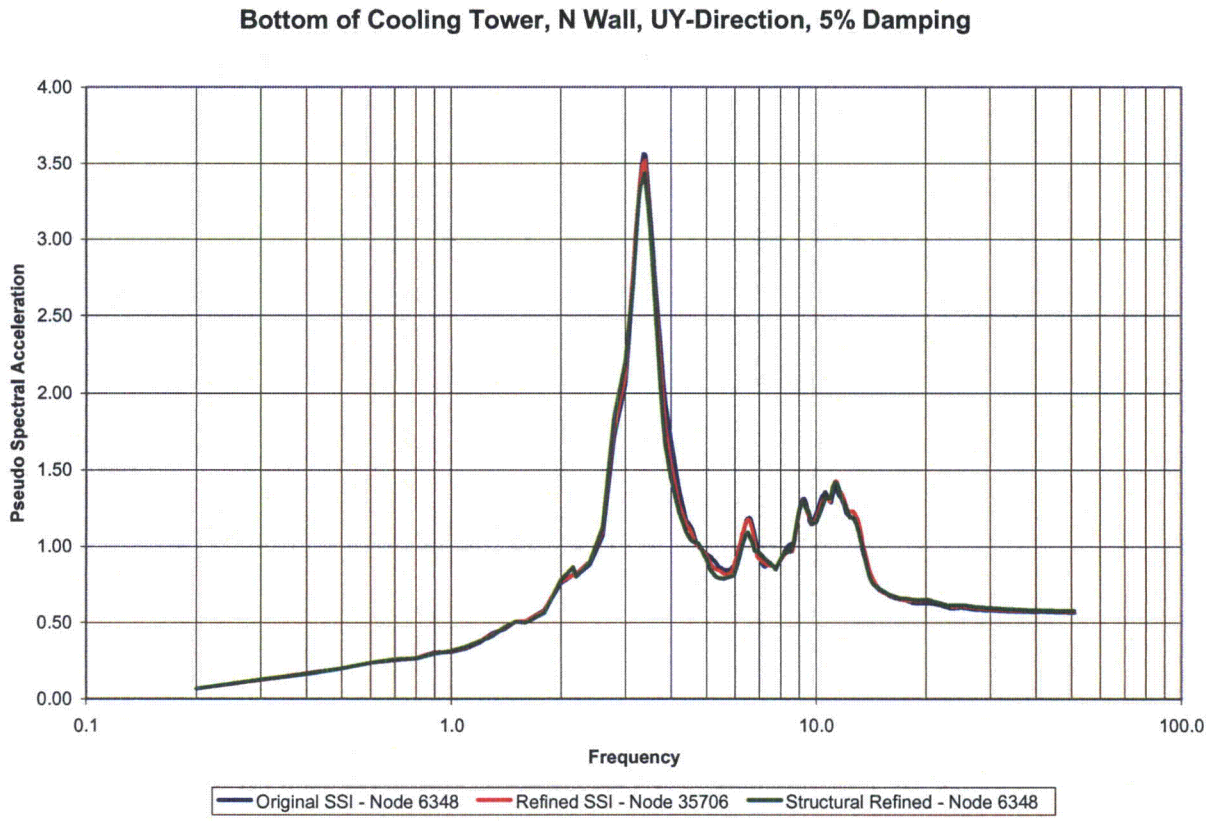

Figure 03.07.02-25.31: Bottom of Cooling Tower North Wall, Y-direction, 5% Damping

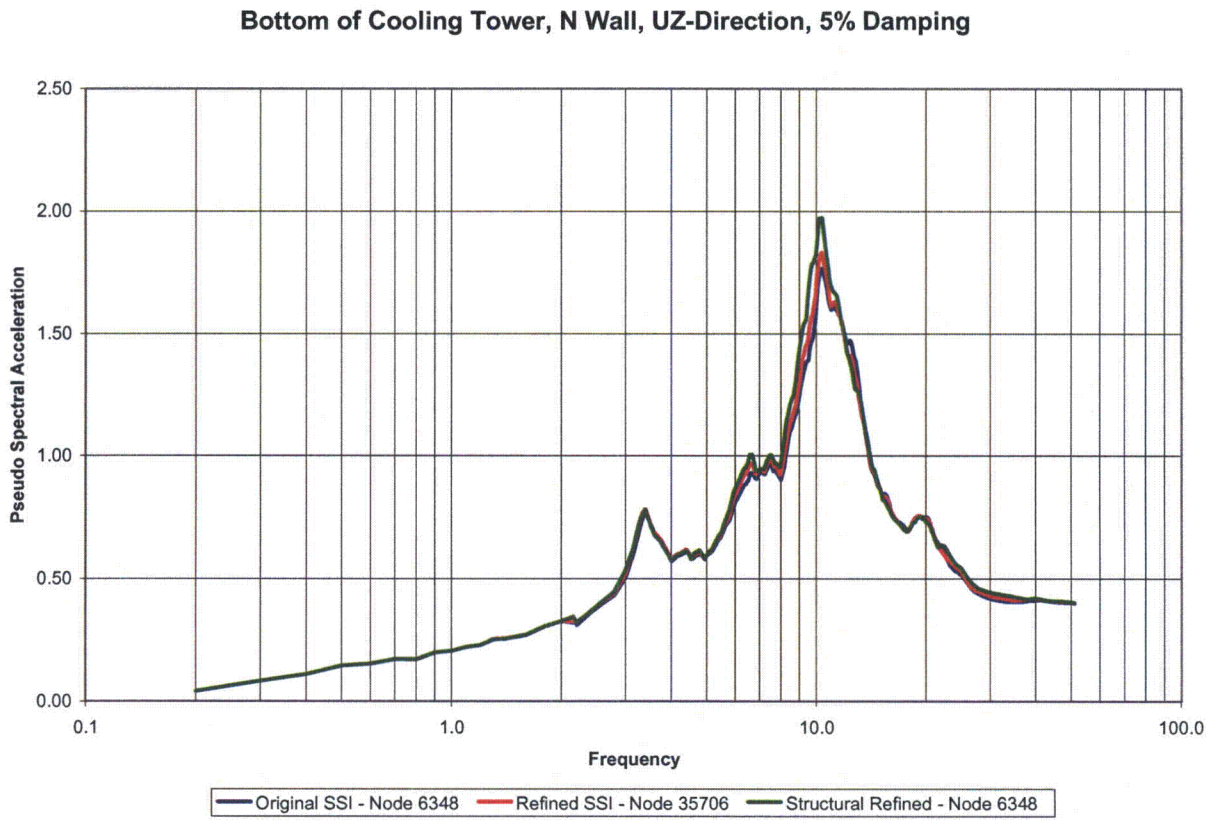

Figure 03.07.02-25.32: Bottom of Cooling Tower North Wall, Z-direction, 5% Damping

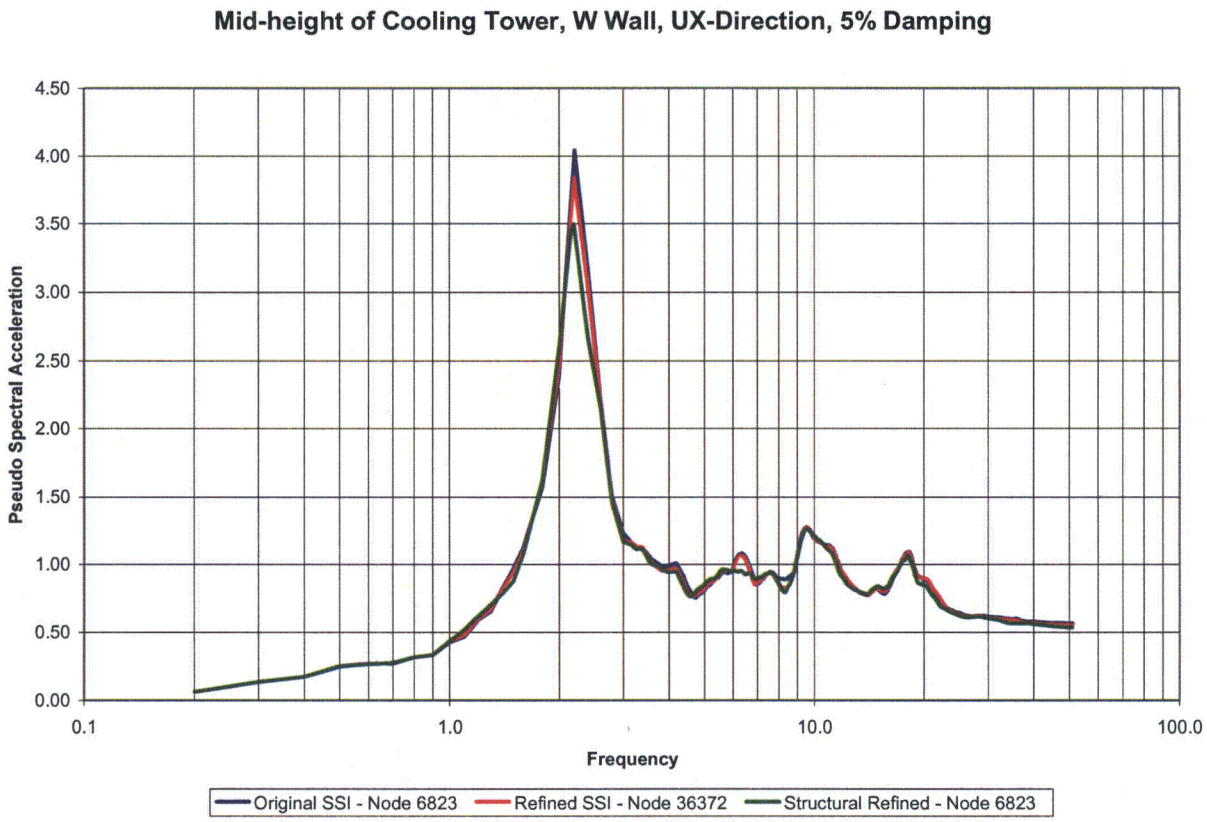

Figure 03.07.02-25.33: Mid-height of Cooling Tower West Wall, X-direction, 5% Damping

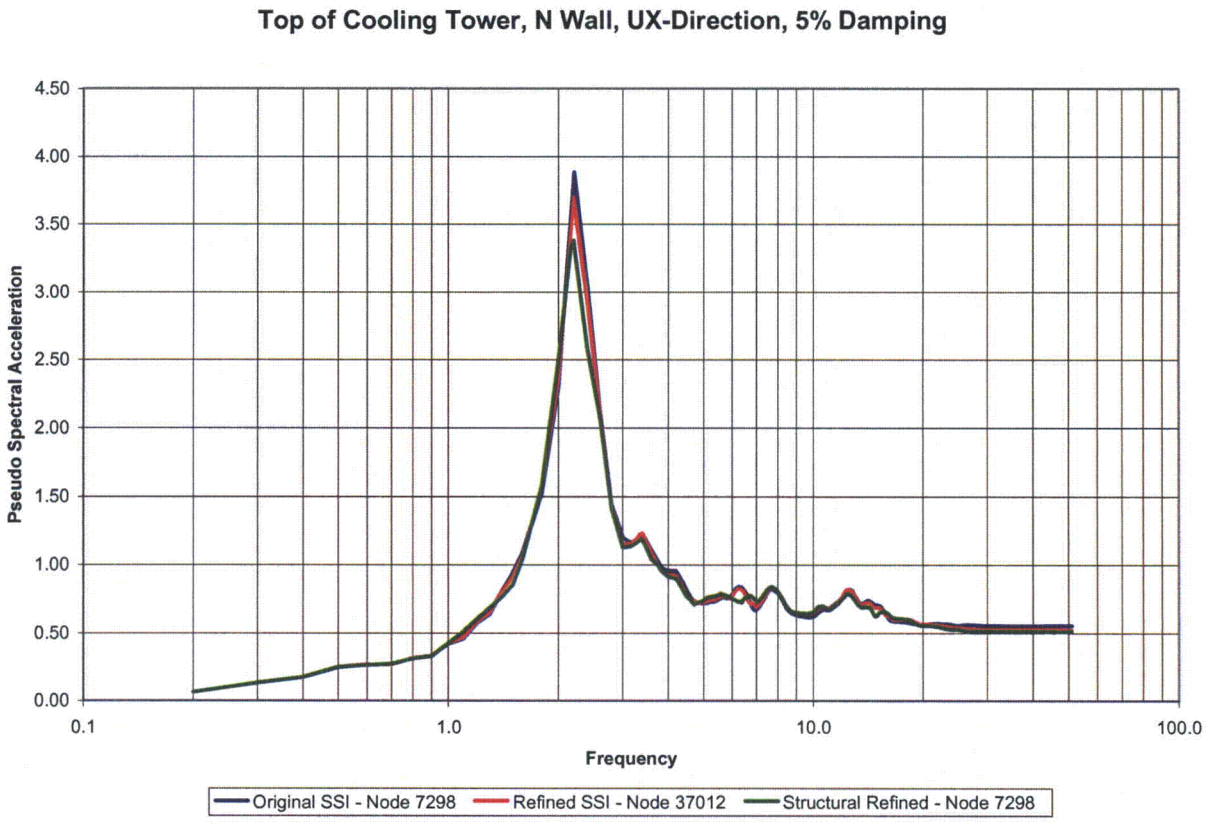

Figure 03.07.02-25.34: Top of Cooling Tower North Wall, X-direction, 5% Damping

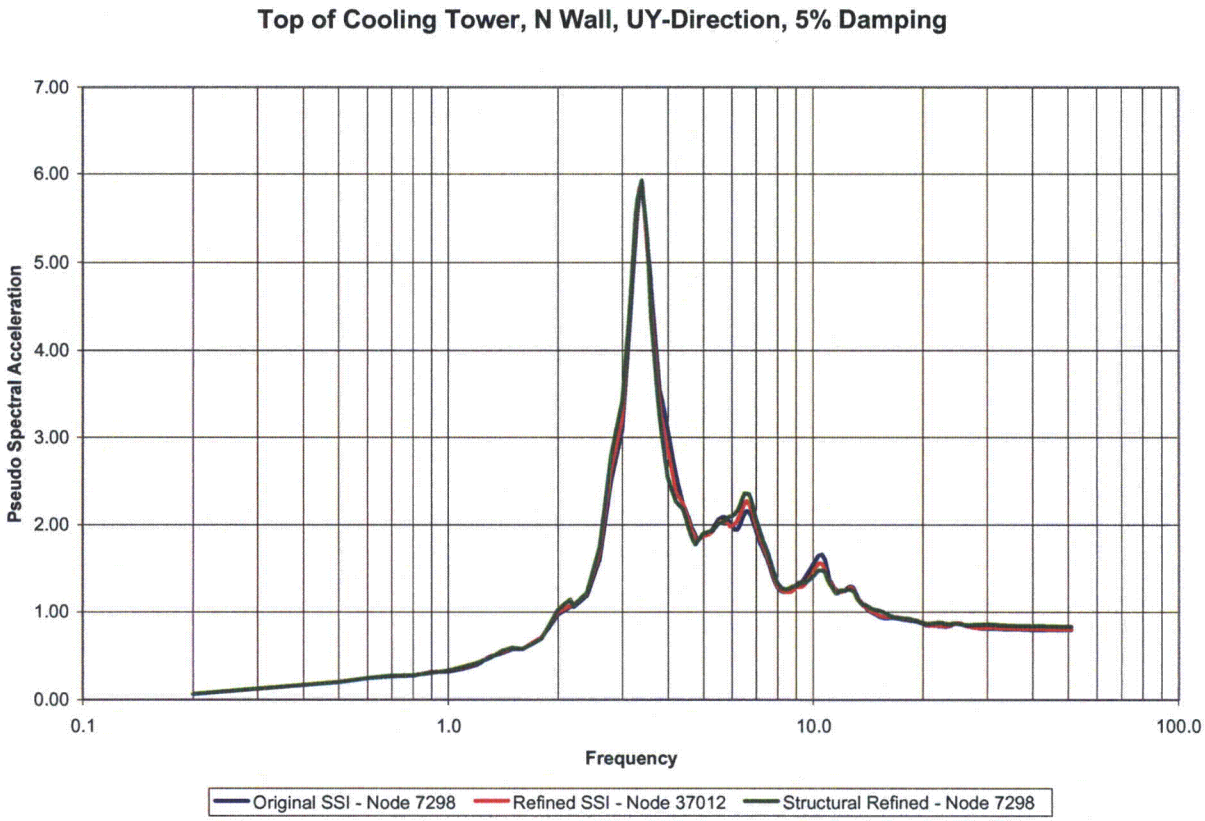

Figure 03.07.02-25.35: Top of Cooling Tower North Wall, Y-direction, 5% Damping

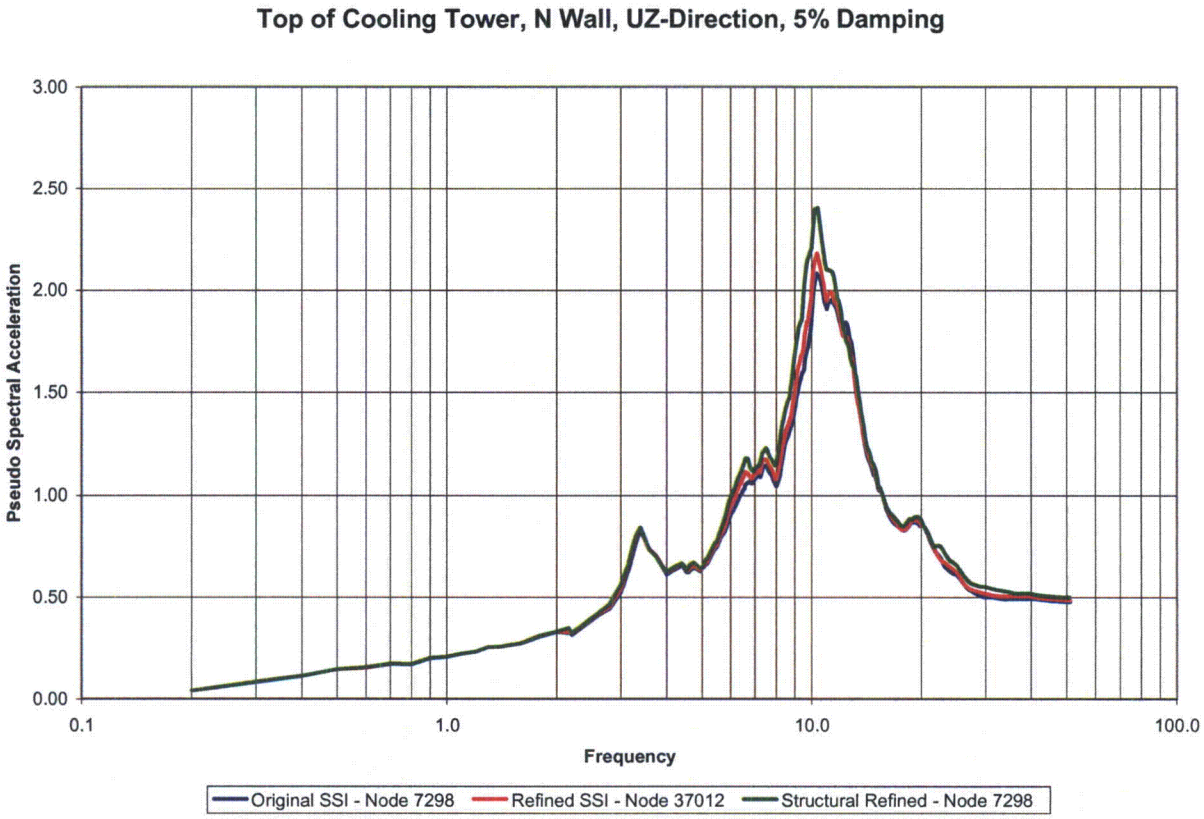

Figure 03.07.02-25.36: Top of Cooling Tower North Wall, Z-direction, 5% Damping

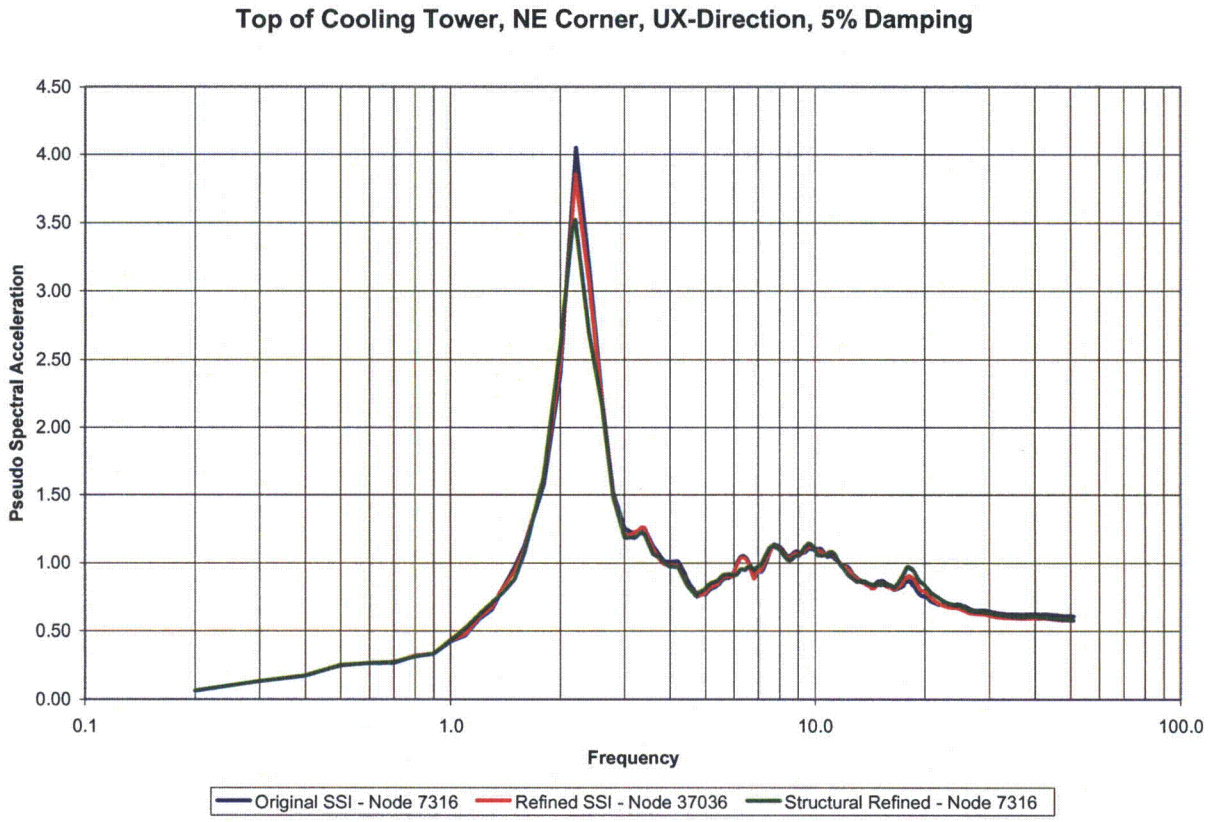

Figure 03.07.02-25.37: Top of Cooling Tower, NE Corner, X-direction, 5% Damping

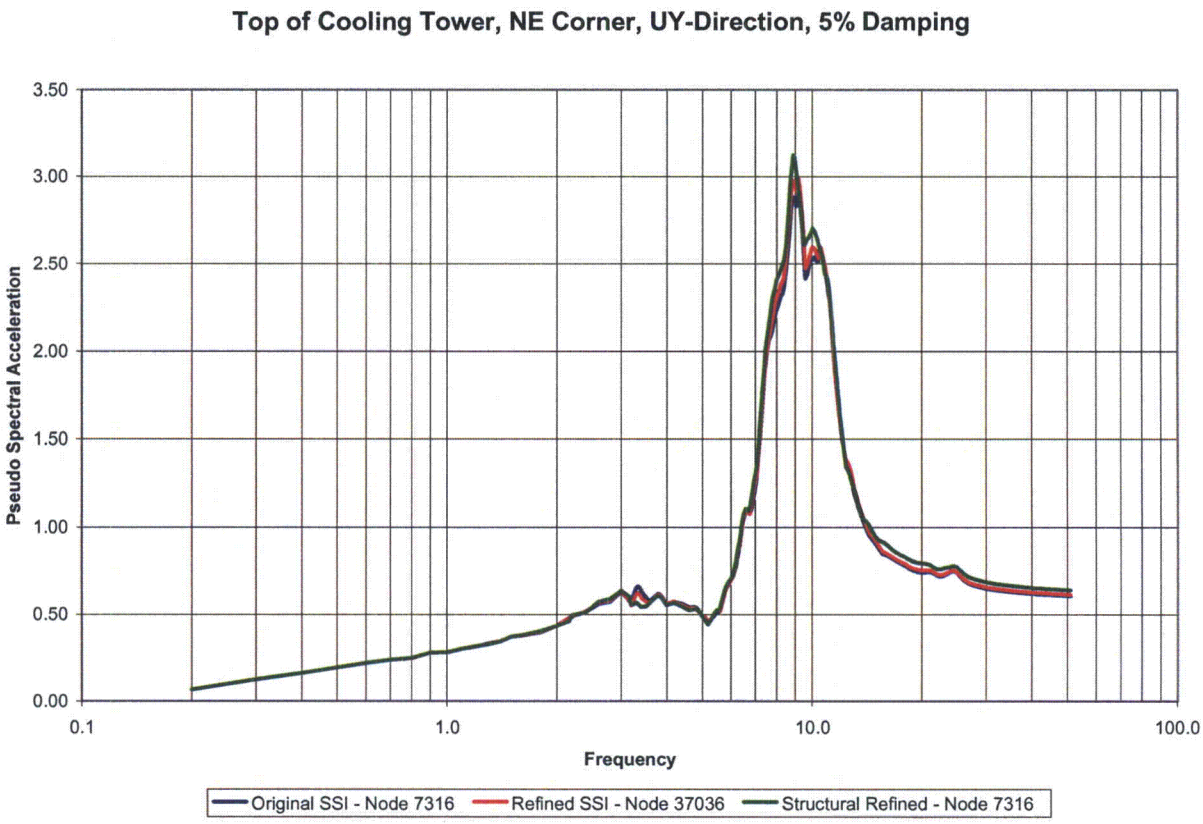

Figure 03.07.02-25.38: Top of Cooling Tower, NE Corner, Y-Direction, 5% Damping

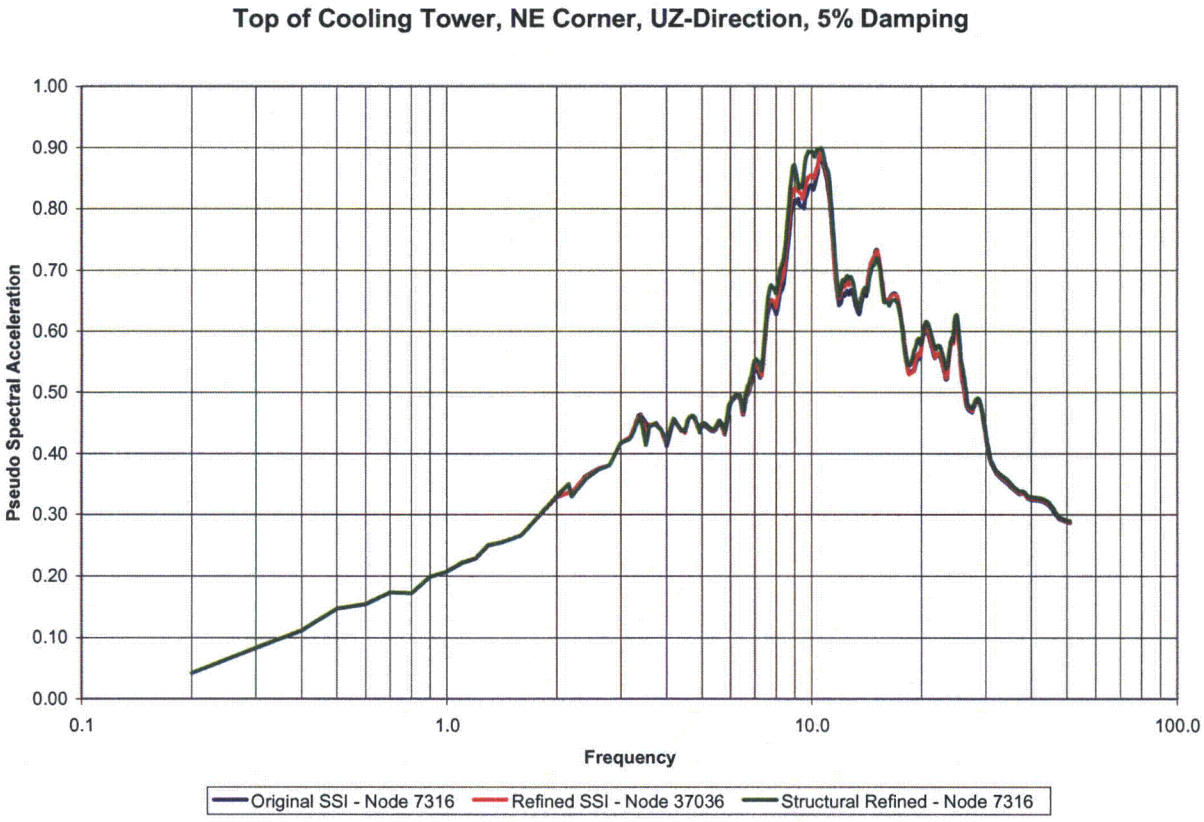

Figure 03.07.02-25.39: Top of Cooling Tower, NE Corner, Z-direction, 5% Damping

Table 03.07.02-25.1: Comparison of Maximum Accelerations

Maximum Accelerations (g)					
Node	**Location**	**Direction**	**Original SSI Mesh**	**Structural Refined Mesh**	**Ratio (Refined / Original)**
4098	PH Operating Floor, W Wall	X	0.242	0.243	1.00
		Y	0.156	0.157	1.01
		Z	0.126	0.127	1.01
4106	PH Operating Floor, Center	X	0.221	0.219	0.99
		Y	0.162	0.162	1.01
		Z	0.739	0.747	1.01
4188	PH Operating Floor, NW Corner	X	0.217	0.218	1.00
		Y	0.166	0.167	1.01
		Z	0.140	0.140	1.00
5608	Top of PH Roof, Center	X	0.284	0.282	0.99
		Y	0.218	0.214	0.98
		Z	0.473	0.598	1.26
5690	Top of PH Roof, NW Corner	X	0.283	0.283	1.00
		Y	0.198	0.200	1.01
		Z	0.152	0.152	1.00
5707	Top of PH Roof, NE Corner	X	0.283	0.281	0.99
		Y	0.188	0.184	0.98
		Z	0.148	0.148	1.00
5737	Basin S Wall	X	0.175	0.172	0.98
		Y	0.337	0.321	0.95
		Z	0.141	0.141	1.00
5841	Basin N Wall	X	0.176	0.173	0.98
		Y	0.360	0.342	0.95
		Z	0.142	0.141	1.00
5943	Basin W Wall	X	0.585	0.553	0.94
		Y	0.220	0.226	1.02
		Z	0.157	0.159	1.01
6180	Top of Basin Wall, SW Corner	X	0.223	0.222	0.99
		Y	0.247	0.253	1.02
		Z	0.159	0.160	1.00
6348	Bottom, Middle, Cooling Tower N Wall	X	0.563	0.499	0.89
		Y	0.559	0.567	1.02
		Z	0.370	0.392	1.06
6410	Top of Basin Wall, NW Corner	X	0.260	0.251	0.97
		Y	0.251	0.249	0.99
		Z	0.160	0.159	1.00
6444	Top of Basin Wall, NE Corner	X	0.215	0.216	1.01
		Y	0.243	0.246	1.01
		Z	0.159	0.160	1.01

Table 03.07.02-25.1: Comparison of Maximum Accelerations (continued)

Maximum Accelerations (g)					
Node	**Location**	**Direction**	**Original SSI Mesh**	**Structural Refined Mesh**	**Ratio (Refined / Original)**
6823	Mid-height Cooling Tower W Wall	X	0.558	0.533	0.96
		Y	0.422	0.441	1.05
		Z	0.192	0.193	1.01
7208	Top of Cooling Tower, SW Corner	X	0.587	0.579	0.99
		Y	0.610	0.640	1.05
		Z	0.257	0.261	1.02
7298	Top, Middle, Cooling Tower N Wall	X	0.550	0.509	0.93
		Y	0.787	0.825	1.05
		Z	0.439	0.470	1.07
7316	Top of Cooling Tower, NE Corner	X	0.596	0.566	0.95
		Y	0.590	0.623	1.05
		Z	0.254	0.259	1.02

RAI 03.07.02-26

QUESTION:

Follow-up Question to RAI 03.07.02-17 (STP-NRC-100035)

10CFR50, Appendix S requires that evaluation for SSE must take into account soil-structure interaction (SSI) effects. To properly account for SSI effect, SSI model should be adequate for transmitting the maximum frequency content of interest which for the site is the PGA frequency (33 Hz) of the site specific GMRS. In the response to Item 1 of RAI 03.07.02-17, the applicant has provided the criteria ((H=Vs / (5* Ft-s)) for determining the maximum soil layer thicknesses in the SASSI SSI model to adequately transmit the highest frequency of interest for mean soil properties. However for the lower bound soil case, the highest transmitted frequency for the in-situ and backfill materials calculated using the criteria stated above is about 26 Hz. As justification, the applicant further states that this lower cutoff frequency (26 Hz) is justified in light of the recommendation of ASCE 4-98, Section 3.3.3.5. However, NRC has not endorsed ASCE-98 acceptance criteria for selecting the cut-off frequency for the SSI analysis. The selection of maximum layer thicknesses based on the shear wave length criteria [as shown by the applicant in Equation H=Vs / (5* Ft-s)], is acceptable to the staff to ensure that a correct variation of ground motion with depth is calculated for site response solution in the SASSI finite element model. In addition for the impedance solution aspect of the SASSI SSI model, the maximum horizontal dimension of the excavated soil elements should also satisfy the above shear wave length criteria, where H is the maximum horizontal dimension of soil elements. As such for the lower bound soil case, the applicant is requested to provide a quantitative assessment demonstrating that the results using the existing soil mesh size will be conservative when compared to an analysis using a more refined soil mesh size (meeting the criteria stated above for both element thickness and horizontal element dimension) capable of transmitting a frequency of 33 Hz. The staff needs this information to ensure that the use of existing soil mesh size used in the SSI analysis adequately accounts for the SSE frequencies of interest in the evaluation of SSI effect.

RESPONSE:

Based on the discussions in the August 4, 2010 NRC public meeting in Rockville, MD., this issue is addressed by the refined mesh study for upper bound in-situ soil, as described in the Supplement 2 response to RAI 03.07.02-24, which is being submitted concurrently with this response.

No additional COLA revision is required as a result of this response.

RAI 03.07.02-27

QUESTION:

Follow-up to Question 03.07.02-19 (STP-NRC-100093)

The COLA markup provided in the response to RAI 03.07.02-19, Revision 1 describes the procedure for establishing the SSE input at the foundation level of the RWB. According to this procedure, five interaction nodes at the depth corresponding to the bottom elevation of the RWB foundation will be added to the 3-D SSI model of the Reactor Building (RB). These five nodes correspond to the four corners and the center of the RWB foundation. The RB SSI model is analyzed for the STP site-specific SSE. The envelop of the resulting response spectra at the foundation level of the RWB (based on the average of responses at the 5 nodes) and 0.3g Regulatory Guide 1.60 response spectra will be used as the design response spectra for II/I evaluation of the RWB. This procedure for estimating the foundation input motion for the seismic SSI response analysis of non-Category I structures is acceptable. However, the procedure does not address the potential increase in dynamic soil pressures on the exterior walls of RWB due to the SSSI effects. The applicant is requested to describe how the increase in dynamic soil pressures on the RWB walls due to the SSSI effects will be accounted for in the design of the RWB exterior walls. The staff needs this information to ensure that the RWB exterior walls are adequately designed to maintain its structural integrity during a SSE in controlling any potential release of radioactive materials to the environment.

RESPONSE:

In order to assess the structure-soil-structure interaction (SSSI) effects on the lateral pressures on the walls of the Radwaste Building (RWB), two dimensional (2D) soil-structure interaction (SSI) analyses were performed for the RWB with and without the adjacent Reactor Building and RSW Piping Tunnel. For the SSSI details refer to the SSSI analysis of the East-West 2D Section of the RSW Piping Tunnel between the RWB and RB described in Part 1 of Supplement 1 response to RAI 03.07.02-24 which was submitted with letter U7-C-STP-NRC-100253, dated November 29, 2010.

The resulting seismic soil pressures on the east and west walls of the RWB from the SSSI analysis are shown in Figures 3H.3-50 and 3H.3-51 in Enclosure 1, respectively.

The RWB east and west walls have been evaluated considering the SSSI seismic soil pressures in Figures 3H.3-50 and 3H.3-51. The evaluation confirmed that the existing design as reported in response to RAI 03.08.04-18, Revision 1, (submitted with letter U7-C-STP-NRC-100124 dated June 2, 2010) is adequate.

Revision 4 of COLA Part 2, Tier 2 Section 3H.3 will be revised as shown in Enclosure 1.

Enclosure 1
Revision to COLA Section 3H.3

3H.3.4.3.1.4 Lateral Soil Pressures (H)

Figure 3H.3-1 shows the at-rest lateral soil pressures. Figure 3H.3-2 shows the dynamic at-rest lateral soil pressures. Figure 3H.3-3 shows the active lateral earth pressures. Figure 3H.3-4 shows the passive lateral earth pressures.

The RWB east and west walls are also designed for lateral seismic soil pressures shown in Figures 3H.3-50 and 3H.3-51, respectively. These soil pressures consider the structure-soil-structure interaction (SSSI) between the RWB, RSW piping Tunnel, and RB. For details of this SSSI analysis, see Section 3H.6.5.3.

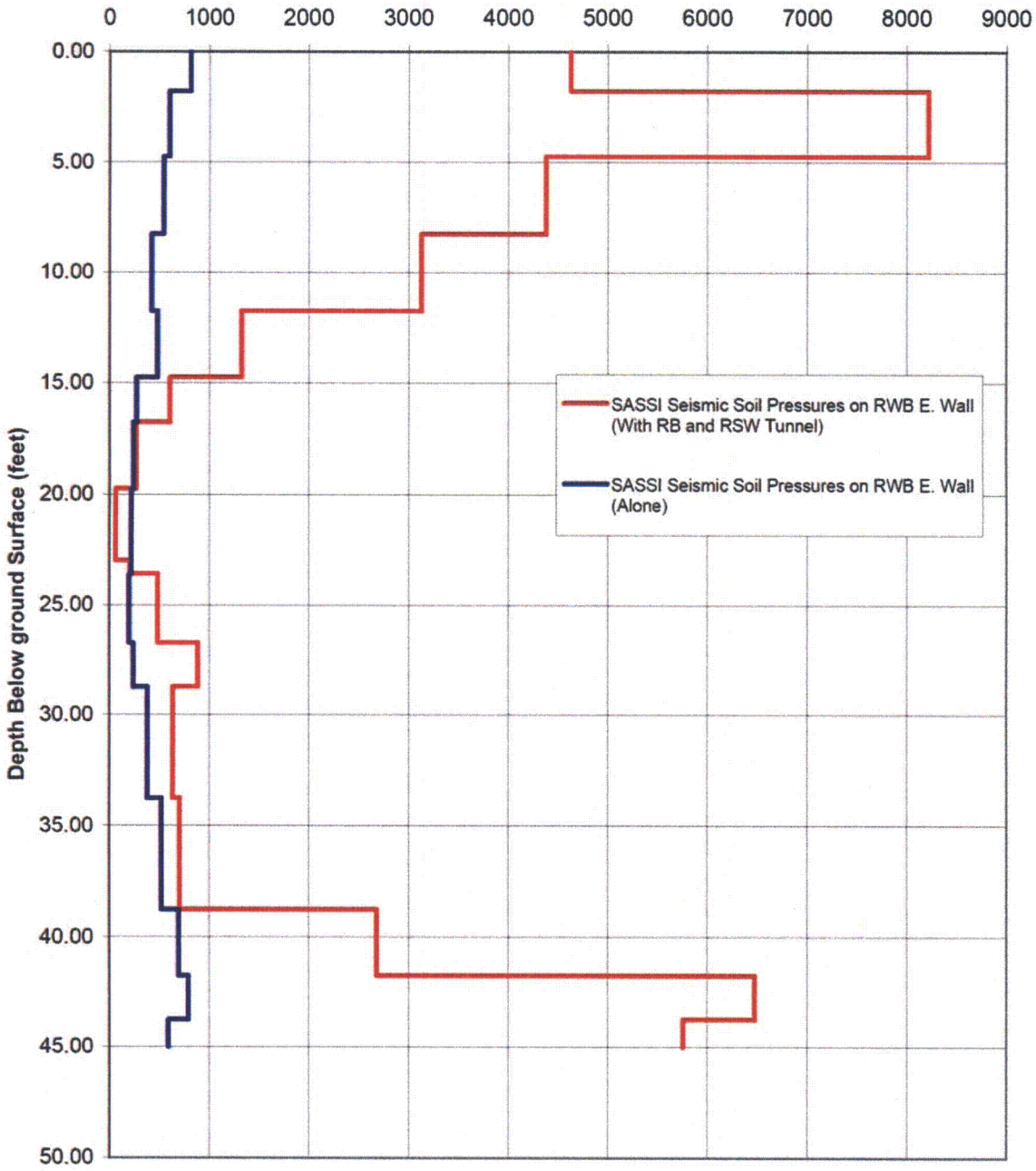

Figure 3H.3-50: SSI and SSSI Lateral Seismic Soil Pressures (psf) on Radwaste Building East Wall

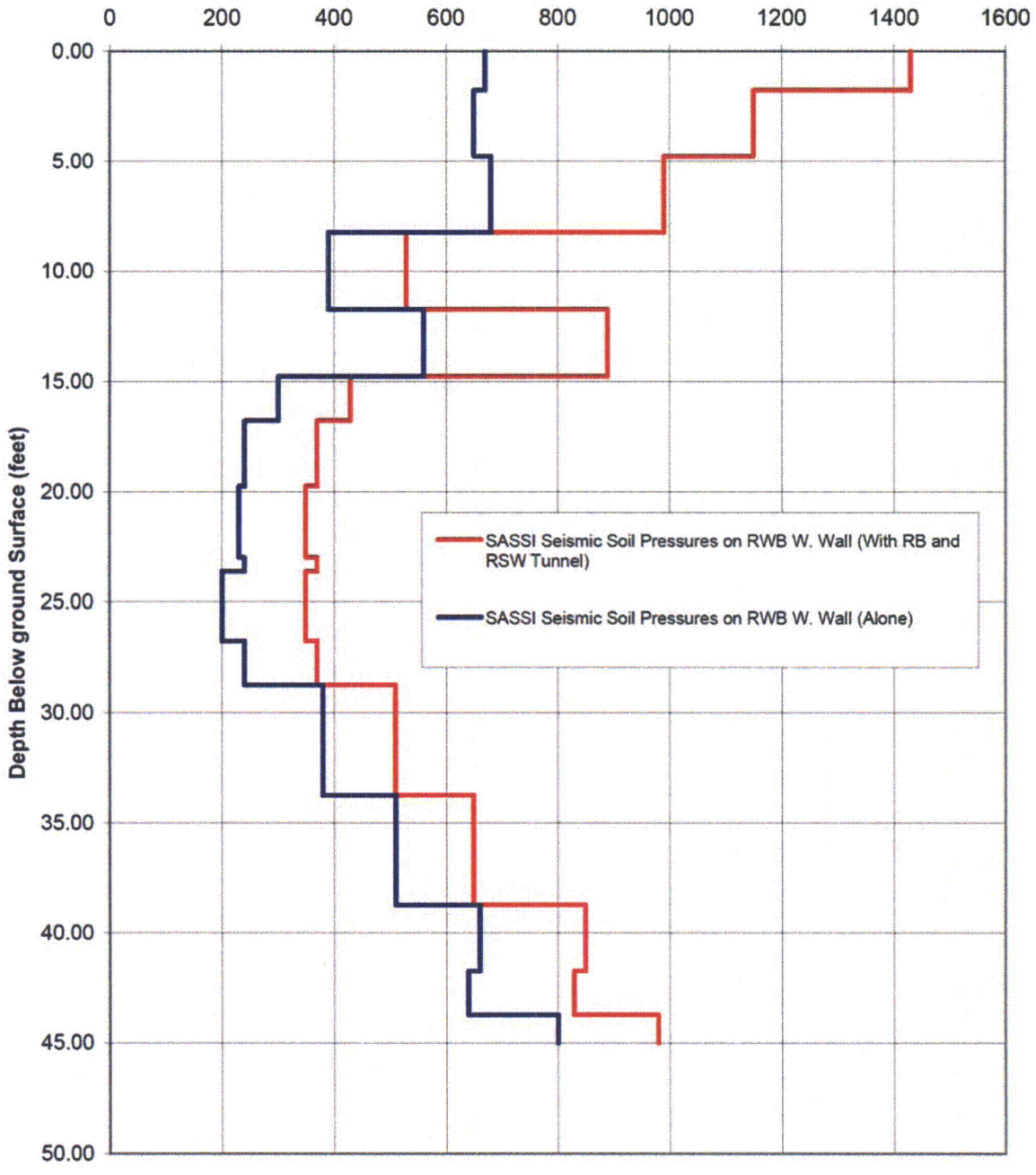

Figure 3H.3-51: SSI and SSSI Lateral Seismic Soil Pressures (psf) on Radwaste Building West Wall